NTNU – Trondheim
Norwegian University of
Science and Technology

Reactive Absorption of CO2 in Single and Blended Amine Systems

Hammad Majeed

Chemical Engineering
Submission date: July 2013
Supervisor: Hallvard Fjøsne Svendsen, IKP

Norwegian University of Science and Technology
Department of Chemical Engineering

Dedicated To

Nature , it's Creator

&

My Parents

ACKNOWLEDGMENT

In the Name of Almighty **ALLAH** to whom my all praises are. He is the one who gave me courage to perform this work.

I am pleased to pay credit to **Chemical Engineering department of NTNU** for offering each possible facility in making my effort triumphant.

I would like to express my profound gratitude to my supervisor, **Professor Hallvard F. Svendsen** for giving me the opportunity to join in the CO_2 capture research group whose brainwave, motivation and stimulating suggestions enabled me to complete this thesis work.

Thanks a lot to my co-advisors **Hanna Knuutila** & **Juliana G. Monteiro** for their exceptional guidance and for readily sharing their profound expertise in the most delightful manner. I would also like to pay gratitude to **Ardi Hartono** for his un parallel suggestions in every field, whether it's an experimental work or modeling. His quest for performing high quality research was inspirational to me.

I hereby declare that this is an independent work according to the exam regulations of Norwegian University of Science and Technology.

NTNU, Trondheim

15.07.2013

Author

ABSTRACT

Global warming scenario is pretty grim and is a well-known worldwide concern, most likely caused by increasing concentrations of CO_2 and other greenhouse gases in the earth's atmosphere due to human activities. CO_2 absorption in amine-based absorbents is an established and proven technology. Unfortunately, this process is still very energy intensive and has high capital costs. The main theme of this work is to characterize new generation solvents; kinetics of CO_2 absorption in single and blended amine system is a part of this mission.

Kinetics of CO_2 in aqueous MAPA system with concentration of 1/2/3/4/5 M and aqueous blended system of MAPA+DEEA with variant concentrations were measured at a temperature range of 298.15-338.15 K. The kinetic experiments for both systems were performed in string of disc contactor. Results for rate constants were interpreted in terms of single step termolecular mechanism proposed by *"Crooks et al., 1989"* for the reaction of CO_2 with amine because of its less number of parameters.

In addition to this work, the physical properties like density from 293.15-353.15 K and viscosity with in span of 293.15-333.15 K were also measured to determine the physio chemical parameters. The solubility of N_2O in aqueous MAPA system and aqueous blended systems were performed to estimate the solubility of CO_2 in MAPA and blended (MAPA+DEEA) solutions at temperature range of 298.15-338.15K.

Densities of systems were measured in Anton Paar DMA 4500M density meter while viscosities were estimated in Physica MCR 100 rheometer and solubility experiments were done in stirred jacketed glass vessel.

Simple model based on temperature and concentration was applied on excel sheet in order to calculate the density, solubility and viscosity. The absorption flux of CO_2 in MAPA and blended systems, Henry's constants, over all mass transfer coefficients and second order rate constants were determined for each case and compared these with the citied data available in order to judge the behavior and performance of current systems.

TABLE OF CONTENTS

List of Figures

List of Tables

Nomenclature

Symbol	Definition	Symbol	Definition
A	Arrhenius constant	L	Liter
AmH	Amine	M	Molarity
B	Base	MAPA	*N*-Methyl-1,3-diaminopropane
CO_2	Carbon dioxide	MFC	Mass flow controllers
DEEA	2-(Diethylamino)ethanol	Mol/mol	Mole
E	Activation energy	N_{CO2}	Flux of CO_2
$E_{A,pen}$	Enhancement factor for penetration theory	n_d	Number of discs
GHG	Green House Gas Emissions	^oC	Celsius scale
H_2	Hydrogen	P^*_{co2}	Partial pressure of CO_2 at interface
Ha	Hatta number	Pz	Piperazine
K	Kelvin scale	Re	Reynolds number
K_{app}	Apparent rate constant	Sc	Schmidt number
K_B	Rate constant of base	Sh	Sherwood number
KG	Overall mass transfer coefficient	Tc	Critical temperature
k_l	Liquid mass transfer coefficient	P	Density
K_{obs}	Observed kinetic rate constant	μ	Viscosity

Chapter 1

Introduction

Energy plays a vital role in world's economic growth. International energy agency *(IEA, 2010a)* presumed that if plans and policies by various governments with respect to energy usage will be implemented then the world primary energy demands will increase by 35% in between 2010 and 2035. That represents an average increase of 1.2% energy demand. On the other hand if policies are not implemented the value of growth per year will be 1.4%. *(IEA, 2010b)* outlined that in 2030 fossil fuel demand will account for 75-80% of world energy usage. In the view of this whole scenario it is pointed out that fossil fuels: coal, natural gas and oil will remain in the most prominent energy sources in an upcoming years.

Global climate change is most obtrusive environmental and energy policy issue of modern age. Industrial processes, burning of fossil fuels and various land use practices are disbursing greatly to the accumulation of greenhouse gases (GHGs) in the atmosphere, which can trap heat and block outward radiation. By far the most rampant of these GHGs is carbon dioxide (CO_2) accounting for 82% of total US GHG emissions.

Among the global prime energy demands the contribution of the fossil fuels are Coal 24%, natural gas accounted 21%, nuclear 5%, hydropower 7% and renewable are 10% *(BP, 2005)*. Power generation plants are the largest source of CO_2emissions *(IEA GHG,2002 b***).** It is also stated that fifth portion of total CO_2 emissions comes from industrial plants *(Zero, 2012).*

1.1 Why to Capture CO_2

Year 1992, international entanglement about climate change led to the United Nations Framework Convention on Climate Change (UNFCCC). The eventual theme of that Convention is "stabilization of greenhouse gas concentrations in the atmosphere at a level that prevents dangerous anthropogenic interference with the climate system".

So in order to minimize the contrary effects of CO_2 there is a need to limit the temperature increase to 2 degrees by 2050 *(Koomey, Krause, 2009).* In Copenhagen, December 2009 accord set a non-binding treaty to limit the global temperature increase to 2^0C above the industrial level. In July, 2009 the G8 leaders ratified to cut the global CO_2 emissions by at least 50% by 2050. To meet these requirements, a reduction in greenhouse gases is urgently required and every option to capture and to store CO_2 should be looked into.

1.2 Carbon Capture and Storage (CCS)

The world is now looking for modifications to increase the energy efficiency like switching from high carbon fossil fuels such as coal to less carbon fuels. Meanwhile technologies have cooperatively come to be known as "carbon capture" to continue the trend of fossil fuel energy sources.

CCS is the family of technologies and has different steps. The very first step is to capture CO_2 at some spot in the energy conversion process, depending on the type of energy technology applied. Following is the separation from mixture gas. It is then proceed towards transportation and storage in a suitable geological sink, where it is kept for suitable long period.

1.3 CO_2 Capture Technologies

There are three main channels to capture CO_2 from origin.

- Pre-Combustion CO_2 capture
- Post-Combustion CO_2 capture
- Oxy-fuel Combustion

1.3.1 Pre-Combustion CO_2 Capture

In pre-combustion CO_2 capture process, the fuel is converted in a reforming or gasification process and the subsequent shift-reaction into a mixture of H_2 and CO_2. The high pressure of this product gas stream expedites the removal of CO_2. The H_2-product can then be burnt in a gas turbine for energy production *(Feron et al., 2005).*

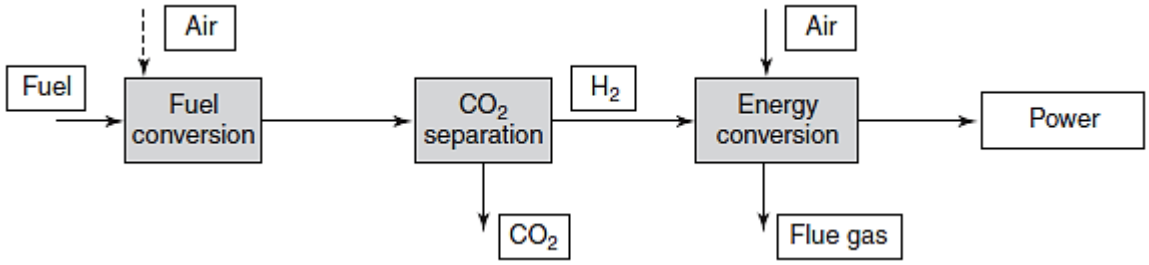

Fig 1.1: Pre combustion Scheme (*Feron et al., 2005*)

1.3.2 Post Combustion CO_2 Capture

In post combustion process, combustion of the fuel takes place first and then CO_2 is going to be captured from the flue gas. Commonly a chemical solvent is used to capture the CO_2 from the flue gas by absorption process. This CO_2 rich solvent is regenerated by heating it up in a stripping column and CO_2 is compressed, transported and stored. Post combustion capture is the facile method to implement on large industrial scale.

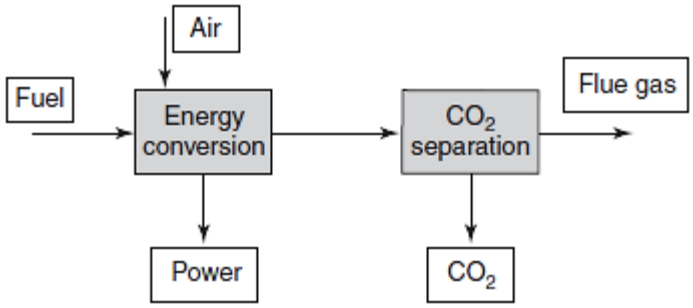

Fig 1.2: Post combustion scheme (*Feron et al., 2005*)

1.3.3 Oxy-Fuel Combustion

Oxy-combustion systems are being developed as flipside to post-combustion. In oxy-fuel combustion pure oxygen is used in gasification instead of air. Separation methodologies are used to extract oxygen from air. As a result of this gasification there will be a very low amount of CO_2 in the flue gases and CO_2 can be easily separated if present in gas streams.

Capture Technology	Advantages	Disadvantages
Pre Combustion	1) Synthesis gas is concentrated in CO_2 and has high pressure. 2) Increased driving force for separation. 3) More technologies available for separation. 4) Potential for reduction in compression costs/loads	1) Applicable mainly to new plants, as few gasification plants are currently in operation. 2) Barriers to commercial application of gasification are common to pre-combustion capture like availability and cost of equipment.
Post Combustion	1) Retrofit technology option.	1) Flue gas will dilute in CO_2 at ambient pressure. 2) Resulting in low CO_2 partial pressure. 3) Significantly higher performance or circulation volume needed for high capture levels than pre-combustion.
Oxy Fuel Combustion	1) Very high CO_2 concentration in flue gas. 2) Retrofit and repowering technology option.	1) Large cryogenic O_2 production requirement may be cost prohibitive. 2) Cooled CO_2 recycle required to maintain temperatures within limits of combustor materials. 3) Low process efficiency. 4) Added auxiliary load.

Table 1.1: Comparison of Capture technologies (Jose´ D. Figueroa et. al., 2008)

In the line of these capture technologies it is essential to discuss the separation of CO_2 from mixture gas.

1.4 Separation Methodologies

Variant schemes are adopted to separate CO_2 from flue or stack gas as follows.

- Chemical absorption
- Physical absorption
- Physical adsorption
- Membrane technologies
- Cryogenic separation

Energy consumption, capture efficiency and process cost are the major aspects on which selectivity of the process is defined.

1.4.1 Chemical Absorption

Chemical reaction takes place between solvent and gas. Chemical absorption utilizes the different reactivity's of various gases with solvent. MEA and other amines can be used in this process, CO_2 recovery rates of 98% and product purity of 99% can be achieved. The reactions should be reversible so that the solvent can be regenerated. Efficient solvents could reduce energy requirements by as much as 40% compared to conventional MEA solvents. There are, however, questions about its rate of degradation in the oxidizing environment of a flue gas and the amount of energy required for regeneration *(CCP, 2008).*

1.4.2 Physical Absorption

Absorption is a process in which atoms or molecules transfer from a gas phase to a liquid phase. In physical absorption, molecules of CO_2 are going to be dissolved in solvent in the absence of chemical reaction. The amount of absorbed gas increases linearly with the increase in its partial pressure according to Henry's law. Physical absorption will be more noticeable if partial pressure of the absorbed gas is high. It also depends upon the temperature; at low temperature the absorption is more efficient.

1.4.3 Physical Adsorption

In adsorption, molecules from gas or from liquid penetrated on solid surface hence creating a film of adsorbate on surface of adsorbent. In this case gas is adsorbed on the solid surface by van der Waals forces.

Separation is based on the difference in gas molecule sizes or different binding forces. Temperature swing and pressure swing adsorption methods are used for separation. The most common adsorbents are activated carbon *(Plaza et al., 2010)* silica gel and aluminum oxide.

1.4.4 Membrane Technologies

The principle behind this method is the pressure gradient. Gas separation membranes allow one component in a gas stream to pass through it faster than the others. High degrees of separation may not be achieved in membranes so multiple stages and/or recycle of one of the streams is essential. That leads to energy consumption, increased complexity and increased operational costs. There are diverse types of gas separation membranes including porous inorganic membranes, palladium membranes, polymeric membranes and zeolites (*CCP, 2008).*

1.4.5 Cryogenic Separation

The principle behind this separation is the difference in the boiling points of various gases. All the gases have different boiling points and this method provide effective gas separation. CO_2 can be separated from other gases by cooling and condensation. Cryogenic separation facilities the direct availability of liquid CO_2 required for transportation. The amount of energy required to provide the necessary refrigeration for cryogenic separation of CO_2 is the major issue in term of cost.

Another problem in this system is to remove any amount of water present, before the gas stream is cooled to avoid any kind of blockage in system. Cryogenics would normally only be applied to high concentration, high pressure gases, such as in pre-combustion capture processes or oxy fuel combustion *(CCP, 2008).*

Panoramic view of separation process

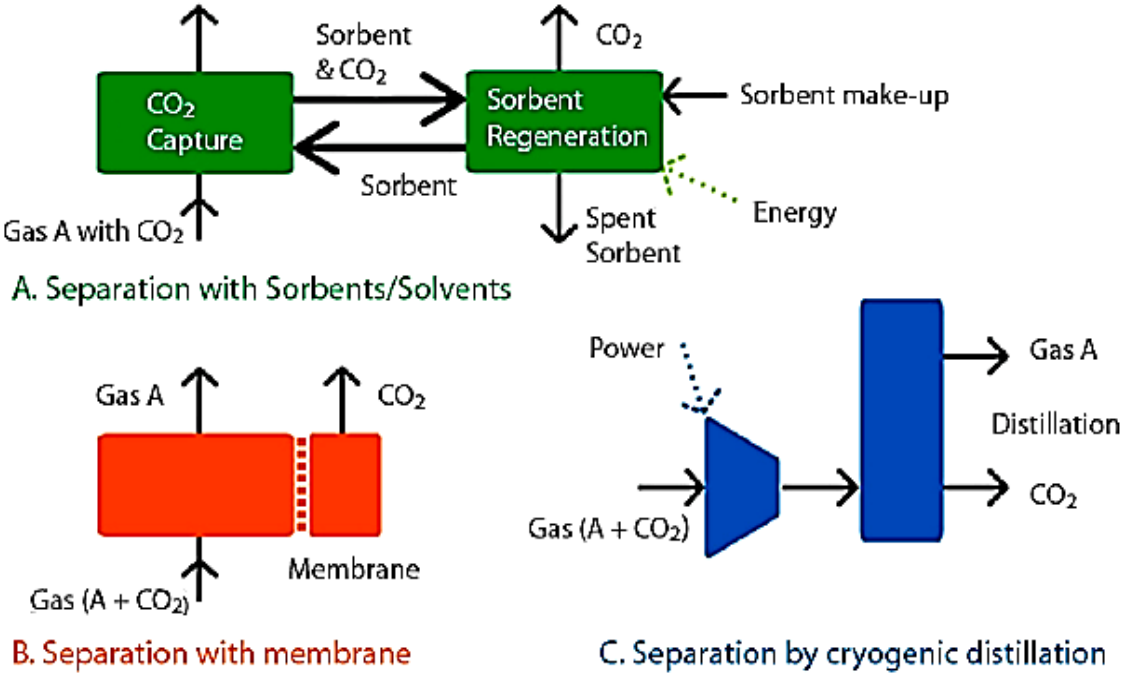

Fig 1.3: Separation processes (carbon capture project CCP, 2008)

1.5 CO_2 Transport and Storage

Deep ocean storage, geological storage and enhanced oil recovery techniques are leadingly followed for CO_2 storage. In deep ocean storage it is suggested that CO_2 can be stored under a depth of 3000m in the form of CO_2 lake under water for thousands of years but this process requires liquefaction and injection of CO_2 to this level. In geological storage, CO_2 is injected under high pressure in deep stable rocks where it can be stored for long period of time. The CO_2 would remain in small pore spaces inherent in rocks. In enhanced oil recovery "EOR" method CO_2 is injected in reservoirs to increase the oil productivity from well where it can be stored as well. CO_2 will be transported through pipeline or by ships *(IPCC, Special report 2005)*.

1.6 Unfolding Concepts and Research for CO_2 Capture

CO_2 capture and separation from large point sources, like power plants, can be achieved through continued research, development, and demonstration. Worldwide research is being performed to abate global climate change and to develop new strategy and processes that increase the efficiency of carbon capture systems while reducing overall expenditure *(IPCC, 2007).*

All the three CO_2 capture technologies citied above are capable of high efficiencies (about 90%). But high cost and energy requirements are major issues for these technologies. There are still gaps in currently available knowledge regarding some aspects of Carbon capture.

There should be some new tactics to find best out of best method and solvent in the form of low cost and less energy requirements for CO_2 capture. Technology roadmaps have been developed in the world for the availability of commercial deployment of CO_2 capture by 2020 *(Fogler, 2010).*

1.7 Interest & Span of Current Work

The paramount focus of current work is to play a part in characterization of new generation absorbents for CO_2. The reason behind this is to optimize the process by amendments in order to reduce overall capture cost. Absorption is considered to be the optimum available technology for post combustion application out of the three traditional methods of CO_2 capture (absorption, adsorption and membrane processes). However, CO_2 absorption by amines requires 2.8–3.2 GJ/ton of recovered CO_2 (as claimed by MHI and Fluor) in a large part due to significant energy consumption associated with the regeneration step *(Mohammad R.M et al., 2007).*

The presage path in development of absorption process is blended amine systems. Some of the blended amine systems can form two liquid phases and hence, end up in high reaction rate on absorption side of process and low energy requirements in the regeneration side. Primary and secondary amines form carbamates, while tertiary amines boost the reaction of hydration of CO_2 that leads to bicarbonate formation *(Donaldson and Nguyen, 1980).* If the lower regeneration heat of bicarbonate, as compared to that of carbamate, is combined with high equilibrium temperature sensitivity, it will end up in to a low stripping steam requirement. From two of the liquid phases one the very rich in CO_2, will be forwarded to regeneration. Due to low circulation

of only one phase this can lead to decreased sensible heat loss, high equilibrium temperature sensitivity and thus over all minimizing the stripping requirement.

Furthermore, the reactive CO_2 absorption in tertiary amines is relatively slow *(Versteeg et al., 1996)* but can be enhanced by addition of primary or secondary amine to generate blended systems.

MAPA (*N*-Methyl-1,3-diaminopropane) a diamine and DEEA (2-(Diethylamino)ethanol) a tertiary alkanolamine have been selected for the reactive absorption of CO_2. The intent of current work is to judge the reaction rates of both the solvents at variant temperatures and driving forces. The kinetics of MAPA and blends of MAPA+DEEA at different temperatures and driving forces of partial pressure of CO_2 were measured. The aqueous blends of DEEA and MAPA are especially captivating for the absorption process because they can form two liquid phases upon CO_2 loading. The upper phase is lean in CO_2 and does not require regeneration, while the lower phase is CO_2 rich and is sent to the stripper column, where DEEA is mainly regenerated *(Liebenthal et al., 2012).*In experimentation of blended systems denotation are made for both amine systems as M denotes MAPA and D denotes DEEA.

System	Concentration (mol/L)	Temperatures (K)	Equipment
MAPA	1,2,3,4,5	298.15-338.15	A String of Discs
MAPA+DEEA	1M1D,1M2D,1M3D,1M5D 2M1D,2M2D,2M3D,2M4D, 2M5D,3M1D,3M3D,4M3D	298.15-338.15	A String of Discs

Table 1.2: Details of current work

Physical properties of solvents were also measured that include density, viscosity and solubility.

System	Physiochemical Property	Concentration (mol/L)	Temperature (K)	Range
MAPA	Density (g/cm^3)	1,2,3,4,5	293.15-353.15	0.9276-0.99359
	Viscosity (mPa.s)	1,2,3,4,5	293.15-333.15	0.6733-12.386
	Solubility ($kPa.m^3/kmol$)	1,3,5	298.15-338.15	4604-14620
MAPA+DEEA	Density (g/cm^3)	1M1D,1M2D,1M3D,1M5D 2M1D,2M2D,2M3D,2M4D, 2M5D,3M1D,3M3D,4M3D	293.15-353.15	0.86631-0.99117
	Viscosity (mPa.s)	1M1D,1M2D,1M3D,1M5D 2M1D,2M2D,2M3D,2M4D, 2M5D,3M1D,3M3D,4M3D	293.15-333.15	0.9886-20.285
	Solubility ($kPa.m^3/kmol$)	1M1D,1M2D,1M3D 1M5D,2M1D,2M2D,2M3D,2M4D 2M5D	298.15 -338.15	1666.59-8354.82

Table 1.3: Experimentally measured physiochemical properties of MAPA and MAPA+DEEA

Chapter 2

Back ground

Detailed characterization of solvent is required for its industrial application. Physiochemical properties like density, viscosity and solubility of CO_2 in aqueous amine solutions are of distinct importance for the development of new solvents in CO_2 capture and design of gas-liquid absorption contactors for gas treatment. Densities and viscosities are required to calculate the liquid Sherwood number. Density is also necessary for determination of physical solubility of CO_2 in the solvent, for the evaluation of kinetics and mass transfer. Viscosity is another requirement to measure diffusivity by using a modified Stokes-Einstein equation, for kinetics and mass transfer *(Versteeg and van swaaij, 1988)*. Solubility of CO_2 in an absorbent is desired for thermodynamic models for the prediction of activity coefficients of CO_2. So in short binary data of system containing (CO_2-water-amine) is utmost hunger to establish the kinetic model. Solubilities, densities and viscosities of CO_2 in the aqueous solutions of MAPA and blends of MAPA+DEAA are estimated at different temperatures and concentrations.

2.1 Physiochemical Properties

2.1.1 Solubility

CO_2 can be chemically bound to an absorbent or it can be in the form of free CO_2 in absorbent solution (physical solubility). The knowledge of the physical solubility of CO_2 at numerous concentrations and temperatures is desired for developing a kinetic model of the system. Here comes a problem that direct measurement of physical solubility is not possible because CO_2 reacts with amine. N_2O which is a non-reacting gas with amine solutions can then be capitalized to measure this property. N_2O analogy is implemented to calculate the solubility of CO_2 into amine solution. N_2O analogy was originally proposed by *(Clarke, 1964)***.** The N_2O analogy then;

Solubility of CO_2 in absorbent = C1 (solubility of N_2O in absorbent)

Where

$$C1 = \frac{Solubility\ of\ \ CO_2 in\ water}{Solubility\ of\ N_2O\ in\ water} \qquad 2.1$$

$$C1 = \frac{H_{N_2O}^{H_2O}}{H_{CO_2}^{H_2O}} \quad 2.2$$

The value of C1 can be calculated according to Varsteeg and van Swaaij *(Versteeg et al., 1988)*.

$$C1 = 3.04e^{-\frac{240}{T}} \quad 2.3$$

This N_2O analogy has been applied to amine systems including blended systems *(Hartono et al., 2008; Versteeg and van Swaij, 1988).*

The solubility of N_2O gas in aqueous amine solvents can be fashioned by an apparent Henry's law coefficient showing the equilibrium between solute concentration in the gas phase and the solute concentration in liquid phase.

The Redlich-Kister equation correlates the solubility at different concentrations and temperatures based on the excess properties. The excess Henry's constant then figured by equation (2.4) *(Edwards et al., 1975) and (Tiepel et al., 1972*.

$$\hat{A} = \ln(K_{H_M}) - x_1 \ln(K_{H_1}) - x_1 \ln(K_{H_2}) \quad 2.4$$

Where K_{H_M} , K_{H_1} and K_{H_2} are Henry's law constant of N_2O in an amine-water mixture. The excess Henry's constant was correlated to Redlich-Kister equation as: *(Prausnitz et al., 1999)*.

$$\hat{A} = x_1 x_2 \sum_{n=1} A_n (1 - 2x_2)^{n-1} \quad 2.5$$

Where x_1 and x_2 are mole fractions of amine and water respectively and An is Redlich-Kister coefficient, determined by regression for each temperature case. Inconsistency in solubility data may leads to non-precise results for reaction kinetics *(Blauwhoff et al., 1984).*

2.1.2 Density

Redlich-Kister model is usually adopted to figure out the densities of aqueous amine solutions. The pure liquid components data in the DIPPR (version 4.1.0, 2004) can be estimated by using the equation (2.6). Critical temperature was used for the regression of the parameters.

$$\rho(gcm^{-3}) = \frac{AM}{B\left[1+\left[1-\frac{T}{T_c}\right]^C\right]1000} \quad 2.6$$

A, B and C are adjusted parameters and M indicates molar mass of the solvent. T is the temperature to be measured while T_c is the critical temperature.

2.1.3 Diffusivity

The diffusivity of the gases like CO_2 and N_2O in water or infinite dilute solution can be estimated by the correlation proposed by Littel *(Littel et al., 1992)* and *Versteeg (Versteeg et al., 1988).* The Stokes-Einstein correlation was proposed for the diffusivity of CO_2 and alkanolamine in aqueous solutions.

2.1.3.1 Diffusivity of CO_2 and N_2O in Water

The diffusivity of CO_2 in water can be calculated as a function of temperature as:

$$D_{CO_2} = 2.35 * 10^{-6} exp\left(\frac{-2119}{T}\right) \ m^2 s^{-1} \qquad 2.7$$

Similarly the diffusivity of N_2O in water as a function of temperature is summed as:

$$D_{N_2O} = 5.07 * 10^{-6} exp\left(\frac{-2371}{T}\right) \ m^2 s^{-1} \qquad 2.8$$

With same routine the diffusivity of N_2O in aqueous alkanolamine solutions can be determined and the general expression for that is "the reciprocal values of the diffusivity data measured and those presented by (*Versteeg et al.1988)* were multiplied by the diffusivity of N_2O in water and sketched against the ratio of viscosity of alkanolamine solutions to water (*Versteeg et al.1988).*

2.1.4 Viscosity

Viscosity is a measure in resistance to flow. Fluids resist the relative motion of the immersed object as well as the motion of the layers with differing velocities in them *(Bird et al., 2002).* Viscosity of both liquid and gas phases are affected by temperature changes but pressure affects, normally, only the viscosity of the gas phase.

The viscosities of aqueous amine solutions are influential for the measurement of the diffusivities. Viscosity of aqueous amine solutions can be correlated to diffusivity by modified Stokes-Einstein relation *(Versteeg et al., 1988).*

Viscosity of aqueous solutions of MAPA and blended system of MAPA+DEEA were measured at different temperatures and compositions. The experimental setup and results from assessments are shown in upcoming chapters.

2.2 Kinetics of Alkanolamines

Alkanolamines are most trendy absorbents in removal of CO_2 from process gas streams, like in ammonia plants to make the gaseous streams free of CO_2, in the production of hydrogen via steam reforming of natural gas, in treating natural/associated gas streams and in thermal power stations to meet the discharge limits for CO_2 in flue gas. Therefore, the CO_2 reaction with alkanolamines is of gigantic importance. The absorption of CO_2 in aqueous amine solutions is based on three mechanisms i-e. Zwitterion mechanism, termolecular mechanism and base catalyzed hydration *(Versteeg et al., 1988)*. Primary, secondary and sterically hindered amines are usually described by zwitterion mechanism while reaction of tertiary amines with CO_2 follows base catalyzed hydration mechanism.

2.2.1 Zwitterion Mechanism

The two-step mechanism originally proposed by Caplow *(Caplow, 1968)* and later on redeem by Danckwerts *(Danckwerts, 1979)*. Reaction between CO_2 and the amine (AmH) proceeds through the formation of a zwitterion as an intermediate is the first step.

$$CO_2 + AmH \underset{k_{-1}}{\overset{k_1}{\leftrightharpoons}} AmH^+COO^- \qquad 2.9$$

This zwitterion undergoes deprotonation by a base B, thereby resulting in carbamate formation in second step.

$$AmH^+COO^- + B \overset{k_B}{\rightarrow} AmCOO^- + BH^+ \qquad 2.10$$

Applying the steady-state principle to the intermediate zwitterion, the rate of reaction of CO_2 in aqueous solutions can then be defined as: *(Versteeg et al., 1996)*

$$r = \frac{k_1(CO_2)(AmH)}{1+\frac{k_{-1}}{k_B(B)}} \qquad 2.11$$

Where K_B *(B)* represents deprotonation of the zwitterion by any base, such as H_2O, OH^- or AmH, as well as by a combination of bases. The reaction rate given by equation (2.11) unveils a fractional order of reaction with respect to the amine concentration.

When deprotonation is instant as compared to the reverse reaction in equation (2.11) ($k_{-1} << k_B$ (B)) then zwitterion formation is said to be rate-determining step.

Than rate of reaction will be:

$$r = k_1(CO_2)(AmH) \qquad 2.12$$

There by proposing that the reaction is of the first order with respect to both CO_2 and amine concentration. When zwitterion deprotonation is rate-determining step ($k_{-1} >> k_B$ (B)), equation (2.12) takes the form:

$$r = \frac{k_1 k_B (B)}{k_{-1}}(CO_2)(AmH) \qquad 2.13$$

The above expression declares the fractional reaction order between one and two with respect to amine concentration. If the amine itself represents base B, then carbamate formation can be expressed as follows:

$$AmH^+COO^- + AmH \rightarrow AmCOO^- + AmH_2^+ \qquad 2.14$$

The overall rate of reaction which accounts for carbamate formation in a solution can be then expressed by the sum of the reactions in equations (2.10-2.14).

$$CO_2 + 2AmH \leftrightharpoons AmCOO^- + AmH_2^+ \qquad 2.15$$

In case of sterically hindered amine, the zwitterion reacts preferably with water and formation of bicarbonate takes place:

$$AmH^+COO^- + H_2O \rightarrow HCO_3^- + AmH_2^+ \qquad 2.16$$

In this scenario the reaction, which narrates for bicarbonate formation, is given by the summation of reactions represented by equations. (2.9-2.16):

$$CO_2 + AmH + H_2O \leftrightharpoons HCO_3^- + AmH_2^+ \qquad 2.17$$

Steric effects reduce the stability of the carbamates formed by the amine with CO_2. Due to the low stability, the carbamates of sterically hindered amines may also readily undergo hydrolysis, forming bicarbonates and releasing free amine molecules. This can be represented as:

$$AmCOO^- + H_2O \rightarrow HCO_3^- + AmH \qquad 2.18$$

The released free ion molecules will again react with CO_2. Thus, presence of bicarbonate ions will be more as compared to that of carbamate ions.

The following reactions may also take place simultaneously in an aqueous amine solution:

$$AmH + H_2O \rightarrow AmH_2^+ + OH^- \quad 2.19$$

$$H_2O \leftrightharpoons H^+ + OH^- \quad 2.20$$

$$CO_2 + H_2O \overset{K_{H_2O}}{\leftrightharpoons} HCO_3^- + H^+ \quad 2.21$$

$$CO_2 + OH^- \overset{K_{OH^-}}{\leftrightharpoons} HCO_3^- \quad 2.22$$

The net rate of CO_2 reactions in an aqueous amine solution is provided by the sum of the reaction rates given by equations (2.10, 2.21, and 2.22) as:

$$r_{overall} = \left[\frac{k_1(CO_2)(AmH)}{1+\frac{k_{-1}}{k_B(B)}}\right] + \{\left[k_{H_2O}(H_2O) + k_{OH^-}(OH^-)\right](CO_2)\} \quad 2.23$$

Assuming that the reaction takes place in pseudo-first regime,

$$r_{overall} = k_{obs}(CO_2) \quad 2.24$$

While k_{obs} denotes observed reaction rate constant that can be measured.

$$k_{obs} = \left[\frac{k_1(AmH)}{1+\frac{k_{-1}}{k_B(B)}}\right] + \{\left[k_{H_2O}(H_2O) + k_{OH^-}(OH^-)\right]\} \quad 2.25$$

For the analysis of experimental data apparent reaction rate constant (k_{ap}), is used and given by:

$$k_{ap} = \left[\frac{k_1(AmH)}{1+\frac{k_{-1}}{k_B(B)}}\right] \quad 2.26$$

k_{ap} can be extracted from k_{obs} as follows:

$$k_{ap} = k_{obs} - \left[k_{H_2O}(H_2O) + (k_{OH^-}(OH^-)\right] \quad 2.27$$

2.2.2 Termolecular Mechanism

Termolecular mechanism was formerly proposed by Crooks and Donnellan *(Crooks et al., 1989)* consider that an amine reacts with one molecule of a base and one molecule of CO_2 at the same time. The reaction proceeds in a single step via a slackly bound encounter complex as an intermediate, represented as: *(Danckwerts et al., 1979)*.

$$CO_2 + AmH \cdots B \leftrightharpoons AmCOO^- + \cdots BH^+ \qquad 2.28$$

The loosely bound encounter complex breaks up to form reactant molecules (CO_2 and amine) while its small fraction reacts with a second molecule of the amine or a water molecule to give ionic products. Da Silva and Svendsen *(da Silva et al., 2004)* recently retreated this mechanism by ab initio calculations and a solvation model. According to their results, the most credible mechanism was similar as suggested by Crooks and Donnellan *(Crooks et al., 1989)*. There might be another alternative that CO_2 forms a bond to amine with solvent molecule stabilizing the zwitterion like intermediate with hydrogen bonds.

The forward rate of reaction for this mechanism is specified by the following equation:

$$r_{overall} = k_{obs}\,(CO_2) \qquad 2.29$$

While k_{obs} can be illustrated as

$$k_{obs} = \left[\, k_{H_2O}(H_2O) + k_{OH^-}(OH^-) + k_{AmH}(AmH) \,\right] (AmH) \qquad 2.30$$

2.2.2.1 Base Catalyzed Hydration Mechanism

According to Donaldson and Nguyen *(Donaldson et al., 1980)* tertiary alkanolamines cannot react directly with CO_2. These amines have a base-catalytic effect on the hydration of CO_2. This was deep-rooted by Versteeg and Van Swaaij *(Versteeg et al., 1988b)* by the absorption of CO_2 into a water free solution of MDEA and ethanol. They clinched that CO_2 was only physically absorbed, proving the proposed reaction mechanism (Versteeg et al., 1988), represented as:

$$R_3N + H_2O + CO_2 \xrightarrow{k'} R_3N^+H + HCO_3^- \qquad 2.31$$

In aqueous solution an amine dissociation reaction may occur:

$$R_3N + H_2O \leftrightharpoons R_3N^+H + OH^- \qquad 2.32$$

Jørgensen and Faurholt *(Jørgensen et al., 1954)* reported that direct reaction between CO_2 and tertiary amines may arise at extremely high pH values, thereby resulting in monoalkyl carbonate formation. On the other hand, at pH values lower than 12, the rate of this reaction can be neglected *(Benitez-Garcia et al., 1991).*

The total rate of all CO_2 reactions in an aqueous solution is therefore expressed by the sum of the reaction rates given by equations (2.10, 2.21 and 2.31):

$$r_{overall} = \left[k_{H_2O} (H_2O) + k_{OH^-} (OH^-) + k' (R_3N) \right] (CO_2) \quad 2.33$$

And k_{obs}:

$$k_{obs} = \left[k_{H_2O} (H_2O) + k_{OH^-} (OH^-) + k' (R_3N) \right] \quad 2.34$$

And k_{ap} by:

$$k_{ap} = [k' (R_3N)] \quad 2.35$$

2.3 Mass Transfer with a Chemical Reaction

Absorption into a liquid agent is the most frequently used channel in gas purification process. Absorption of gas is a unit operation in which soluble components of a gas mixture dissolve in a liquid agent. This heterogeneous process is carried out in various equipment's ranging from a bubbling absorber to a packed column.

In order to polish the overall rate of the process, an intimate gas–liquid contact has to be developed and mass transfer has to be improved by increasing turbulence in both liquid and gas phases. Though, at the interface boundary layers are always present, in which mass transfer takes place by a fusion of diffusional and chemical mechanisms, so that, the overall rate of the process is administered by both chemical reaction and mass transfer *(Ma'mun 2005).*

The absorption rate of CO_2 in aqueous amine solution will increase if the mass transfer is accompanied by chemical reaction. The absorption flux will be then:

$$N_A = \frac{1}{\frac{1}{E_A k_l} + \frac{R_T}{H k_G}} \left(C_A^* - C_{A,b} \right) \quad 2.36$$

E_A denotes the enhancement factor which is defined as the ratio of liquid side mass transfer coefficient with chemical reaction to the mass transfer coefficient without chemical reaction.

The absorption flux can be simplified in two ways:

- For very low loadings of CO_2 the concentration of solute (CO_2) in the liquid bulk will be zero and absorption flux equation thus reduced to:

$$N_A = \frac{1}{\frac{1}{E_A k_l} + \frac{R_T}{H k_G}} \left(C_A^* \right) \qquad 2.37$$

- Gas side resistance to mass transfer can be ignored if pure CO_2 is used. In that case absorption flux will be:

$$N_A = E_A k_l C_A^* \qquad 2.38$$

When mass transfer is accompanied by chemical reaction then E_A is an influential parameter. Enhancement factor can be calculated from equations based on mass transfer models like surface renewal model, film theory and penetration theory.

2.3.1 Two Film Theory

Two film theory was first suggested by Whitman (1923) and by Lewis and Whitman (1924). To illustrate the process, a gas phase is brought in contact with a liquid phase *(Froment and Bischoff, 1990)*. According to this theory a stagnant film of thickness δ is supposed to exist at liquid and gas interface as sketched in Figure 2.1. Mass transfer occurs by a steady molecular diffusion through the film. This theory predicts mass transfer rate on the basis of first order dependency.

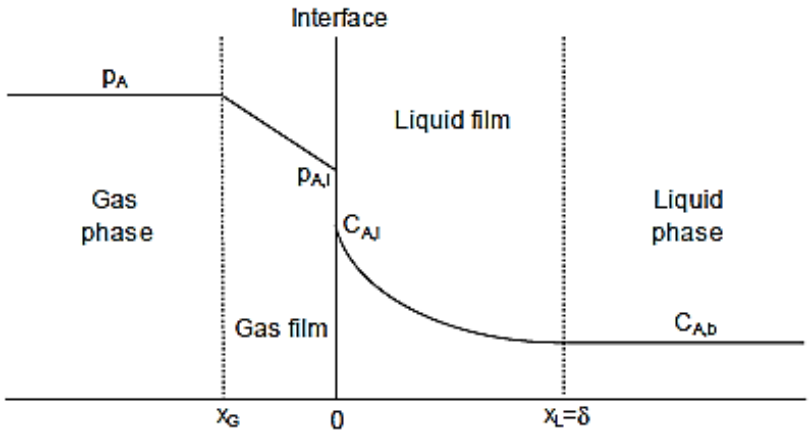

Fig 2.1 Mass transfer concept b/w gas and liquid based on two film theory (Ma'mun, 2005)

The absorption rate is determined by molecular diffusion in the surface layers. Although the diffusional and turbulence transport will apparently vary on continuous basis with depth below the surface, So therefore it is useful to take as a model a completely stagnant layer having an effective thickness δ, overlying liquid of uniform composition. It is assumed that the thickness is small enough for the absorption process to be treated as one, steady–state diffusion through the stagnant layer.

The mass transfer equation in physical absorption is determined from the mass balance of the solute (CO_2) at steady state as:

$$D_A \frac{\partial^2 C_A}{\partial x^2} = 0 \qquad for\ 0 \leq x \leq \delta \qquad 2.39$$

While the Boundary limits are:

When X=o , $C_A = C_{A,i}$

When X=δ, $C_A = C_{A,b}$

Integrating and applying boundary conditions yields,

$$C_A = C_{A,i} + (C_{A,b} - C_{A,i})\frac{x}{\delta} \qquad 2.40$$

The mass transfer flux will then be

$$N_A = -D_A \frac{dC_A}{dx}\Big|_{x=0} = \frac{D_A}{\delta}(C_{A,b} - C_{A,i}) = k_l(C_{A,j} - C_{A,b}) \qquad 2.41$$

k_l denotes the coefficient of mass transfer for liquid side, equals to $\frac{D_A}{\delta}$.

Hatta (Hatta, 1932) proposed the analytical solution for the mass transfer through a film. Mass balance for the solute is given as under:

$$D_A \frac{\partial^2 C_A}{\partial x^2} = k_l C_A for\ 0 \leq x \leq \delta \qquad 2.42$$

Boundary Conditions:

X=o , $C_A = C_{A,i}$

X=δ, $D_A\left[\frac{\partial C_A}{\partial x}\right]_\delta$

Enhancement factor is given by:

$$E_{A,film} = \frac{Ha}{\tanh(Ha)} \qquad 2.43$$

If Ha >>1, then $E_{A,film} \cong Ha$.

2.3.2 Surface Renewal Model

Surface renewal model for mass transfer was proposed by Danckwerts (Danckwerts, 1951) as extension of penetration theory. It is based on the assumption that the liquid elements do not stay on the surface (gas-liquid contact) at the same time. It is the complex model of fluid mechanics.

In surface renewal model, the interface is observed as being formed by a number of elements, and each one of which has been brought to the surface some time *t* before the instant of observation.

The distribution of the surface element contact times is described by a distribution function $\psi(t)= se-st$, where

$$\psi(t) = \frac{1}{t^*} \; for \; t < t^* \qquad \text{and} \qquad \psi(t) = 0 \; for \; t > t^*$$

The absorption rate at the surface stated by Danckwerts' age function is:

$$N_A(t) = \sqrt{D_A(k_1 + s)C_{A,i}} = \sqrt{D_A\left(k_1 + \frac{k_l^2}{D_A}\right)C_{A,i}} = k_l C_{A,i}\sqrt{1 + \frac{k_l D_A}{k_l^2}} \qquad 2.44$$

While

$$k_l = \sqrt{D_A s} \qquad 2.45$$

Hence the enhancement factor E_A can be illustrated as:

$$E_A = \sqrt{1 + \frac{k_l D_A}{k_l^2}} = \sqrt{1 + Ha^2} \qquad 2.46$$

A number of literature such as Perry and Pigford *(1953)*, Brian *(1964)*, Secor and Beutler *(1967)*, and Onda *et al. (1970).* Danckwerts and Kennedy *(1954)*, Porter *(1966)*, DeCoursey *(1974, 1982*) and Olander *(1960)* is available for correlation of enhancement factor for other type of reactions based on penetration theory and surface renewal theory.

2.3.3 Film-Penetration Theory

In contrast to surface renewal model, the film-penetration theory adopts the unsteady state molecular diffusion mechanism. Higbie *(Higbie, 1935)* was first who come up with the film penetration theory based on the hypothesis that, liquid-gas interface is composed of tiny liquid elements that are incessantly brought to the surface from bulk of the liquid. These elements are considered as stagnant. When liquid element reached the surface, the dissolved gas concentration in the element is supposed to be equal to the liquid bulk concentration. So therefore mass transfer will then be:

$$D_A \frac{\partial^2 C_A}{\partial x^2} = \frac{\partial C_A}{\partial t} \qquad 2.47$$

Initial and Boundary Conditions:

$$C_A(0,t) = C_{A,i}$$

$$C_A(\infty,t) = C_{A,b}$$

$$C_A(x,0) = 0$$

The mass transfer rate with above conditions gives a solution:

$$N_A = k_l\left(C_{A,i} - C_{A,b}\right) \qquad 2.48$$

Where K_l denotes the mass transfer coefficient

$$k_l = 2\sqrt{\frac{D_A}{\pi t^*}} \qquad 2.49$$

The enhancement factor E_A for pseudo first order irreversible reaction can be voiced as:

$$E_{A,pen} = \left[\left\{1 + \frac{\pi}{8Ha^2} erf\left[\sqrt{\frac{4Ha^2}{\pi}}\right] + \frac{1}{2Ha} exp\left(\frac{4Ha^2}{\pi}\right)\right\}\right] \qquad 2.50$$

$E_{A,pen} \cong$ Ha, If Ha >> 1,

2.4 Chemical Equilibrium

Chemical equilibrium governs the extent of dissociation and reaction and so the distribution of species.

The equilibrium condition stoichiometric formulation is:

$$\sum_{i=1}^{n} \vartheta_i . \mu_i = 0 \qquad 2.51$$

Where ϑ_i is stoichiometric coefficient of component i and μ_i characterizes the chemical potential of component i. Conventionally, the chemical equilibrium is defined by the equilibrium constant , K.

$$K = \prod_{i=1}^{n} \alpha_i^{vi} = \prod_{i=1}^{n} \gamma_i^{vi} . x_i^{vi} \qquad 2.52$$

While γ_i dontes the activity coefficient and xi is liquid phase composition *(Kohl & Nielsen, 1997).*

2.4.1 Chemical Equilibria in (CO_2-Water- DEEA System)

Dissociation of CO_2 from gas phase to liquid phase

$$CO_{2(g)} \rightleftharpoons CO_{2(l)} \qquad 2.53$$

Ionization of water

$$2H_2O \rightleftharpoons H_3O^+ + OH^- \qquad 2.54$$

Hydrolysis of dissolve CO_2

$$CO_2 + 2H_2O \rightleftharpoons HCO_3^- + H_3O^+ \qquad 2.55$$

Dissociation of carbonate ion

$$HCO_3^- + H_2O \rightleftharpoons CO_3^{2-} + H_3O^+ \qquad 2.56$$

Amine Protonation

$$DEEA + H_3O^+ \rightleftharpoons DEEAH^+ + H_2O \qquad 2.57$$

Base catalytic effect on hydration of CO_2

$$DEEA + H_2O + CO_2 \rightleftharpoons DEEAH^+ + HCO_3^- \qquad 2.58$$

2.4.2 Chemical Equilibria in (CO_2-Water- MAPA System)

Dissociation of CO_2 from gas phase to liquid phase

$$CO_{2(g)} \rightleftharpoons CO_{2(l)} \quad 2.59$$

Ionization of water

$$2H_2O \rightleftharpoons H_3O^+ + OH^- \quad 2.60$$

Hydrolysis of dissolve CO_2

$$CO_2 + 2H_2O \rightleftharpoons HCO_3^- + H_3O^+ \quad 2.61$$

Dissociation of carbonate ion

$$HCO_3^- + H_2O \rightleftharpoons CO_3^{2-} + H_3O^+ \quad 2.62$$

Amine Protonation

$$MAPA + H_3O^+ \rightleftharpoons MAPAH^+ + H_2O \quad 2.63$$

Carbamate formation

$$MAPA + H_2O + CO_2 \rightleftharpoons MAPACOO^- + H_3O^+ \quad 2.64$$

Protonated carbamate formation

$$MAPACOO^- + H_3O^+ \rightleftharpoons H^+MAPACOO^- + H_2O \quad 2.65$$

2.5 Reaction Regime

The influence of a reaction on the absorption rate can be expressed by a dimensionless ratio term φ, or can be determined from Hatta number and enhancement factor. Extent of reaction can also be identified by the relative rates of diffusion and reaction *(Astarita et al., 1983)*.

$$\varphi = \frac{Diffusion\ time}{Reaction\ time} \quad 2.66$$

$$\varphi = \frac{t_D}{t_R} \quad 2.67$$

The Hatta number, Ha;

$$H_a^2 = \frac{Maximum\ conversion\ in\ film}{Maximum\ transport\ through\ film} = \frac{k_{obs}D}{k_l^2} \quad 2.68$$

Reaction regimes in terms of relative rates of reaction and diffusion can be expressed as:

2.5.1 Slow Reaction Regime

When $\varphi \ll 1$, the reaction is too slow and have no significant effect on the diffusion phenomena and fundamentally no absorption rate enhancement will take place. This case then refers to as slow reaction regime.

2.5.2 Fast Reaction Regime

When $\varphi \gg 1$, the reaction will be fast, in result there will be a significant rate enhancement, dropped it on to fast reaction regime.

2.5.3 Instantaneous Reaction Regime

When $\varphi \rightarrow \infty$ the reaction is infinitely fast, chemical reaction and the rate enhancement grasps its maximum achievable limit. Chemical equilibrium is established instantaneously and regime is said to be instantaneous reaction regime.

The enhancement factors E_A for these three regimes, according to Astarita *et al.* (1983):

Slow reaction regime

$$E_A=1 \qquad 2.69$$

Fast reaction regime

$$EA= \sqrt{\varphi} \qquad 2.70$$

Instantaneous reaction regime

$$E_A = E_{A\infty} = \frac{(C_{A,i}-C_{a,b})_{eq.}}{(C_{A,i}-C_{a,b})} \qquad 2.71$$

Now the reaction regimes in terms of Hatta number are summarized as:

2.5.4 Slow Reaction Regime

Ha < 0.3 and $E_A=1$. The rate of reaction is faster than diffusional transfer of solute to liquid phase. This transfer of solute is rate controlling step. Mass transfer coefficient and absorption flux will depend on liquid flow rate *(Aronu et al., 2011).*

2.5.5 Fast Reaction Regime

Fast reaction regime follows; 3 < Ha ≪ EA. Diffusion and chemical reactions are proceeding parallel. The liquid phase retention time is not of considerable importance because all reaction takes place in reaction film. Absorption flux is independent of physical mass transfer coefficient so therefore independent of liquid flow rate.

2.5.6 Instantaneous Reaction Regime

$3 < E_{A\infty} \ll$ Ha and $E_A = E_{A\infty}$, applies for instantaneous reaction regime. The reaction is too fast in case of irreversible reaction, the reactants cannot co-exist in film. By reaction diffusion the absorption flux is limited.

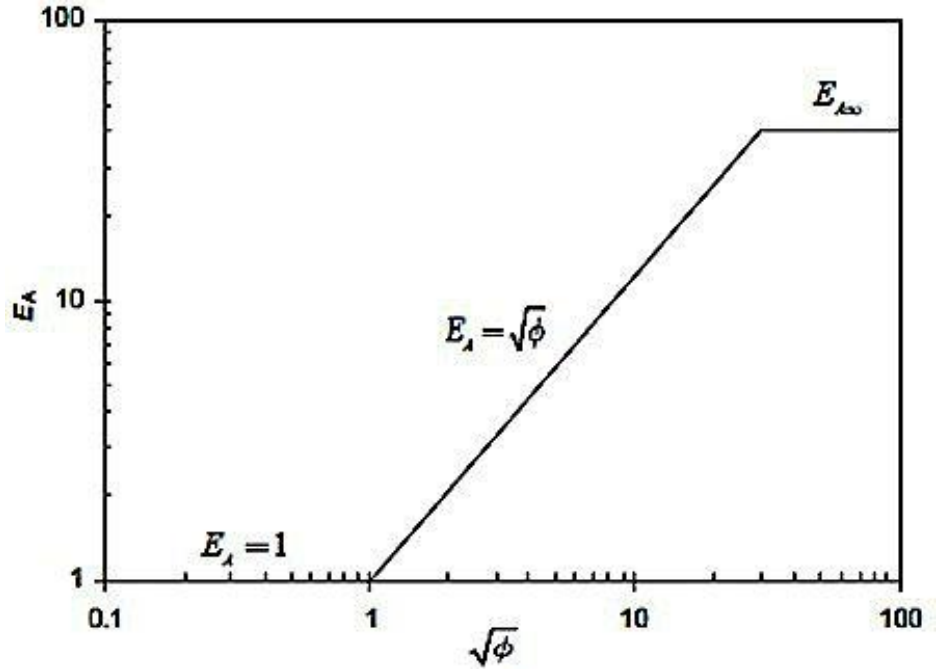

Fig 2.2: Asymptotic behavior for enhancement factor EA = $f(\varphi)$ (Ma'mun, 2005)

2.6 Gas Side Resistance

The soluble gas essentially diffuses through insoluble gas to reach interface in a gas blend of soluble and insoluble gasses. That's why the partial pressure of the soluble gas at the interface is less than that in the bulk gas. According to Danckwerts *(Danckwerts, 1970)*, the stagnant gas film of finite thickness across which the soluble gas is transferred by molecular diffusion alone while bulk gas has uniform composition is said to be gas film resistance. The mass balance of the soluble gas for both the liquid and gas film at steady state condition will then be as:

$$N_A = k_g(p_A - p_{A,i}) = E_A k_L^0(C_{A,i} - C_{A,b}) \qquad 2.72$$

In correspondence to Henry's law ($P_{A,i} = HC_{A,i}$) at the liquid interface to eliminate interfacial concentrations, and $E_A k_L^0 = k_L$, the absorption flux is given as under:

$$N_A = K_g(p_A - HC_{A,b}) = K_l\left(\frac{p_A}{H} - C_{A,b}\right) \qquad 2.73$$

While

$$\frac{1}{K_G} = \frac{1}{k_g} + \frac{H}{k_l} \qquad 2.74$$

$$\frac{1}{K_L} = \frac{1}{k_l} + \frac{1}{Hk_g} \qquad 2.75$$

Expression in equations (2.74 and 2.75) provides the overall resistance as the sum of the resistances in two films. The values of k_g and k_l vary from point to point in reality.

The average over all resistance and summation of two averaged resistances are not considerably different in practical cases, based on (*Mannford Doble 1996)* experimentations *(Aronu et al., 2011)*.

According to equation (2.73) there are two possible limiting behaviors in system explicitly as:

2.6.1 Liquid Phase Control

$$\text{If} \quad \frac{k_l}{Hk_g} \ll 1 \qquad \text{Then} \quad N_A = K_L\left(\frac{P_A}{H - C_{A,b}}\right) \qquad 2.76$$

In this scenario mass transfer in gas phase is easier than in liquid phase, it means that over all force of driving is exclusively consumed in liquid phase so that $P_{A,i}$ is almost equal to P_A.

2.6.2 Gas Phase Control

$$\text{If} \quad \frac{k_l}{Hk_g} \gg 1 \qquad \text{Then} \quad N_A = K_G\left(P_A - HC_{A,b}\right) \qquad 2.77$$

Mass transfer in liquid phase is much more favorable as compared to that of gas phase showing that driving force is mainly involved in gas phase *(Aronu et al., 2011).*

2.7 Liquid Film Mass Transfer Coefficient

Stephens and Morris *(Stephens et al., 1951)* proposed a correlation for strings of disc contactor in order to calculate liquid side mass transfer coefficient: *(Dindore, 2004).*

$$\frac{k_l}{D} = \alpha\left(\frac{4\Gamma}{\mu}\right)^n\left(\frac{\mu}{\rho D}\right)^{0.5} \qquad 2.78$$

While α = 17.92 and *n* = 1.0, μ and ρ are the viscosity and density of the liquid. Where D is the diffusivity of the solute in the liquid phase and Γ is wetting rate of the apparatus: *(Hartono et al., 2009)*

$$\Gamma = \frac{(liquid\ flow\ rate)\times(length\ of\ string)}{Surface\ area\ of\ string} \qquad 2.79$$

The Stephens–Morris correlation has been used by some writers to correlate the liquid–side mass transfer coefficient with operating and physical parameters for this system. There is no agreement on the values of α and *n* among the authors. The difference in these correlation of the parameter values is due to variations in factors such as disc–type, disc morphology etc *(Ma'mun, 2005)*.

It is important to have the gas film resistance as small as possible while measuring the liquid film mass transfer coefficient.

2.8 Gas Film Mass Transfer Coefficient

The gas film mass transfer coefficient for strings of disc contactor can be estimated by correlation provided by Stephens and Morris *(Stephens et al., 1951)* which is given as under.

$$\frac{k_G P}{v\rho_d} = 0.3281\Gamma^{0.13}\left(\frac{vd\rho}{\mu}\right)^{-0.33}\left(\frac{\mu}{\rho D}\right)^{-0.56}\left(\frac{P}{Pi}\right) \qquad 2.80$$

ρ_d is the density of the solute gas, "d" denotes the equivalent diameter for gas flow, "P" is the total pressure, "v" is the gas velocity and "P*i*" is the partial pressure of solute gas.

Dindore *(Dindore, 2004)* used SO_2 absorption into aqueous NaOH solution to determine the gas–side mass transfer coefficient for the disc contactor defined as: *(Ma'mun, 2005)*

$$Sh = 0.11Re^{0.73}Sc^{-0.56} \quad 2.81$$

2.9 Kinetic Rate Constant

The rate constant (apparent) in terms of zwitterion ion mechanism and termolecular mechanism are expressed as under.

2.9.1 Rate Constant for Zwitterion Mechanism

The apparent kinetic rate constant for the zwitterion mechanism can be elaborated by following expression:

$$k_{ap} = k_2 (AmH) \quad 2.82$$

$$k_{ap} = \frac{(AmH)}{\frac{1}{k_2} + \frac{1}{\{k_{AmH}(AmH) + k_{H_2O}(H_2O)\}}} \quad 2.83$$

While k_{AmH} , $k_{\boldsymbol{H_2O}}$ are kinetic parameters and for single zwitterion mechanism these parameters can be calculated by two methods:

- Non-linear regression:

This method will be used to determine the kinetic parameters if the assumption for water concentration to be constant is not valid, or not considered.

- Plotting method:

Another method to estimate kinetic parameters is graphical/plotting method. According to that if water concentration can be assumed constant for low amine concentrations, and graph is sketched between AmH and $\frac{k_{ap}}{(AmH)}$ then slope of that plot will give the value for k_{AmH} and the intercept of the plot will give the value of k_{H_2O}.

2.9.2 Rate Constant for Termolecular Mechanism

For the single-step termolecular mechanism, the apparent kinetic rate constant will then be:

$$k_{ap} = \{k_{AmH}(AmH) + k_{H_2O}(H_2O)\}(AmH) \quad 2.84$$

Similarly, in order to estimate kinetic parameters for termolecular mechanism the overhead nonlinear regression method and plotting method can be applied.

2.10 Activity Based Rate Constant

Kinetic constants are dependent on temperature, concentration and also types of the ions in the solution. They are not real constants. The kinetic expression based on activity can be stated as *(Pinsent et. al., 1956)*:

$$r = k_2^{\gamma} C_A C_B \gamma_A \gamma_B \quad 2.85$$

k_2^{γ} in above expression depends solely on temperature and should be independent of concentration. CO_2 distribution between liquid and vapor phase is modeled, based on Henry's law constant at infinite dilution.

$$\varphi_{CO_2}(T,P,y) y_{CO_2} P = \hat{\gamma}_{CO_2}(T,P,x) x_{CO_2} H^{\sim *}_{CO_2}(T) \exp\left\{\frac{\bar{V}_{CO_2}\left(P - P^{sat}_{H_2O}\right)}{RT}\right\} \quad 2.86$$

Apparent Henry's constant is used to estimate the concentration of species for calculation of kinetic rate constant. Apparent Henry's law constant is basically a ratio of partial pressure of gas above solution to concentration of gas in solution and can be expressed numerically as:

$$H_A^{App} = \frac{P_{A,i}}{C_{A,i}} \quad 2.87$$

Relating equations (2.86 and 2.87):

$$H_A^{App} x_A = x_A \gamma_A H_A^{\infty *} \quad 2.88$$

While the overall gas side mass transfer coefficient is:

$$N_A = E^{\gamma} k_L^o \left(a_{A,i} - a_{A,b}\right) \quad 2.89$$

$$K_{ov,G} = \frac{1}{\frac{1}{k_G} + \frac{H^{\sim *}_{co2}/C_{tot}}{E^{\gamma} k_L^o}} = \frac{1}{\frac{1}{k_G} + \frac{H^{\sim *}_{CO2}}{E^{\gamma} k_L^o}} \quad 2.90$$

Reaction rate for irreversible first order reaction is accounted by film theory, depicted by under texted eq:

$$r = a_A k_1^{\gamma} = k_1^{\gamma} \gamma_A C_A \qquad 2.91$$

While Hatta number is scripted as:

$$Ha^{\gamma} = \frac{\sqrt{k_1^{\gamma} \gamma_A D_A}}{k_L^o} \qquad 2.92$$

The activity based kinetic rate constant for first can be determined by equation (2.93).

$$k_1^{\gamma} = \frac{H_A^{\infty 2} \gamma_A}{\left(\frac{1}{K_{ov,G}} - \frac{1}{k_g}\right)^2 D_A} \qquad 2.93$$

While the second order rate constant by equation (2.94):

$$k_2^{\gamma} = \frac{k_1^{\gamma}}{C_B \gamma_B} \qquad 2.94$$

Chapter 3

Materials and Experimental Setup

A diamine and a tertiary alkanolamine are picked up for kinetics examination of CO_2 absorption as solvents.

MAPA (≥ 99%) with CAS no. 6291-84-5 was obtained from Sigma Aldrich. It is important to be acquainted with some of his general properties.

- Clear and color less liquid
- Freezing point = -72 ^{0}C
- Boiling point = 140 ^{0}C
- Completely soluble in water
- pH = 11.5 at 20 ^{0}C
- Structure:

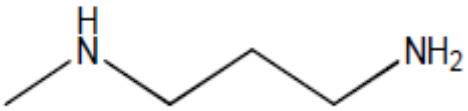

Similarly DEEA (≥ 99%) with CAS no.100-37-8 was also obtained from Sigma Aldrich.

- Clear liquid with pale yellowish color
- Freezing point = -70 ^{0}C
- Boiling point = 163 ^{0}C
- Completely soluble in water
- Structure:

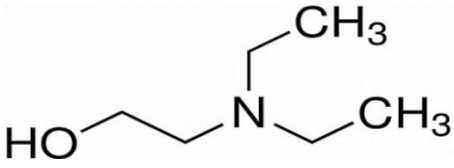

The CO_2 (purity > 99.999 mol % from AGA Gas GmbH) and Nitrogen N_2 (purity > 99.999 mol% from YARA PRAXAIR) were used for calibration, loading and flushing. While N_2O was used in solubility experiments also obtained from YARA PRAXAIR.

3.1 Chemicals for CO_2 and Amine Analyses

All of standard solutions were prepared from underneath stated chemicals and de-ionized water.

3.1.1 Standard Solutions

- 0.1N NaOH (ampoule for 1000 mL supplied Merck KGaA)
- 0.1N HCl (ampoule for 1000 mL supplied Merck KgaA)
- 0.2N H_2SO_4 (2, 0.1 ampoules for 1000 mL supplied by Merck KgaA)
- 0.1N $BaCl_2$ (244 g $BaCl_2.2H_2O$/2L with purity > 99% supplied by SIGMA-ALDRICH)

3.1.2 Filters

- 0.45µmHAWP supplied by MILLIPOR

Analysis technique will be described later on.

3.2 Experimental Setup

Kinetic measurements of CO_2 absorption were performed on a string of discs contactor. In the line of these experiments, solubilities, densities and viscosities were also measured.

3.2.1 String of Discs Contactor Apparatus (SDC)

The rate of CO_2 absorption in an aqueous amine solutions were evaluated by means of string of discs contactor. String of discs contactor comprises an arrangement of 43 discs that are at right angel to each other having a diameter of 1.5 cm and thickness of 0.4 cm. The characteristic active length of the column is 64.5 cm while the active mass transfer area for this arrangement is 226.15 cm^2 *(Ma'mun, 2005)*.

The SDC is equipped with Fisher–Rosemount BINOS® two CO_2 channels; 2000 ppm and 1vol% CO2; a BRONKHORST HI–TEC mass flow controller, a peristaltic liquid pump (EH PROMASS 83), five K–type thermocouples and a gas blower are also a part of this setup. Figure 3.1 sketched the whole apparatus.

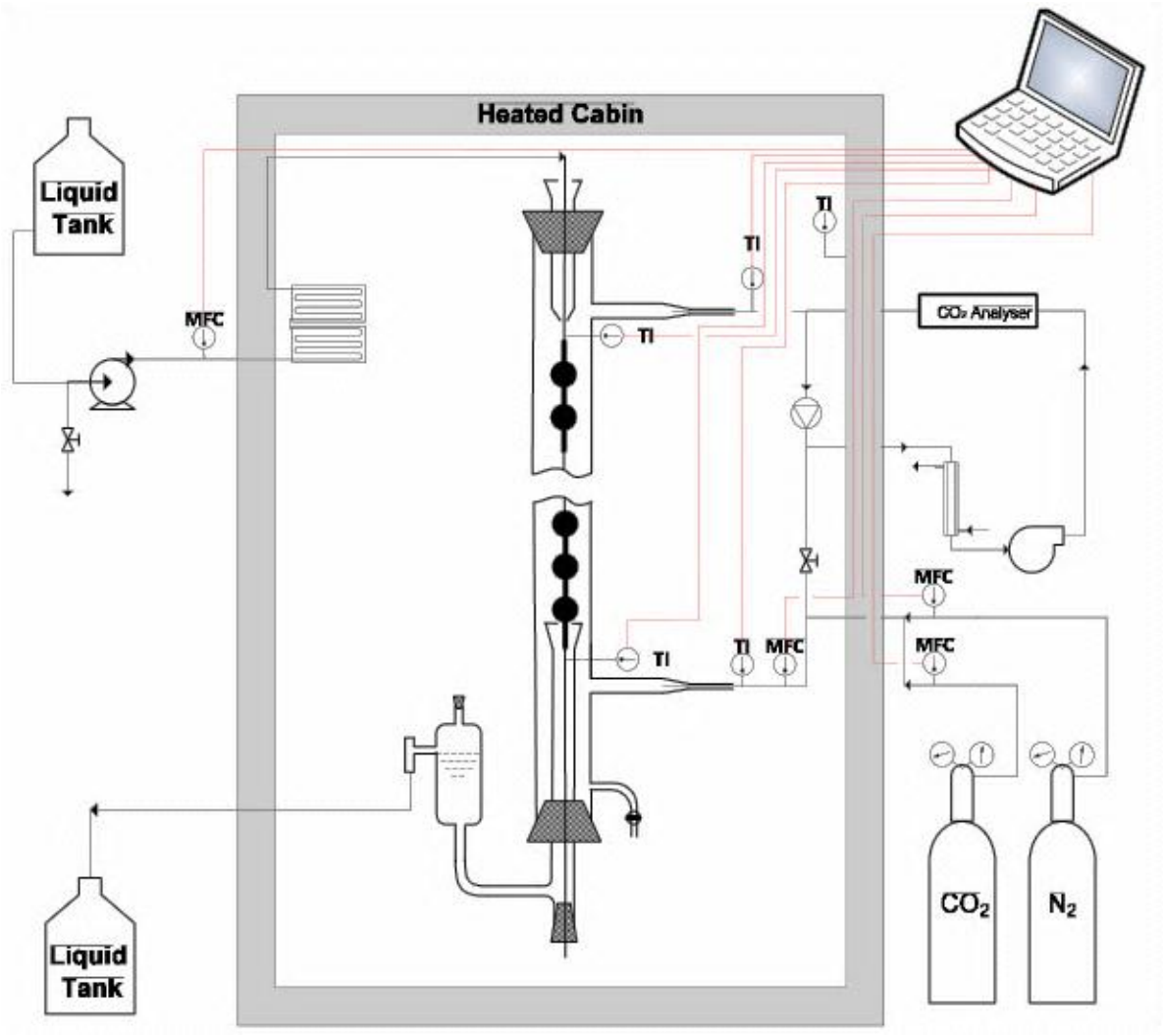

Fig 3.1: Kinetic apparatus "String of discs contactor" (Hartono et al., 2009)

SDC is operated in counter-current mode with liquid flow from top to bottom on discs and gas flows vice versa. Thermocouples are mounted at the inlet and outlet of liquid, inlet and outlet of gas and inside the cabinet. The liquid and gas flows can be independently adjusted by a liquid pump and gas blower respectively.

The flow of the blower is controlled by a Siemens Micro Master Frequency Transmitter and has a maximum flow rate of 1.75 Nm^3/hr. The active mass transfer area is calculated by the following expression *(Hartono, 2009).*

$$A_{active}(m^2) = \left\{2.\pi\left(\frac{d}{2}\right)^2 + \pi dw - 2w^2\right\}.n_d \qquad 3.1$$

3.2.1.1 Calibration Process

- CO_2 and N_2 injection valves were opened
- Turned on fan and fan regulators and adjusted to desired level
- Mass flow controllers (MFC) were on calibration mode
- Flow of condensate water valve regulated to open position
- Experimental valve adjusted to closed position for calibration
- Log file in system was created on labview program for data acquisition and sample readings

After performing the essential startup tasks for calibration, it's time to start with the process of calibration. Firstly leakage test was done in order to check any malfunctions in system by altering the valve of N_2 MFC to low flow range. Bubbles were popped up in gas outlet cylinder indicating that system was leakages free. On the other hand if gas bubbles weren't trickled out then system had some leakage that should be looked in to for further proceeding.

Afterwards, calibration was initiated for 0 to 1 vol% CO_2 channel by maintaining the zero opening of CO_2 MFC and 100% for N_2 MFC opening in order to get the first calibration point. Variant openings of CO_2 MFC using channel 3 (starting from 70% to 0% opening) were used while the opening for N_2 MFC remained same for all readings. 10-20 minutes were allotted for each opening and waited for the point to get stable. These points were recorded in the sheets that are attached to appendix in kinetic calculations.

3.2.1.2 Experimental Layout

When the calibrations were done, the calibration valve was also closed and experimental valve was opened. Solution was prepared in the beginning of the experiment .The 5 liter flask at liquid inlet was filled with the desired solution, heating element was turned on and adjusted to required temperature. Five K-type thermocouples were used to register the 4 inlet and outlet gas/liquid temperatures and the temperature inside the chamber *(Ma'mun, 2005).* Before starting every

experiment it was desired to clean the disc of SDC by pumping it firstly with hot water then with DI water. Direct drained valve was used to remove any air trap inside lines, in order to avoid pump failure, so some of the solution was evacuated first from that valve. Now the solution from 5 liter filled flask was allowed to enter in to SDC. The initial amount of solution that entered in SDC was removed in an empty beaker after passing through it to make sure that there were no contaminations on disc remaining. The liquid flow rate was adjusted to 50mL/min. The flow of liquid was controlled by peristaltic liquid pump. The flow rate of gas which is flowing in counter current direction was also adjusted to desired level. Opening of N_2 MFC was defined to 6% (low value) and this value will remain unchanged throughout all the experiments. This value was stated because by increasing the amount of N_2 more than that of 6%, wouldn't have immense effect on flux. Then hit and trial method was used to adjust the amount of CO_2 to 2 kPa on analyzer (Fisher-Rosemount BINOS 100 NDIR CO_2 analyzer) by opening CO_2 MFC. Most of the experiments were performed to this partial pressure with desired temperature levels. It was waited for liquid and gas temperatures to get stable at the desired set point. After point stabilization reading was documented and temperature was changed. During temperature stabilization the flow of liquid and gas was kept close. Liquid and gas flows were re-started after the stabilizing of temperature. Experiments were executed from 298.15 K-338.15 K. When 5 liter of solution was finished in the first run, then the solution from the outlet flask was returned to the inlet flask.

The string of discs contactor involved in this kinetic study has been characterized by *(Dindore 2004)* in order to evaluate hydrodynamics of liquid and gas flow.

The CO_2 flux can be calculated by implementing solute balance over whole system. The difference between CO_2 flow rate in the system and CO_2 out of the system gives the absorption flux of CO_2 *(Hartono, 2009, Ma'mun, 2005, and Aronu, 2011).*

$$r_{CO_2}^{abs}\left(\frac{kmol}{s}\right) = Q_{CO_2}^{in} - Q_{CO_2}^{out} \qquad 3.2$$

Where $r_{CO_2}^{abs}$ indicates molar absorption rate.

The amount of CO_2 which is going out of the system as indicated on analyzer can be determined from:

$$Q_{CO_2}^{out} = Q_{N_2}^{in}\frac{y_{CO_2}^{out}}{1-\left(\frac{p_{solution}}{P}\right)-y_{CO_2}^{out}} \qquad 3.3$$

When the experimentation was completed, the clean-up and shut down procedure was executed.

All of the solution was drained out from system. Hot water and DI water was injected from inlet again to rinse it and to remove any traces of amine solution remaining in it. Liquid pump speed reduced to zero from labview program, and system was shutdown afterwards. It was made sure that all the gas bottles, valves and cooling water line were closed.

3.2.2 Solubility Assessment

A stirred jacketed glass vessel as sketched in figure* 3.2 was used for N_2O solubility measurements. Glass vessel had a calibrated volume of $1.07*10^{-3}$ m^3. On the other hand there was a stainless steel gas holding vessel with a calibrated volume of $1.04*10^{-3}$ m^3. A vacuum pump, condenser, cooling medium and external heating attachment was also a part of system. In a startup procedure valves of gas bottles were turned on and absorption flask was ensured to be dry and free of impurities by injecting N_2. The absorption flask/glass vessel contained the N_2O, Liquid and vacuum inlet lines. After flushing with N_2 the flask was sealed and vacuum was generated in flask by using vacuum pump and pressure was reduced to maximum achievable limit. During vacuum the liquid inlet line remained open to generate vacuum in it as well to suck solution in to flask after wards. Labview program for solubility measurement was clicked from system. Then it's time to prepare amine solution. Solution was weighed and injected up to marked level in the absorption vessel. The remaining solution was reweighted and difference was calculated that will give the exact amount of amine solution inside the absorption vessel.

After injection, liquid inlet line was closed and vessel was degassed again in order to remove any trapped gas bubbles inside liquid and in vessel down to 20 mbar and at ambient temperature. Before degassing the vessel cooling medium was turned on and temperature of the vessel top reduces to 277.15 K in order to condense any amine vapors if present, so that they may not lost and changed the concentration of amine during degassing of the vessel.

When these two steps were finished stirrer was switched on to ensure homogeneous mixing and to attain the equilibrium and it was adjusted to 1000 RPM. The temperature of stirred glass vessel was managed by a heating medium (LAUDA E300) glycol bath.

* Apparatus for current work is somehow similar to Ma'mun, 2005

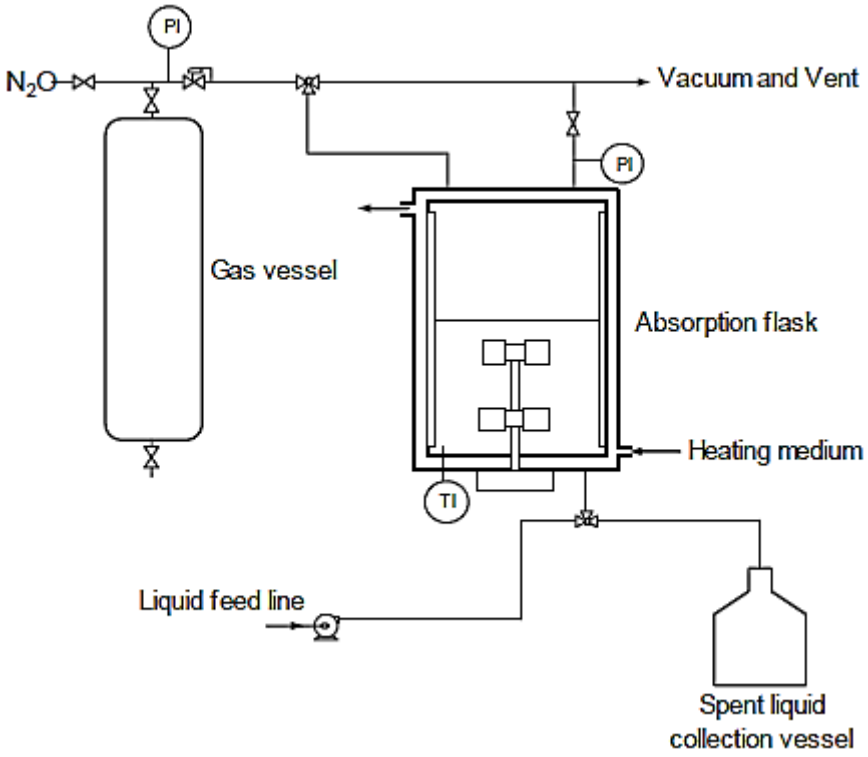

Fig 3.2: N_2O solubility experimental arrangement (Ma'mun, 2005)

Temperature in solubility measurements ranged from 298.15 K to 338.15 K when temperature of gas and temperature of liquid stabilized for one certain temperature the point was noted and temperature was altered for next reading. When 338 K was achieved and all points were recorded, then it's time to inject N_2O in vessel by opening the N_2O inlet line. The commercial N_2O gas was supplied by AGA Gas GmbH with a purity of 99.999%. After the injection temperature and pressure of absorption vessel and steel vessel were measured and catalogued. The amount of N_2O injected in absorption flask was calculated from the difference in pressure of the gas vessel before and after injecting N_2O. Temperature was decreased from 338.15 K to 298.15 K in the same fashion as it was increased and points were recorded similarly for every temperature change.

Temperature was measured by two K type thermocouples and pressure was measured by two pressure transducers (Druck PTX 610 and PCE28). Transducer attached to absorption flask will go up to 8 bar while the transducer in steel vessel measured up to 6 bar.

The amount of N_2O that was added can be calculated as *(Hartono, 2009)*:

$$n_{N_2O}^{added} = \frac{V_V}{RT_V}\left[\frac{P_{v1}}{z_1} - \frac{P_{v2}}{z_2}\right] \quad 3.4$$

Where P_v, T_v, are pressure and temperature while z_1, z_2 are compressibility factor of gas at initial and final conditions and R is universal gas constant respectively. Peng Robinson equation of state was used to calculate compressibility factor.

The amount of N_2O in gas phase of the absorption vessel can be estimated by the following equation:

$$n_{N_2O}^{gas} = \frac{P_{N_2O}(V_R - V_S)}{zRT_R} \quad 3.5$$

While Vs is volume of solvent and can be measured from solvent density and V_R expressed volume of reactor. P_{N_2O} is the partial pressure of N_2O and quoted as:

$$P_{N_2O} = P_R - P_S^o \quad 3.6$$

P_R is the total pressure of absorption glassed vessel and P_S^o indicates the solvent vapor pressure.

The amount of N_2O in the liquid phase can be assessed by:

$$n_{N_2O}^{liq} = \left(n_{N_2O}^{added}\right) - \left(n_{N_2O}^{gas}\right) \quad 3.7$$

The solubility of N_2O can be calculated by Henry's law constant relation:

$$P_{N_2O} = H_{N_2O} C_{N_2O} \quad 3.8$$

Where C_{N_2O} indicates concentration of N_2O, will be calculated by following equation:

$$C_{N_2O} = \frac{\left(n_{N2O}^{liq}\right)}{V_S} \quad 3.9$$

3.2.3 Density Measurement

The (Anton Paar DMA 4500M) density meter was used to analyze densities of amine samples as shown in figure 3.3. Density of all solutions of MAPA and blends of DEEA+MAPA were measured.

First of all test vials were cleaned and it was made sure that there was no contamination in vials. These test vials will then be filled with amine solution up to 9.5 ml measured volume and sealed with caps. DI water filled vials were put at the start and end of amine samples in order to check accuracy and percentage error in measurements.

Program was called from density meter and was operated from lavish touch screen. Sample data was fed in according to the positions in rotating disc in which vials were adjusted. Before running the experiment the DI water and ethanol bottles used for cleaning and drying of sensor were checked. Temperature was set to the desired value and started the measurement. Densities were measured from 293 K to 353.15 K for each individual sample. Densities of water were also measured at these temperatures in order to check the system accuracy. Data was saved automatically in system memory that was extracted afterwards.

Fig 3.3: "Anton Paar DMA 4500M" density meter (Representative Anton Paar 2013)

3.2.4 Viscosity Determination

The (Physica MCR 100) rheometer was used for the viscosity assessments. This apparatus is operated by US 200 Software which is windows based. Amine samples of MAPA and blends of DEEA+MAPA were analyzed. Software window was opened and correctly chose the measuring system (DG 26.7) and measuring cell (TEK 150P-C). The EC motor shaft position was adjusted to lift up position as sketched in figure 3.4 as well and desired temperature was adjusted. Temperature was controlled by fluid circulation.

Then white protection cylinder was removed from apparatus to couple the cylindrical measuring system but it was very important to make sure that coupling should be aligned as indicated by mark on shaft. In MCR rheometers the one hand quick coupling system, solvent trap and evaporation blocker enhanced its measuring capacity.

Fig 3.4: "MCR 300 Physica" rheometer (APTL)

When coupling was done then bottom (concentric) cylinder was fitted to rheometer base and filled with 4ml of solution. After wards the measuring position tab was clicked from software and EC motor shaft rotated downwards to base. Furthermore was time to wait for the temperature to be stabilized. Then reset the NF to zero and started the measurement.

For one temperature the apparatus took 5-8 minutes depending upon the number of points selected. 20 data points were selected in these experiments for most of the cases to observe the shear stress and shear rate. Newton1 method was used to calculate the viscosity of aqueous solutions, while taking an assumption that amines behave as Newtonian fluids. The data points showing linear trends were included by selecting those desired points and that value was recorded as viscosity of the given solution. Same procedure was followed for rest of the temperatures and concentrations. Viscosity measurements were done for temperature range of 293.15 K to 333.15 K while the sample solution was changed after every two temperature analysis.

3.3 Process of Analyzing

3.3.1 CO_2 Analyses of Samples

In order to calculate the amount of CO_2 in samples, precipitation titration method was used.

Following steps were adopted:

- Liquid sample from closely tight sample bottle which was to be analyzed obtained and added to flask. The amount of the liquid sample added, dependent on the total CO_2 content in the sample.
- 50 cm^3 sodium hydroxide (0.1 N NaOH) and 25 cm^3 barium chloride (0.1 N $BaCl_2$) freshly prepared solution was taken in 250 cm^3 Erlenmeyer flask and measured.
- Tare the weight balance and measured amount of liquid sample is added in Erlenmeyer flask.
- The Erlenmeyer flask was heated for four minutes on heated plate until it boiled in order to enhance the barium carbonate ($BaCO_3$) formation, and then cooled to ambient temperature.
- The mixture was filtered with a 0.45 µm Millipore paper and rinsed with de-ionized water in order to check any leakage in filtration flask.
- The filter covered by $BaCO_3$ cake was transferred to a 250 cm^3 beaker. De-ionized water (100 cm^3) was added into the beaker, and enough hydrochloric acid (0.1N HCl) was added to dissolve the cake of $BaCO_3$.
- The amount of hydrochloric acid (0.1N NaOH) added was measured.
- The solution with 0.1 N NaOH with an end-point of pH 5.25 was titrated in an automatic titrator (Metrohm 809 Titrando).
- After the titration the following equation was used to calculate the amount of CO_2 in the liquid phase.

$$Amount\ of CO_2\left(\frac{mol}{kg}\right) = \frac{[(Hcl_g - NaOH_{ml}) - (Hcl_{g(blank)} - NaoH_{ml\,(blank)})]}{10 * 2 * wt.of\ Sample_g} \quad 3.10$$

$$CO_2\left(\frac{mol}{litre}\right) = CO_2\left(\frac{mol}{kg}\right) * \rho_{sol}\left(\frac{kg}{liter}\right) \quad 3.11$$

3.3.2 Amine Analysis of Samples

There was a possibility of solvent loss during operation, so the amine concentrations were determined by titration afterwards.

Following steps were adopted:

- A liquid sample of 0.5 cm^3 was diluted in 50 cm^3 de-ionized water in plastic beaker and titrated with 0.2 N sulphuric acid (H_2SO_4) using the metrohm 702 SM Titrino.
- High concentration samples were analyzed by using 0.2N H_2SO_4 as titrant and low concentration samples were analyzed by using $0.02NH_2SO_4$.
- LabX software program was used for determination of the amine concentrations by titration. Weighed quantities of the samples were placed in rotating disc and program was started.
- Before starting the program the diaode was cleaned with DI water and adjusted in sampling place.
- The end point was obtained at pH 2.5. The Amine concentrations were found in mol/kg and these concentrations were used to get loading (mol CO_2/ mol amine).

3.4 Accuracy / Uncertainty

There is no such thing as a perfect measurement. Experimentations and measurements can never be exact; there will be some errors due to one of the following reasons.

- Systematic uncertainties
- Difficulty of temperature control
- Limitations of theoretical Laws
- Random uncertainties
- Time lag of instrumentation and Control system
- Human Errors
- Numerical Errors
- Limited precision

- Comparison uncertainties
- Response time of IR analyzer
- Impurity of Materials used

Measurements have always errors and uncertainties, no matter how hard someone might try to minimize them.

System accuracy is basically an accreditation in measured value and the correct value. To avoid air and O_2 pressures in SDC and in solubility equipment, N_2 was flushed through equipments prior to experimentations.

Standard equipments like pressure transducers, thermocouples, balances, weighing, analyzer, Pumps, blowers, fans were used in order to minimize the uncertainties in readings. A standard was maintained from preparation of solution till CO_2 and amine analysis in order to generate precise data. State of the art controllers were used during whole process. Well accepted and best fitted equations for kinetic measurements were a part of this work.

Appropriate care was taken during rinsing of the equipments with hot water then de-ionized water. Atmospheric pressure from lab mounted barometer was taken after every reading and compared with the equipment generated atmospheric pressure for counter check. For calculation in excel sheets data fixed at four places after decimal point and taking every possible precaution in every step of experimental and computational work. In spite of all above protections and precautions the equipment uncertainties; human error; material impurities; ground conditions and limitations of governing theoretical laws and computational models cannot be totally disregarded.

Chapter 4

Results & Discussions

Physiochemical properties and kinetics were performed for MAPA and blends of MAPA+DEEA.

4.1 Density Evaluations:

(Aqueous MAPA System)

Experimental densities were performed for the aqueous solution of 1/2/3/4/5M MAPA system at variant temperatures, ranging from 293.15K - 353.15K. All the data points achieved are tabulated in appendix A1. While the densities are sketched against temperatures as shown in figure 4.1.

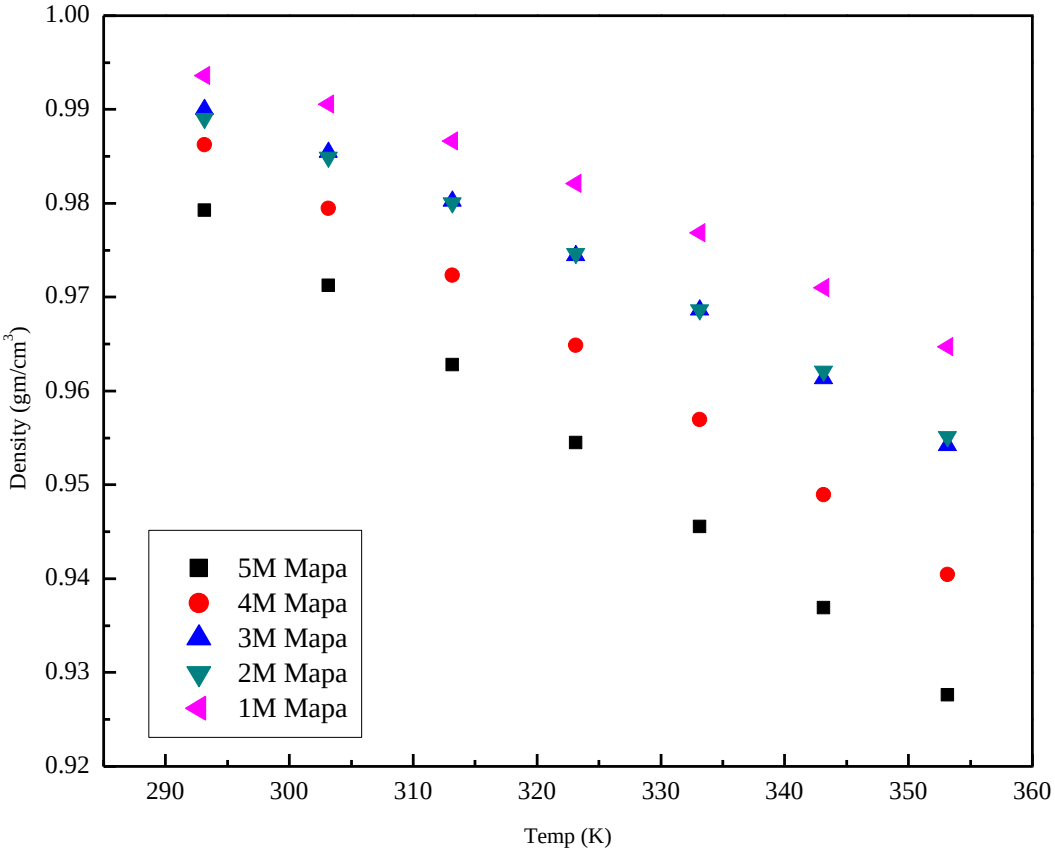

Fig 4.1: Experimental densities of "MAPA" system at different temperatures

The parallel measurements were compassed for each sample in order to ensure the reproducibility of the data. The uncertainty in the parallel measurements was approximately less than $\pm 0.01\%$ (see tables in appendix A1) hence showing system accuracy.

Densities of deionized water were also measured by placing test vials at the start and end of actual samples in order to assure the working efficiency of current equipment (Appendix A4).

From plotted data it is observed that with the increase in concentration of aqueous amine solutions, density decreases accordingly. It is spotted that highest density achieved is (d= 0.99359 gm/cm^3) at 293.15 K. At low temperatures the density difference in between all concentrations is small. While with the increase in temperature the difference in densities is quite large, as density is a relation of mass to volume so with the increase in temperature volume increases hence density decreases. The experimental results revealed that the density difference for 2M and 3M MAPA system are not very much, therefore curves for both systems pursued the same trend. Points at each concentration followed likely the same polynomial behavior as it was observed for the other amine systems.

The equation (4.1) is used in order to model the density calculation of aqueous MAPA system at all temperature and concentration while the modeled graph is also attached to appendix C1.

$$\rho\left(\frac{gm}{cm^3}\right) = K_1 - \frac{K_2.X}{T} + \frac{K_3.X}{T^2}.exp\left(\frac{K_4}{T} - \frac{K_5}{T^2}\right) \qquad 4.1$$

While ρ indicates density, T for temperature in K, X is the mass fraction and K_1, K_2, K_3, K_4, K_5 are the parameters and are tabulated in appendix A2. The value of AARD is 0.2%.

(Aqueous Blended System)

Blended (MAPA+DEEA) systems were also evaluated for density measurements. Same experimental procedure was adopted as before and two parallel density measurements were also performed for this system. Tabulated densities of blends are a part of appendix A3 and also graphed against variant temperature as depicted in figure 4.2. Denotations are made in order to simplify plot area, M indicates MAPA while D indicates DEEA and integers indicates molar concentrations.

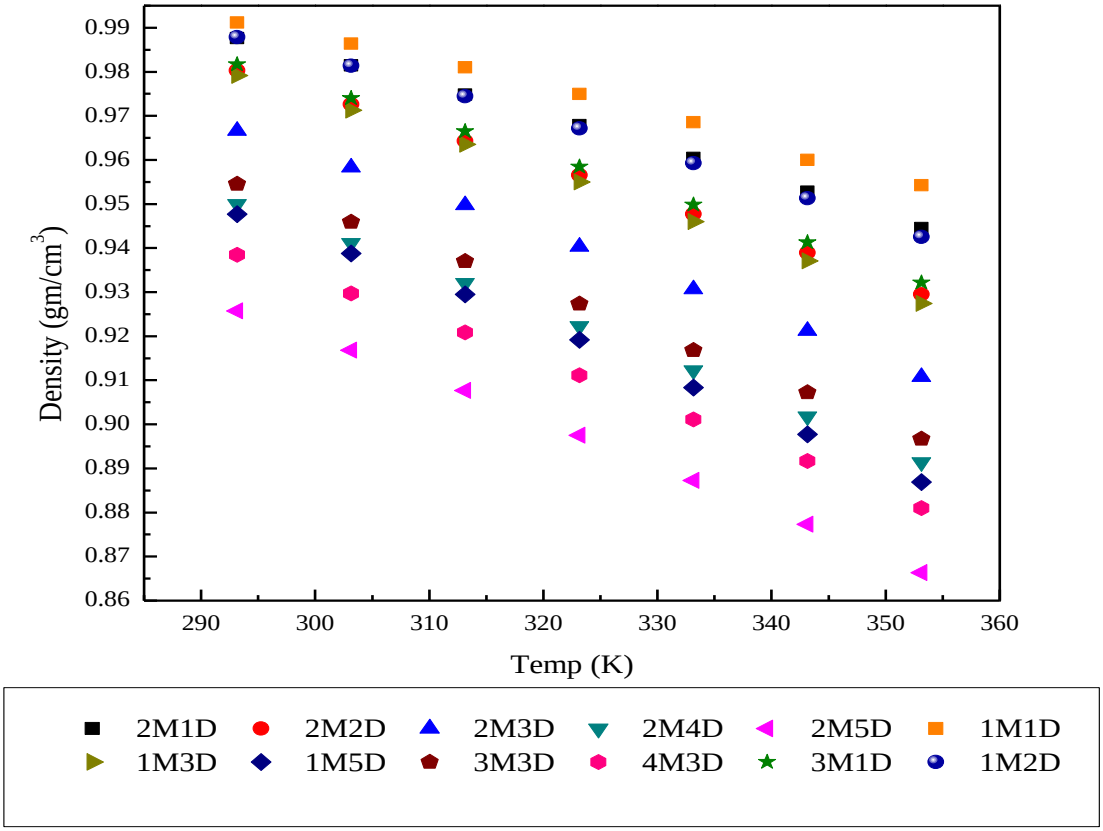

Fig 4.2: Experimental densities of Blended "MAPA+DEEA" system at different temperatures

The main focus is on two different sets of blended systems that are examined for densities, one in which 1M concentration of MAPA is constant but concentration of DEEA varies. Second is in which 2M concentration of MAPA is constant and concentration of DEEA varies again. Blended systems have the same trend as for single solvent that with the increase in temperature the density of blended system decreases and vice versa. While higher densities are examined at lower concentrations and lower temperatures and phenomenal differences in densities are observed at higher concentration and lower temperatures. As physical properties like density and viscosity are related to overall total molar concentration rather than that of individual amine constituents. So density measurements of some of the blended systems extensively overlap each other, although the number of moles of MAPA and DEEA are not the same in both the cases as declared by the plot of 1M2D and 2M1D.

Similarly 1M3D, 3M1D and 2M2D blended systems show approximately the same values and density differences at all temperatures in these systems are not much eminent. Overall the graphical representation of the data points showed the polynomial behavior as observed in single amine system.

Considering two sets of density measurement it is also concluded that with the increase in concentration of DEEA with constant concentration of MAPA the density of blended system decreases.

4.1.1 Density Comparison (Current Work & Literature)

The experimental measurements of current work should be analyzed and verified by comparing it with the literature data. This section will cover the comparison of densities of single and blended amine systems with literature. It is worth mentioning here that current work and literature may not behave as it is. Current work and literature have different performances and characteristics and experimented under different conditions.

(Aqueous MAPA System)

Density measurements were reviewed in literature in order to find out the same solvent to compare it with current work but unfortunately no as such density measurements are available on single MAPA system. MAPA being a diamine contains one primary and one secondary group. Extensive literature is available on primary and secondary amines so current work can be compared either with primary, secondary amines or with diamine to have a complete over view of density evaluations.

Fig 4.3 contains the density measurements of current work, the MAPA system and MEA (Monoethanolamine) system by *"Erwin D. Snijder et al., 1993"*. Both the data points are in agreement with each other. The data points of current work and *"Erwin D. Snijder et al., 1993"* followed the same polynomial trend. The values of the densities of current work are slightly lower than *"Erwin D. Snijder et al., 1993"*.

The current work is also compared with a diamine, the HDMA (1,6-hexamethyldiamine) system by *"Prachi Singh et al., 2011"*. Fig 4.3 showed that current work and *"Prachi Singh et al., 2011"* both are in agreement with each other. Both the systems have the same trend and at lower concentration i.e. 1M of *"Prachi Singh et al., 2011"*exhibts the same character as of 2and 3M concentrations of current work. Similarly density measurements of 2.5M *"Prachi Singh et al., 2011"* followed the 5M concentration of current work.

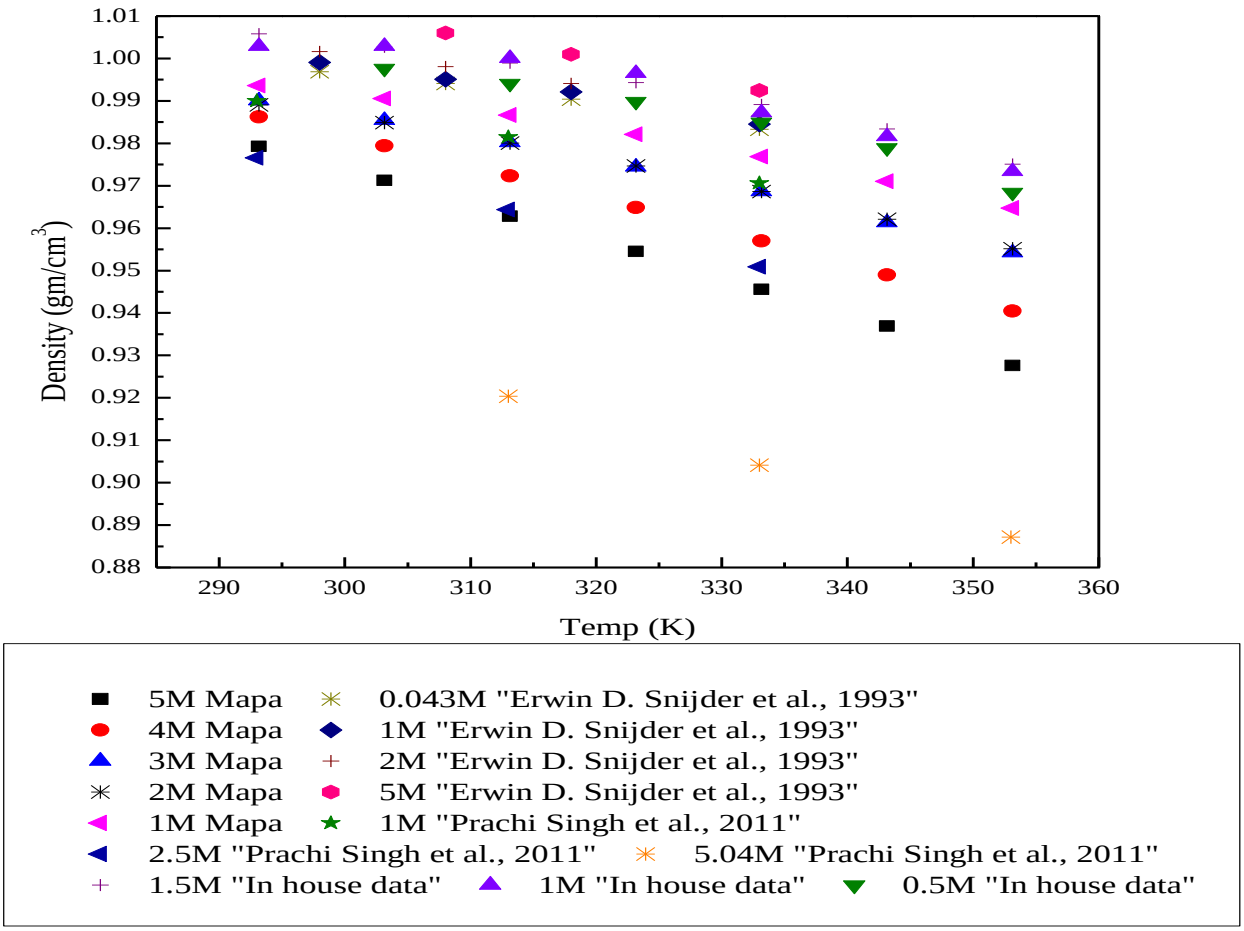

Fig 4.3: Comparison of current work MAPA system with MEA system by "Erwin D. snijder et al., 1993", HDMA system by "Prachi Singh et al., 20011", Pz system by "In house data"

Similarly the current work is compared with Pz (piperazine) system of *"In house data"*. The current work is in agreement with *"In house data"* at lower concentrations in terms of trend but densities of *"In house data"* are higher than current work. As literature data is not available at higher concentrations it is believed that at higher concentrations literature work will follow the same polynomial behavior as of current work. (Some simplification is required to elaborate *"In house data"*, it is the data available with in research group still not published but done by another master's student).

(Aqueous Blended System)

It is declared that there is no as such literature available on the density measurements of MAPA+DEEA blended system. There are literatures available on some other primary and tertiary blends like MEA+TEA (Monoethanol amine + Triethanol amine) system by "*Shyh-Yun Horng et al., 2002*", MEA+MDEA (Monoethnaol amine + *N*-Methyldiethanolamine) system by *"Daniel P. et al., 1994"*. There is another citied data on density measurements of blends like MDEA+ PZ (*N*-Methyldiethanolamine + Piperazine) system by "*Arunkumar Samantaa et al., 2011*". Density measurements of current work MAPA+DEEA blended systems are not appropriate to compare with these published data's because the concentrations of citied data are very much lower as compared to that of current system and blended concentration of amines are different, although graphs were plotted to estimate the behavior of current work with literature and all these systems followed the same trend line.

4.2 Viscosity Evaluation

(Aqueous MAPA System)

Experimental viscosities were also carried out for aqueous MAPA system. The data points of 1/2/3/4/5M MAPA systems are attached to appendix A5 and graphical illustration is presented by graph 4.4.

Sketched area indicates that with the increase in temperature the viscosities of the amine solution decrease accordingly. It is observed that difference in the viscosities of amine solution at higher temperature is limited, even at 333.15 K viscosities of 2/3/4/5 M MAPA systems have almost the same numerical values. This effect is due to rise in the kinetic energy of molecules with increase in the temperature and hence the relative motion of the molecules which decrease the resistance to flow. While at lower temperature the difference in term of viscosities increases rapidly.

The 2M and 3M MAPA system has exactly the same behavior as it was observed in density measurements that data points of both systems followed the same path.

On the other hand side data points of 1/2/3 M MAPA systems have likely the same trends and points are somehow conjugated to each other, while drastic change in viscosities are detected for 4&5 M MAPA system at lower temperatures.

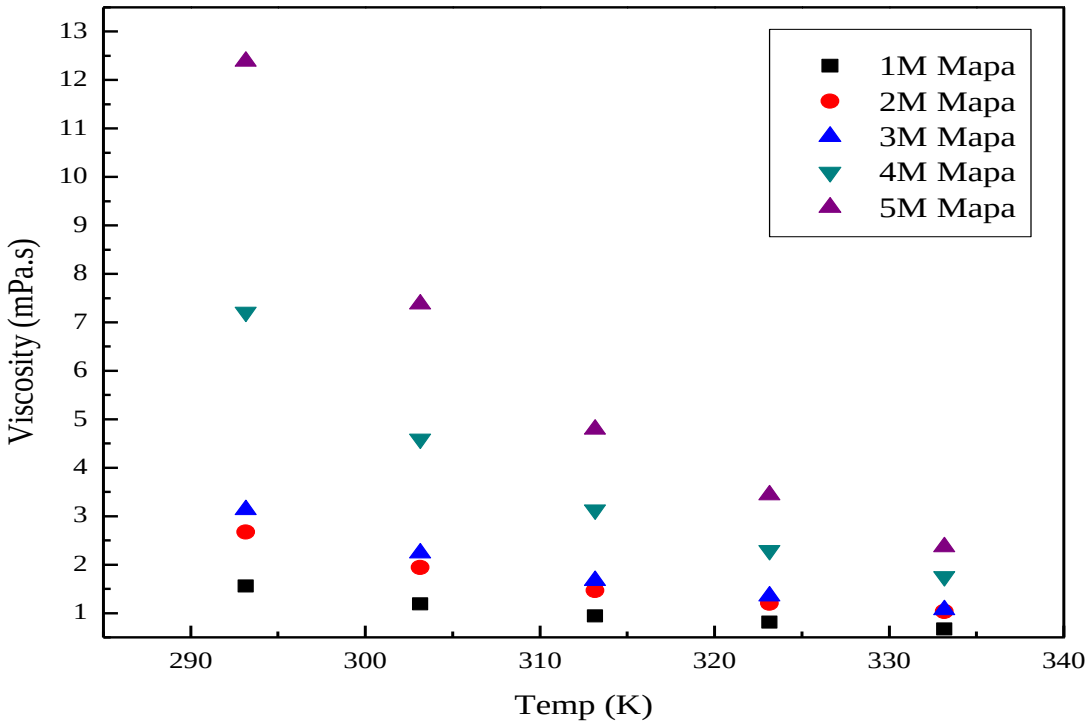

Fig 4.4: Experimental viscosities of "MAPA" system at different temperatures

Similarly if the focused area is concentration of the amine system, then with the increase in concentration at one specific temperature the viscosity increases.

Equation (4.2) is used in order to model the viscosity calculations of aqueous MAPA system as follows:

$$\mu(mPa.s) = K_1 - \frac{K_2.X^2}{T} + \frac{K_3.X}{T^3}.exp\left(\frac{K_4}{T} + \frac{K_5.X^2}{T^2}\right) \qquad 4.2$$

While μ indicates viscosity, T for temperature in K, X is the mass fraction and K_1, K_2, K_3, K_4, K_5 are the parameters and are tabulated in appendix A6 along with the graphical representation of data in appendix C2 with an AARD value of 4.9%.

(Aqueous Blended System)

Aqueous blended systems were also passed through the same experimental procedure in order to determine viscosity. Tabulated values are attached to appendix A7 while graph is plotted here in figure 4.5 to discuss.

Blended systems present the same trend as for single system that with the increase in temperature the viscosity of the system decreases. At higher temperature (e.g. 333.15 K) the viscosities of blended systems are align (vertical stream line) to each other means viscosity difference is small, but with the decrease in temperature the alteration in viscosity values increases accordingly. The viscosities of 2M4D/1M5D/3M3D/4M3D/2M5D followed exactly the same exponential behavior with temperature it might be because of likely same total molar concentrations. Similarly 1M3D/3M1D/2M2D have also the same conjugated exponential path with a slight change in numerical values.

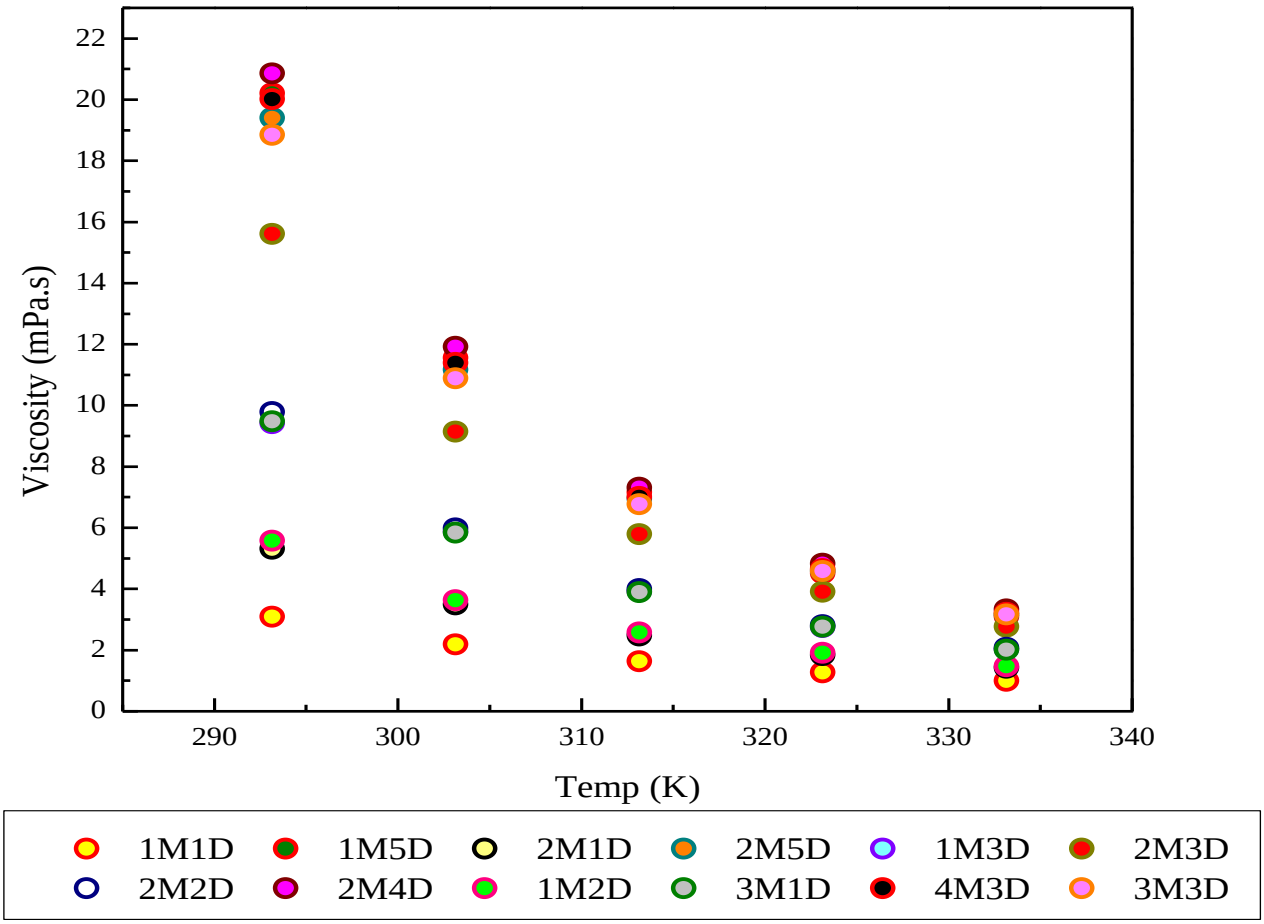

Fig 4.5: Experimental viscosities of Blended "MAPA+DEEA" system at different temperatures

Considering again the two sets of viscosities with constant 1&2M MAPA with varying concentrations of DEEA, viscosity increases exponentially with the increase in DEEA concentrations.

Furthermore, by changing / increasing the concentration of blended system at one specific temperature, immense changes in viscosities are observed specially at low temperatures.

4.2.1 Viscosity Comparison (Current Work & Literature)

The experimental measurements of viscosities of single and blended systems are analyzed with the literature data available.

(Aqueous MAPA System)

Literature was reviewed in order to examine the current work against the published work. Similar to that of densities, citied data is not available for aqueous MAPA system.

So viscosities of current work, aqueous MAPA system are compared with Pz (piperazine) system by *"Peter W. Derks, 2005"* and Pz (Piperazine) system of *"In house data"*. The *"Peter W. Derks, 2005"* data and the *"In house data"* both are done at low concentrations. Form figure 4.6 it is observed that current work, *"Peter W. Derks, 2005"* and *"In house data"* are in good agreement with each other at low concentrations. It is believed that at if literature data is extrapolated to higher concentrations it will follow the same exponential behavior as of current work.

Current work is also compared with HDMA (1,6-hexamethyldiamine) system a diamine by *"Prachi Singh et al., 2011"*. The current work is in good agreement with *"Prachi Singh et al., 2011"* and is presented in figure 4.7. One higher concentration i.e. 5.04M in literature is available similar to that of current work that show good adjustment in curves. All the data points of current work and literature followed the same exponential behavior.

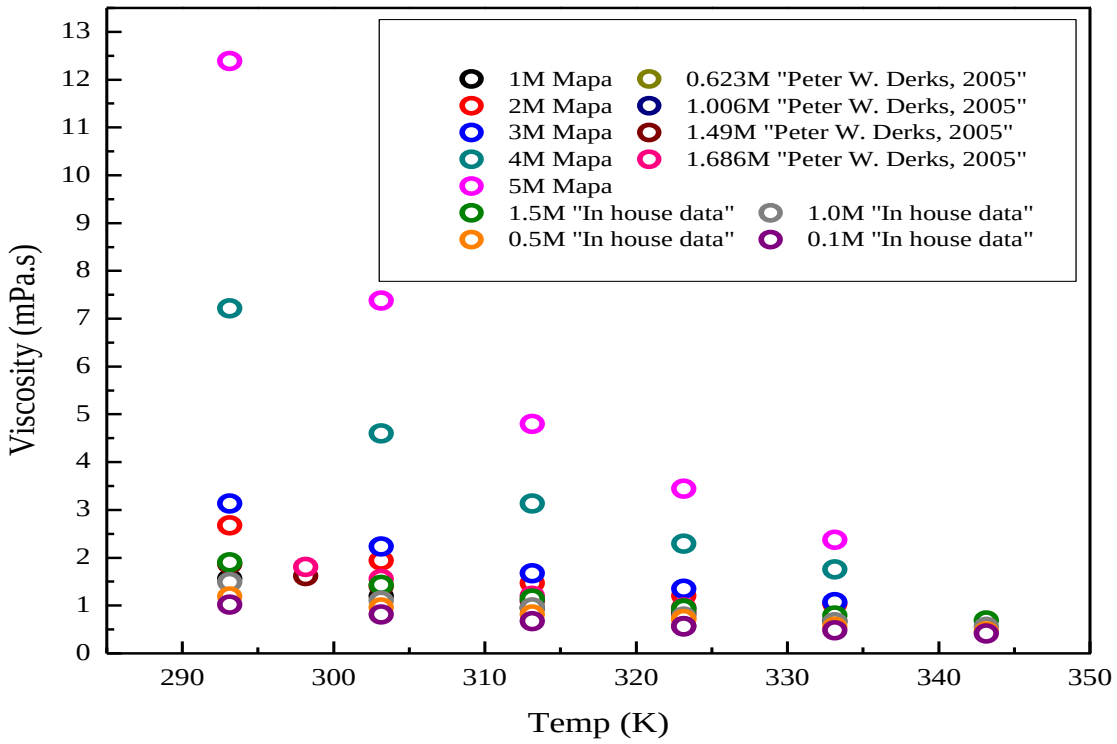

Fig 4.6: Comparison of current work MAPA system with Pz system by " Peter W. Derks, 2005" and Pz system by "In house data"

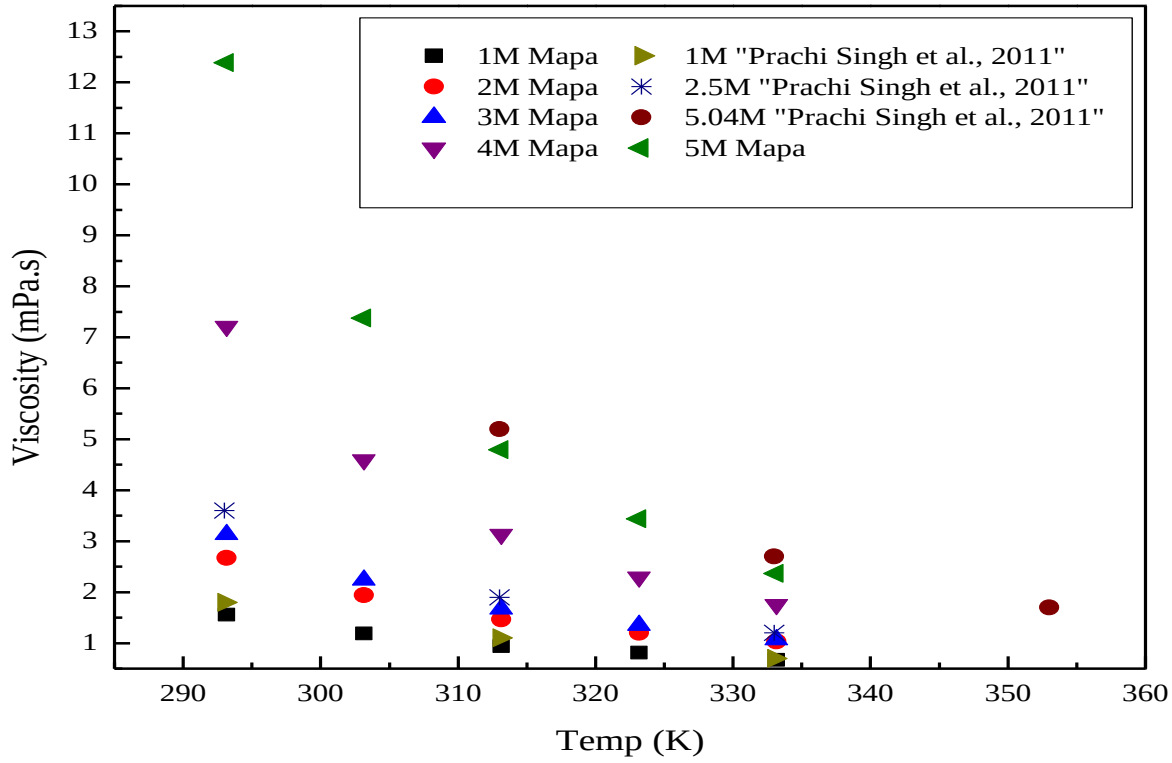

Fig 4.7: Comparison of current work "MAPA" system with "HDMA" system by "Prachi Singh et al., 2011"

(Aqueous Blended System)

Considering the viscosities of blended systems, literature data is currently unavailable for MAPA+DEEA blended system. There are some published works available on blends like MDEA+PZ (*N*-Methyldiethanolamine + Piperazine) system by *"Arunkumar Samantaa et al., 2011"* , MEA+TEA (Mono ethanol amine + Triethanol amine) system by *"Shyh-Yun Horng et al., 2002"* and MEA+MDEA (Monoethnaol amine + *N*-Methyldiethanolamine) system by *" Daniel P. et al., 1994"*.

Viscosity measurements of current work MAPA+DEEA blended systems are not appropriate to compare with these published data's because the concentrations of citied data are very much lower as compared to that of current system and blended concentration of amines are totally different, although graphs were plotted to test the behavior of current work with literature and all these systems followed the same exponential behavior as of current work.

4.3 Solubility Determination

Solubility experiments were performed in order to estimate henry's constant that are essential in order to predict kinetics of specific system.

(Aqueous MAPA System)

Measured henry's constant against variant temperatures in aqueous MAPA systems are attached to appendix A8, while graph is sketched in fig 4.8 in order to explain the behavior.

The plotted area indicates that with the increase in temperature the henry constant increases accordingly. Similarly concatenation has also direct decency on henry constant. At lower temperatures the difference in values of henry constant is excessive but as the temperature increases the difference in values at all concentration reduces.

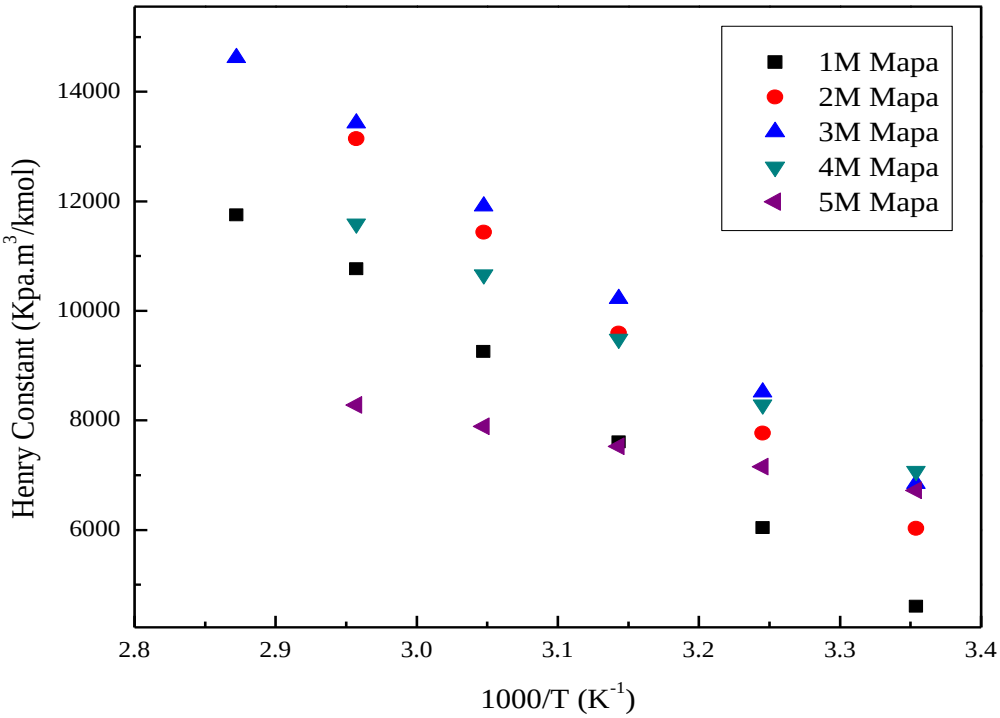

Fig 4.8: Experimentally determined henry's constant of "MAPA" system at different temperatures

An abrupt behavior is observed in higher concentration i.e. 5M that at higher temperatures it follows the trend likely similar to 1M. There might be a problem in doing experimentation at that particular time, details including gas saturation by solvent (mostly water), any potential leakage, neglect of the influence of the room pressure fluctuations, and imperfect purging of N_2 in the equilibrium cell at the start of experiment. Beside this, solubility experiments were performed for alternative 1/3/5M MAPA system while for 2&4M MAPA system values are obtained by interpolation. That's why same rough behavior can be seen in 4M MAPA system as it is derived from 1/3/5 MAPA system by interpolation. N_2O solubility in aqueous MAPA system is predicted by the Redlich-Kister equation as mentioned in chapter 2.

The equation (4.3) is used in order to model the henry's constant of aqueous MAPA system at all temperature and concentration while the modeled sketch is also presented in fig 4.9.

$$H_{N_2O}\left(\frac{kPa.m^3}{mol}\right) = K_1 - \frac{K_2.X^2}{T} + \frac{K_3.X}{T^2}.exp\left(\frac{K_4}{T} + \frac{K_5.X^2}{T^2}\right) \qquad 4.3$$

Where T indicates temperature in K, X is the mass fraction and K_1, K_2, K_3, K_4, K_5 are the parameters and are tabulated in appendix A9, with an AARD of 4.3%.

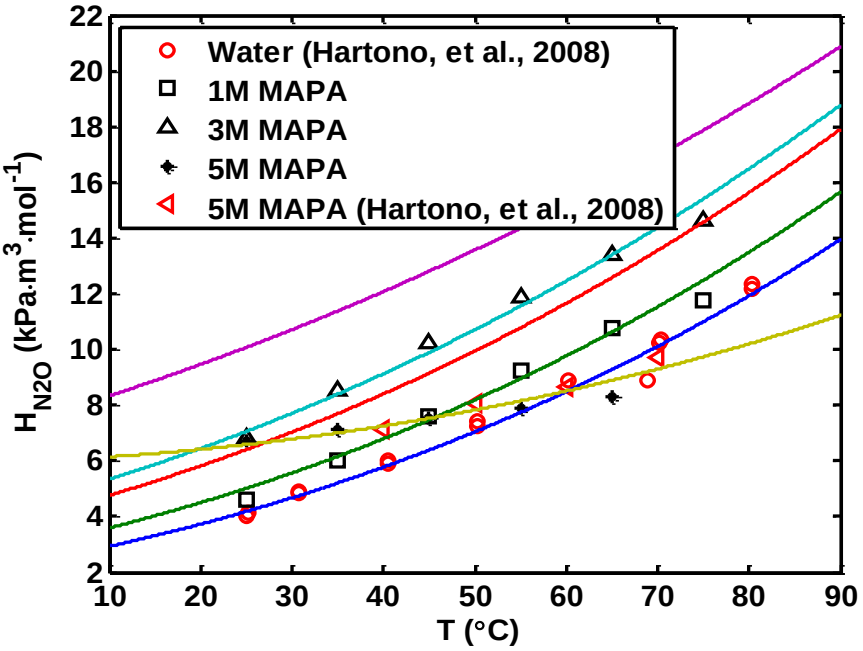

Fig 4.9: Experimental and modeled Henry's constant of "MAPA" system

(Aqueous Blended System)

Same experimental procedure was adopted in order to calculate the henry's constant for blended amine systems. The tabulated values are attached to appendix A10 while graph is presented in fig 4.10.

Blended systems exhibit the same characteristic behavior as observed in single amine system, that with the increase in temperature the henry's constant increases. As two different cases are discussed in density and viscosity evaluation so for solubility of blended systems those two cases are again of main consideration i.e. constant 1M MAPA with varying DEEA concentration similarly constant 2M MAPA with varying DEEA concentration. At very low concentrations i.e. 1M1D (1M MAPA+1M DEEA) the values of henry constant are higher, as the concentration of DEEA increases in it the values reduces respectively. Similarly for 2M1D (2M MAPA+1M DEEA) the henry constant is higher but by increasing the amount of DEEA values reduces equally. It is also observed that constant 1M MAPA set has higher henry's constant values as compared to that of constant 2M MAPA set. All the solubility experiments in case of blended system were performed except 3M1D/3M3D/4M3D.

So the solubilities in these three cases are obtained by interpolation from experimental data points of performed systems.

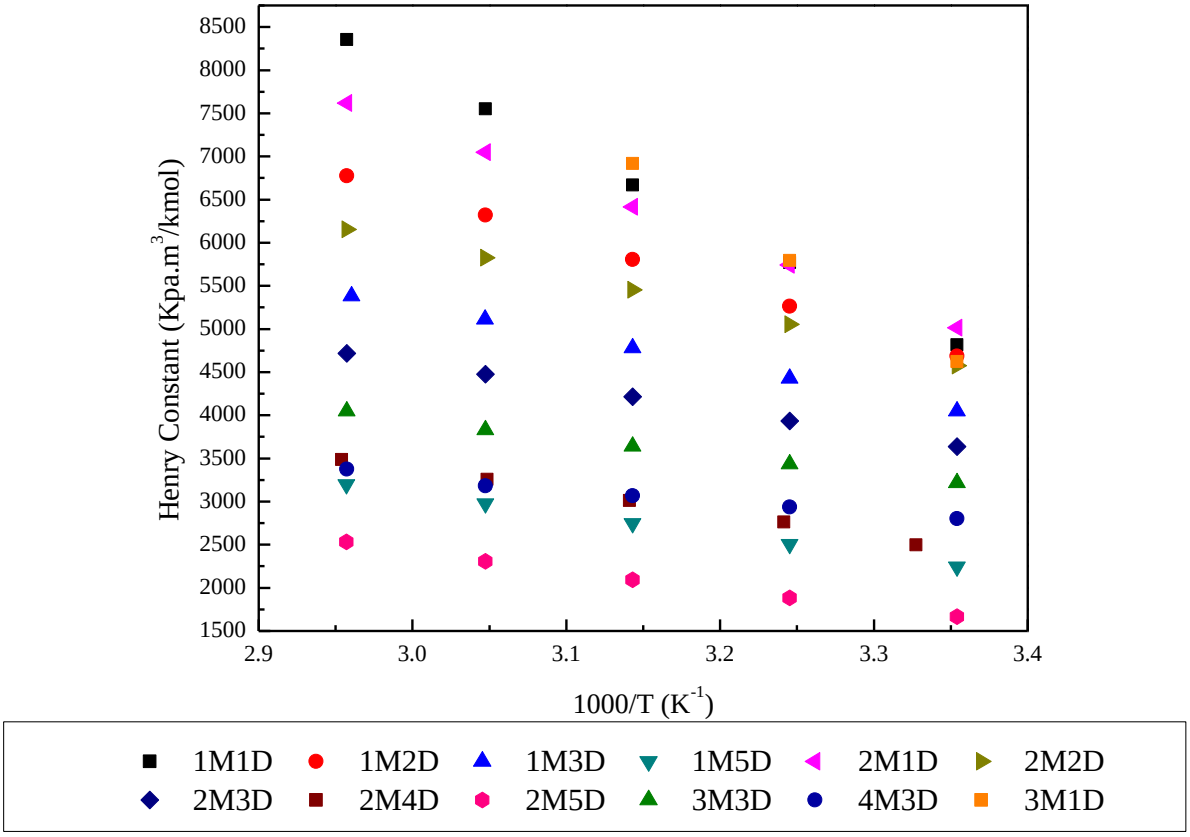

Fig 4.10: Experimentally determined henry's constant of Blended "MAPA+DEEA" system at diff. temperatures

4.3.1 Solubility Comparison (Current Work & Literature)

Literature data was considered to compare the current work results and previously available data.

(Aqueous MAPA System)

It is reported that as such there is no citied data available on aqueous MAPA system but similar systems are available to compare with. The results of MEA (Monoethnaolamine) system by *"Basma Yaghi et al., 2008"* is compared with current system at lower concentrations , depicts that values of henry's constant of current work are higher than MEA system and the data points of literature work are bit scattered as compared to that of current work.

Another MEA (Monoethnaolamine) system by *"Mandal et al., 2005"*, MEA (Monoethnaolamine) system by *"Li et al., 1995"* for higher concentration indicated that solubility of current work is very much higher when compared with these systems as well.

(Aqueous Blended System)

Blended systems like, MEA+MDEA (Monoethnaolamine + *N*-Methyldiethanolamine) system by *"Daniel P. et al., 1994"*, MDEA+PZ (*N*-Methyldiethanolamine + Piperazine) system by *"Arunkumar Samantaa et al., 2011"* and MEA+TEA (Monoethanolamine + Triethanolamine) system by *"Shyh-Yun Horng et al., 2002"* are readily present in literature but this data is not well suited to compare with current work. The molar concentrations of current systems are too high as compared to that of all available literature, in addition to it the range of these systems are limited to few specific temperatures. The aim of current work in case blended systems is to judge the changes by varying concentrations rather than that of analysis with past work.

4.4 Kinetic Evaluation of Aqueous MAPA System

Kinetic measurements were done for single and blended systems on string of discs equipment. Different concentrations of single and blended systems were performed at different temperatures. Results are displayed in this way that aqueous MAPA system will be discussed first then blended systems joined the discussion afterwards. Kinetics data for aqueous MAPA system is attached to appendix B1.

4.4.1 Absorption Flux

The measurements of absorption flux of CO_2 were also achieved during kinetic experiments. Five different molar concentrations of single MAPA systems were performed as graphed in fig 4.11.

According to experimental results that are presented in graph, indicates that variation in the temperature of the amine solution has a significant effect on the absorption rate. With the increase in temperature the rate of CO_2 absorption increases accordingly. Considering the concentration as second factor, the absorption flux has direct dependency on it. It can be observed that with the increase molar concentration of amine solution the rate of absorption of CO_2 increases the same way.

There is another factor that has an influence on flux that is the mass transfer area, both have an inverse relation by decreasing it the absorption rate/flux of CO_2 increases and vice versa.

The order of the flux will then be 5M>4M>3M>2M>1M. Sudden increase in flux noted at higher temperature for 5M MAPA system. On the other hand side difference in flux values for lower concentration i.e. 1&2M MAPA system is small. The maximum value of flux achieved is 3.45E-03 (mol/m^2.sec) for the case of 5M MAPA at higher temperature. During kinetics calculations temperature was averaged for liquid inlet and outlet because the temperatures attained during experimentations were not exact integers like 293.15K or 303.15K. The reason behind this is the poor temperature control in string of discs apparatus. The amine solution continuously dripped out in to the discharge storage tank, and it will remain outside under ambient conditions until and unless 5L batch of amine solution is finished. When amine solution was recirculated the set temperature disturbed.

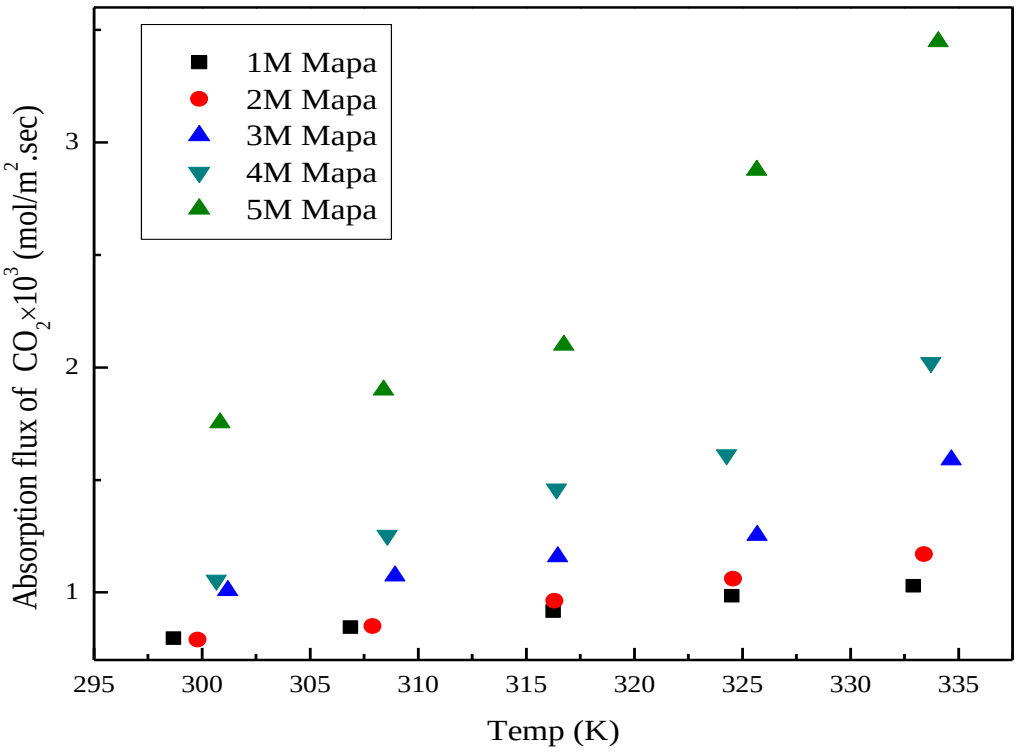

Fig 4.11: Absorption flux of CO_2 for "MAPA" system at different temperatures

4.4.1.1 Absorption Flux Comparison (Current work & Literature)

Current work is also compared with the citied data. Literature was reviewed in order to find the kinetics on aqueous MAPA system but as such no experimental measurements were obtained. So current work is compared with the similar systems available.

Absorption flux of CO_2 of current work is analyzed with the Pz (Piperazine) system of *"In house data"* and DETA (Diethylenetriamine) system by *"Hartono et al., 2009"* and is presented in fig 4.12. The graphical representation indicates that the current work is in agreement with the literature data,

although higher concentration of cited data are not available but it is believed that it will follow the same behavior as higher concentrations of current work.

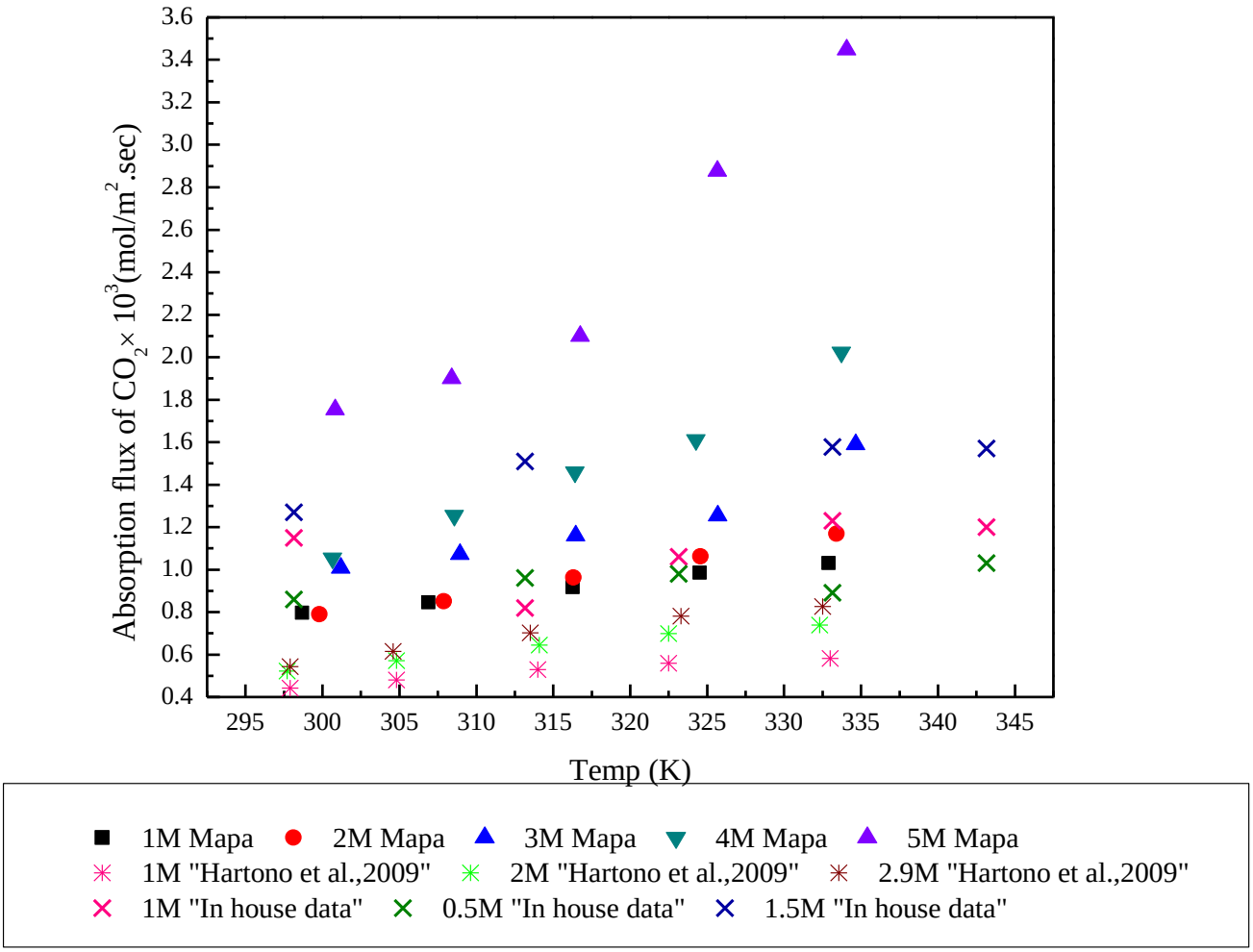

Fig 4.12: Comparison of absorption flux of current work and DETA system by "Hartono et al., 2009", Pz system by "In house data".

At lower concentrations i.e. 1M concentration of Pz (Piperazine) system *"In house data"* is in agreement with the 1M concentration of current work. Moreover the 1.5M concentration of Pz (piperazine) system *"In house data"* is showing slightly higher flux values as compared to that of 2M concentrations of current work but the fashion of both works are similar. Data points of *"In house data"* are bit scattered as compared to that of other systems.

Considering the DETA (Diethylenetriamine) system by *"Hartono et al., 2009"* the absorption rate of CO_2 is lower as compared to that of current work at lower concentrations.

Even by increasing the concentration of DETA (Diethylenetriamine) system by *"Hartono et al., 2009"* to 2.9M the values of fluxes are lower than that of 1M concentration of current work,

indicating that the current system is fast in terms of absorption rate when comes in comparison to DETA (Diethylenetriamine) system by *"Hartono et al., 2009"*.

4.4.2 Overall Mass Transfer Coefficient

The overall mass transfer coefficient for different concentration of single MAPA system is sketched in fig 4.13.

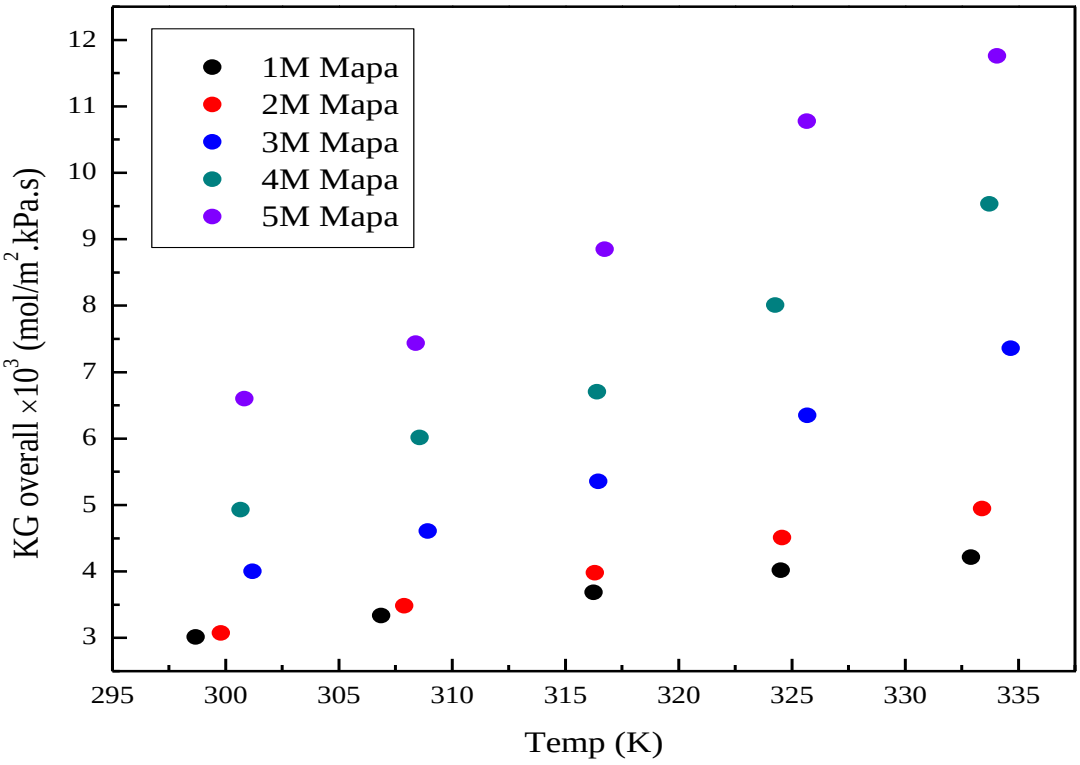

Fig 4.13:Overall mass transfer coefficient of "MAPA" system at different temperatures

According to the experimental results obtained, it is observed that overall mass transfer coefficient is enhanced with the increase in temperature. The same behavior is recognized with the increase in concentration of the amine solution as well, that over all mass transfer coefficient increases with the concentration. It means that there is more ease for the mass transfer at higher concentrations than at lower concentrations. With the increase in absorption flux of CO_2 the overall mass transfer coefficient increases accordingly as by definition flux has direct relation with overall mass transfer coefficient.

According to sketched behavior of overall mass transfer coefficient it is examined that at lower concentration i.e. 1&2M MAPA system the values of mass transfer are very much close . As the concentration increases rapid difference in values of overall mass transfer coefficient is observed.

4.4.2.1 Overall Mass Transfer Coefficient Comparison (Current Work and Literature)

Literature was citied in order to analyze the current work and data already available. It is stated that no as such material is available on over all mass transfer coefficient for this system (Aqueous MAPA system) or similar system. Although kinetic evaluations are done like Pz (Piperazine) system by *"P.W.J. Derks et al., 2006"* , HDMA (1,6-hexamethyldiamine) system by *"Prachi Singh et al., 2011"* and EDA (Ethylenediamine) system by *"Juelin Li et al., 2007"* but no one from these, reported over all mass transfer coefficient details to judge and estimate the behavior of current work.

4.4.3 Observed Kinetic Rate Constant

The observed kinetic rate constant is sketched against temperature and plotted in fig 4.14.

Termolecular mechanism (Direct mechanism) is followed in order to interpret kinetics. The number of fitting parameters in this mechanism is lower than that in the zwitterion mechanism. Termolecular mechanism can satisfactorily explain fractional and higher-order kinetic. It is a straightforward procedure for kinetic estimation and is briefly out-lined in previous chapters.

It is clear from these results that the temperature affects the kinetics for CO_2 absorption. With the increase in temperature the rate constant increases accordingly. Similarly concentration of amine solution is also focusing its influence on kinetic rate constant, by increasing the concentration the observed kinetic rate constant increases. It can be noticed that at higher concentrations and higher temperature i.e. 4&5M the rate constant increases rapidly as compared to that of lower concentrations and lower temperature.

The observed kinetic rate constant has an inverse relation with the diffusivity of CO_2, if diffusivity increases than kinetic rate constant decreases in the same fashion. Similarly by varying the enhancement factor (Ea) the observed kinetic rate constant vary, as Ea has direct relation with it.

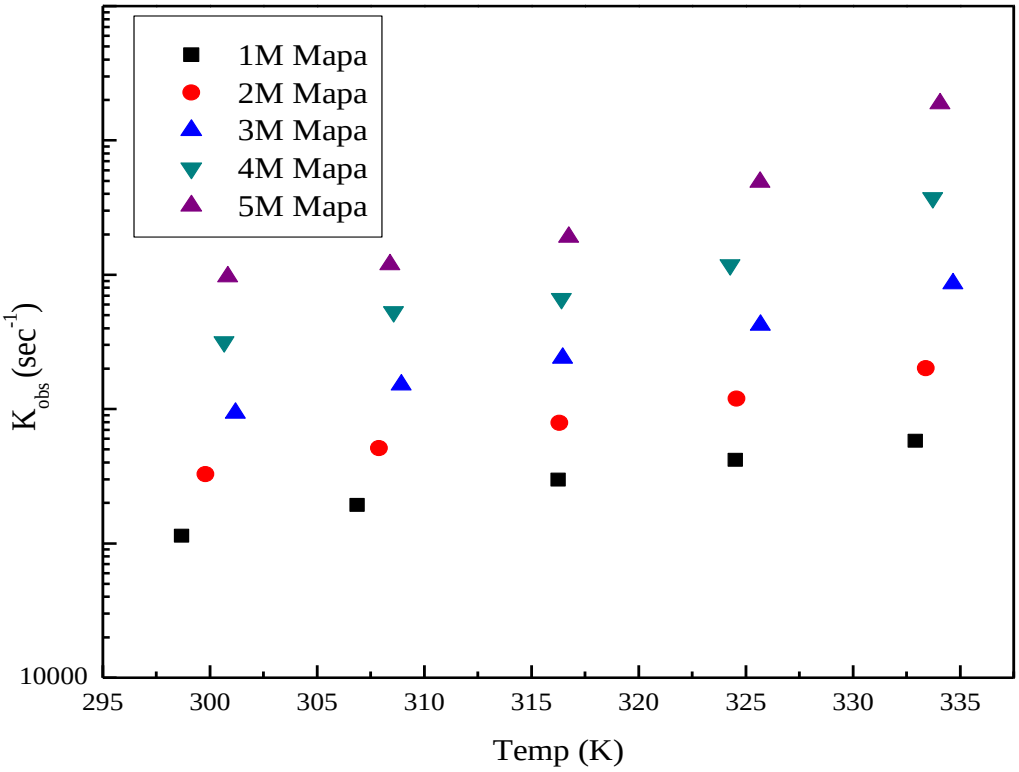

Fig 4.14: Observed kinetic rate constant of "MAPA" system at different temperatures

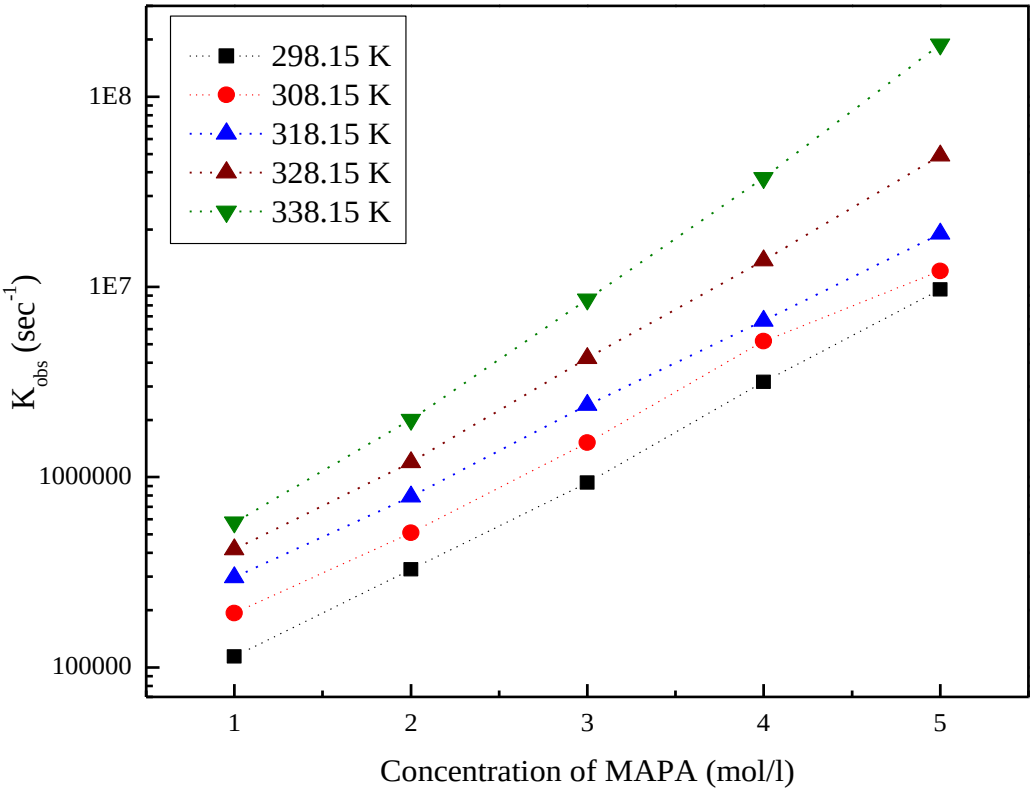

Fig 4.15: Observed kinetic rate constant at variant "MAPA" concentrations

More over in order to show the effect of concentration on observed kinetic rate constant semi log graph is plotted as shown in fig 4.15, that indicates effect of increased molar concentration on rate constant which is significant. The concentration dependency of the observed kinetic rate constant is the reaction order with respect to the MAPA concentration.

4.4.3.1 Comparison of Observed Kinetic Rate Constant (Current Work and Literature)

Literature was studied in order to analyze the behavior of current work. Observed kinetic rate constant of the current work is compared with Pz (Piperazine) system by *"P.W.J. Derks et al., 2006"*, Pz (Piperazine) system of *"In house data"* and HDMA (1,6-hexamethyldiamine) system by *"Prachi Singh et al., 2011"*. Graphed is plotted and presented in fig 4.16.

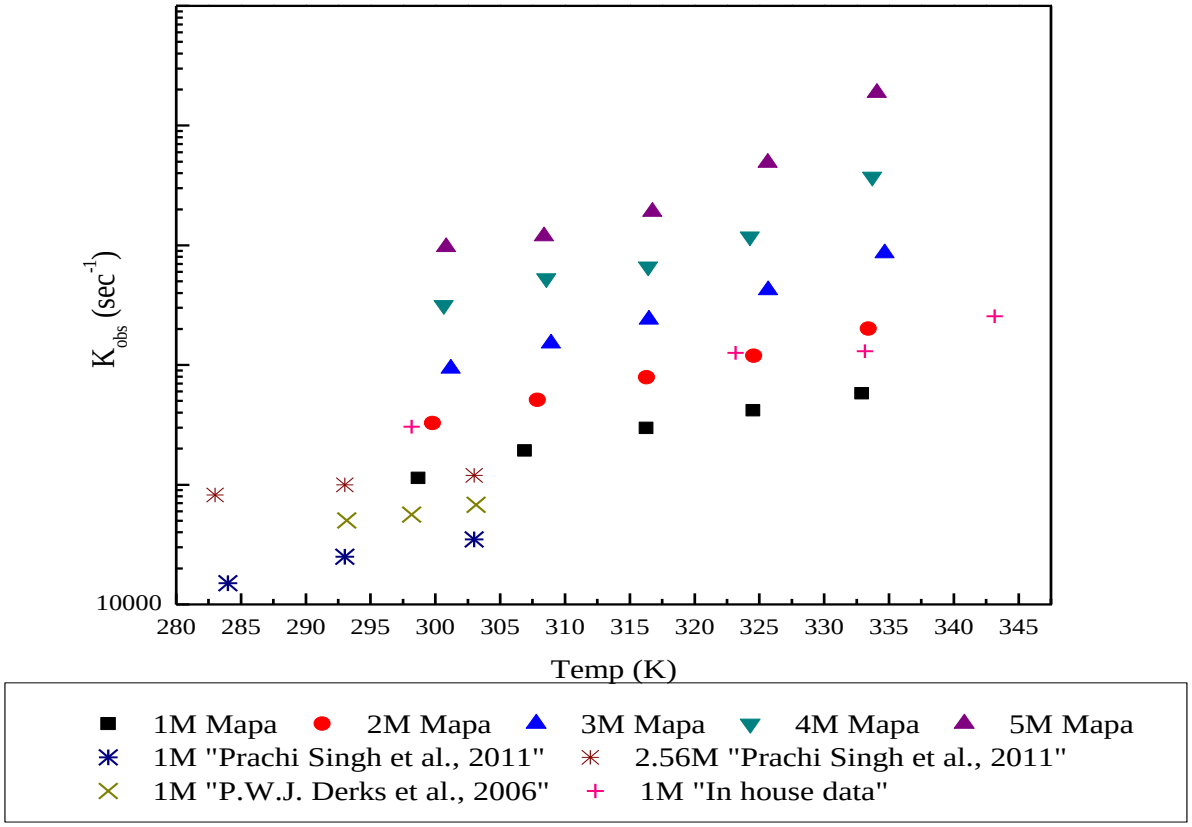

Fig 4.16: Comparison of overall mass transfer coefficient of current work and Pz system by "P.W.J. Derks et al., 2006", HDMA system by "Prachi singh et al., 2011"

It is examined from the graph that current work and literature are likely in agreement with each other. The 1M concentration of Pz (Piperazine) system by *"P.W.J. Derks et al., 2006"* followed the same

path as of current work but values are lower. On the other hand the rate constant in 1M concentration of Pz (Piperazine) system by "In house data" is higher as compared to that of current work and *"P.W.J. Derks et al., 2006"*. Both the literatures are not in good agreement with each other.

Furthermore the current system is showing higher values in terms of observed kinetic rate constant than that of HDMA (1,6-hexamethyldiamine) system by *"Prachi Singh et al., 2011"*.

4.4.4 Second Order Kinetic Rate Constant

Experimental kinetic rate constants for aqueous MAPA system are presented in fig 4.17.

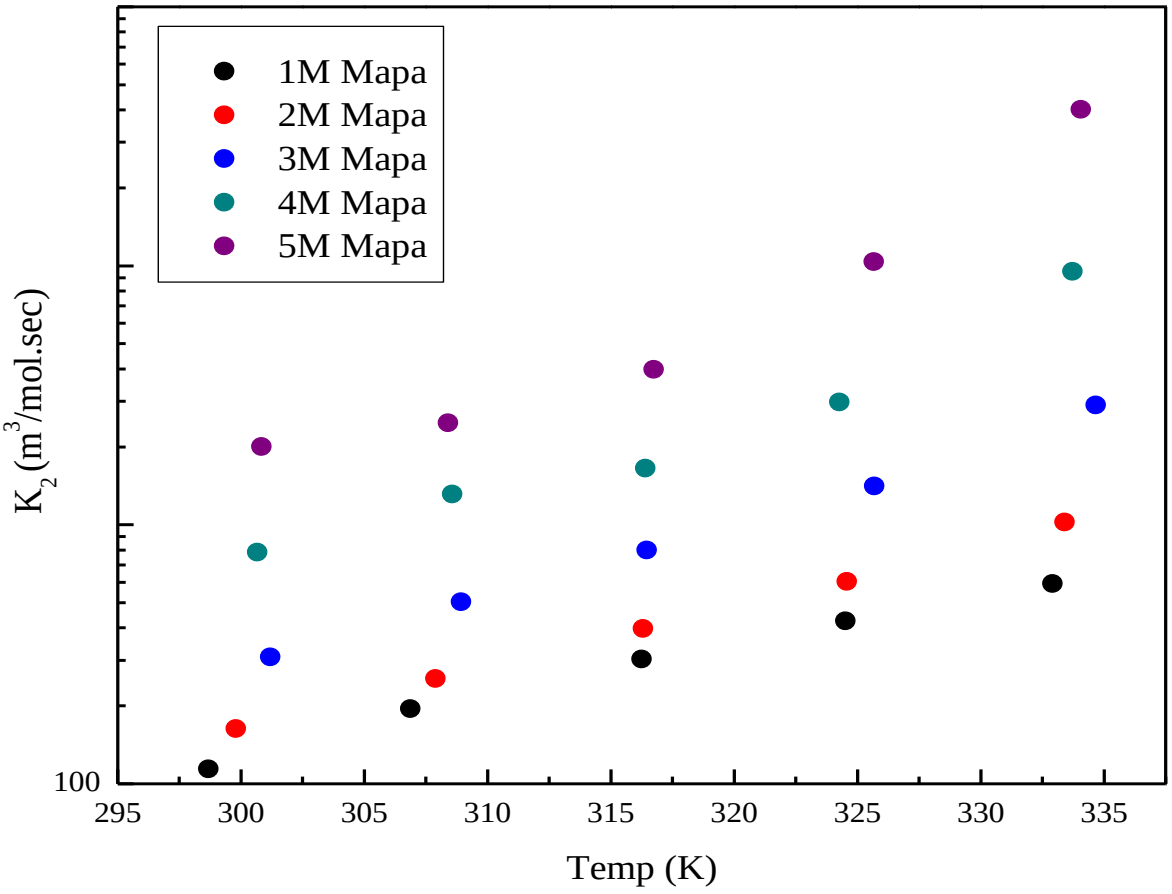

Fig 4.17: Second order kinetic rate constant of "MAPA" system at different temperatures

Parity plot of kinetic rate constant has a direct dependency over temperature and concentration of amine solution. It can be observed that with the increase in temperature the kinetic rate constant increases accordingly. The data points for all concentrations show linear behavior although at higher concentrations i.e. 5M there is a deviation from the linearity at higher temperatures it is because of sensitivity of measured physiochemical properties.

The difference in the values of rate constants at lower concentration are small, it perhaps of very close physiochemical properties at lower temperatures and lower concentrations which affects the K_2 values. The solubility data affects the K_2 values more than density and viscosity. Secondly the very low flow rates of CO_2 on MFC were used during experiments on SDC (string of discs) and that creates the uncertainty in flux. On the other hand side as the concentration increases difference in rate constant values exaggerate as well.

Furthermore the reaction rate constant (k_{MAPA} and k_{water}) can also be determined by single step termolecular mechanism as proposed by *"Crooks et al., 1989"*. These parameters are obtained from experimental observed kinetic rate constant (k_{obs}) at various MAPA concentrations and regressed at given temperatures. The values of observed kinetic rate constant (k_{obs}) divided by the concentration of MAPA result in a linear equation as expressed in eq. (4.4).

$$\frac{k_{obs}}{[MAPA]} = k_{MAPA}[MAPA] + k_{H_2O}[H_2O] \qquad 4.4$$

Isotherms for each individual temperature are sketched for $\frac{k_{obs}}{[MAPA]}$ versus concentration of MAPA and best fit linear curves are extracted in order to get rate constants (k_{MAPA} and k_{water}) as all the data points are not showing linearity in behavior. From linear equations at each individual temperature slope indicates k_{MAPA} while intercept divided by water concentration gives k_{Water}.

By taking an average value against each averaged temperature, the reaction rate constants of MAPA and those of water that are calculated from the plots are presented in Table 4.1.

Temp ^0C	k_{Mapa} $l^2/mol^2.sec$	k_{water} $l^2/mol^2.sec$
27.08	2.39E+04	8.86E+02
34.98	2.83E+04	1.24E+03
43.28	4.25E+04	1.22E+03
51.79	7.60E+04	5.42E+02

Table 4.1: Reaction rate constants of MAPA and those of water

Rate constants (k_{MAPA} and k_{water}) are sketched against 1000/T (K) to attain an Arrhenius–plot. The reaction rate constant of k_{MAPA} and that of water k_{H_2O} calculated from this plot can be expressed by the following Arrhenius correlations.

$$k_{MAPA} = 1.6654 \times 10^9 \, exp\left(\frac{-3359.6}{T}\right)$$

$$k_{H_2O} = 4.777 \times 10^5 exp\left(\frac{-1871.0}{T}\right)$$

By applying these equations at each individual temperature modeled/calculated kinetic rate constant can be estimated.

4.4.4.1 Comparison of Second Order Kinetic Rate Constant (Current Work and Literature)

Experimentally determined rate constants were citied in order to analyze the present work.

MEA (Monoethnaolamine) system by *"Haruo Hikita et al.1979"* has lower concentrations as compared to that of current work for kinetic rate constant. Trend of 1M concentration of *"Haruo Hikita et al.1979*" acquire the same behavior as of current work but current system is very much fast as values of kinetic rate constant are much higher than reported data.

4.4.5 Comparison of Modeled and Experimental (Absorption Flux and K_2)

Experimentally determined and calculated/modeled absorption flux of CO_2 and second order kinetic rate constant are presented in figures 4.18 and 4.19.

According to sketched area the calculated and experimental absorption flux of CO_2 showing good agreement with each other at all concentrations. While in case of kinetic rate constant the lower concentrations are showing similarity as the concentration approaches to 5M, there is a slight change in modeled and experimental values it's because of sensitivity of henry's constant values of 5M MAPA system.

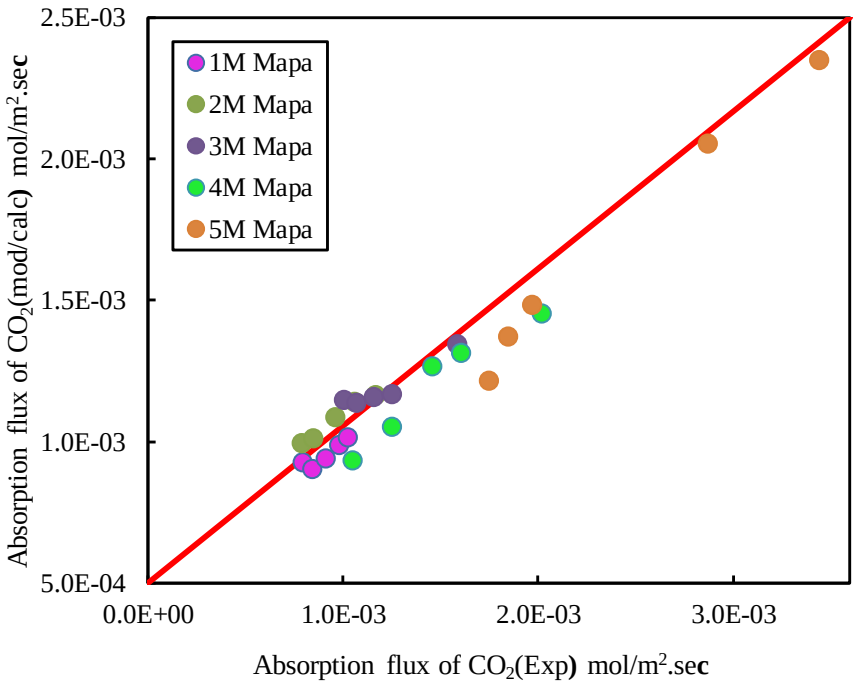

Fig 4.18: Experimental and calculated/modeled absorption flux of CO_2 in "MAPA" system

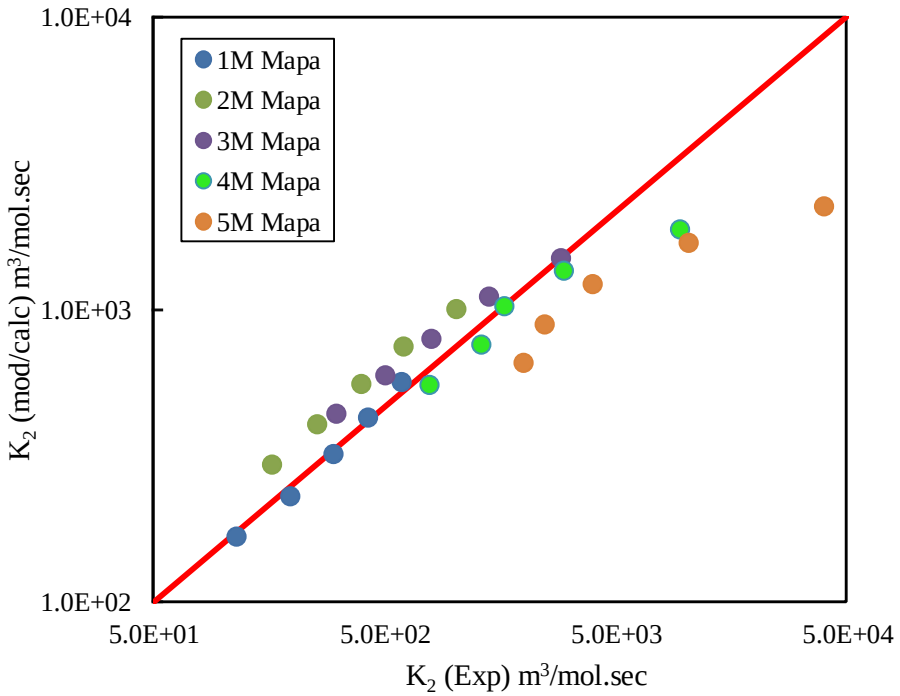

Fig 4.19: Experimental and calculated/modeled second order kinetic rate constant in "MAPA" system

4.5 Kinetic Evaluation of Aqueous Blended System

Kinetic evaluations of blended systems were performed on same experimental setup as for MAPA system. Kinetics data of blended system is attached to appendix B2.

4.5.1 Absorption Flux

The experimentally determined absorption flux of CO_2 at variant concentration and blended schemes are presented in fig 4.20.

According to experimental results that are expressed in graph indicates, with the increase in temperature the rate of CO_2 absorption increases accordingly. Similarly the concentration of blended systems has significant effect on absorption flux. It can be observed that absorption rate of CO_2 increases when the concentration of the blended amine solution increases. As concentration has direct relation with flux.

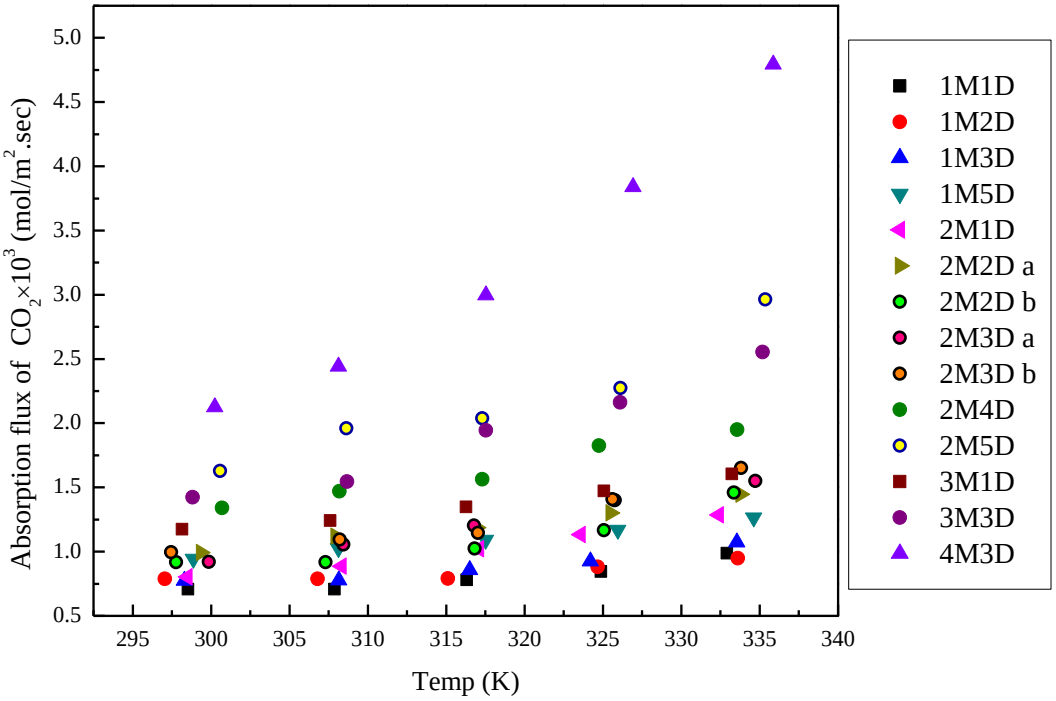

Fig 4.20: Absorption flux of CO_2 for Blended "MAPA+DEEA" system at different temperatures

In case of blended systems two different set of experiments are of considerable importance one with constant 1M MAPA and variable DEEA concentrations, and second is of constant 2M MAPA with variable DEEA concentrations.

As the concentrations of DEEA increases in blend the absorption flux tends to increase in the same manner. At lower temperatures the difference in values of fluxes are limited as the temperature raises

the difference in flux boosts. 4M3D system depicts high absorption flux at higher temperature. Additionally when concentration of MAPA increases from 1M to 2M an apparent increase in flux is observed. If the DEEA concentration is kept constant and concentration of MAPA varies from 1M to 2M an intensive increase in flux can be observed i.e. 1M5D and 2M5D.

There is another factor that has an influence on flux that is the area of mass transfer. The absorption flux has an inverse relation with flow area. Flux will be higher when mass transfer area will be less.

In order to ensure the experimental data points for flux, two blended systems were repeated as indicated by 2M2D a, 2M2Db similarly 2M3Da, 2M3Db. The data points of these two systems are in good agreement with each other ensuring the reproducibility of data.

Temperature values were averaged for liquid inlet and outlet. The reasoning behind averaged values is the imperfect temperature control in string of discs apparatus. The amine solution continuously dripped out in to the discharge storage tank, and it will remain outside under ambient conditions until and unless 5L batch of amine solution is finished. The solution collected at the outlet when recirculated the set temperature disturbed.

4.5.1.1 Absorption Flux Comparison (Current work & Literature)

Literature data was reviewed on blended systems in order to judge the trends of current work but blends of MAPA+DEEA have not done yet. Single literature that is reported for the blends of MEA+MDEA (Monoethnaolamine + *N*-Methyldiethanolamine) system by *"Daniel P. et al., 1994"* presents the data points for absorption flux at only one temperature. Current work can't be compared with the literature reviewed as molar concentrations of reported system are very low as compared to that of current and only available for single data point.

The main theme of blended system (current work) is to judge the efficiency by varying concentrations either DEEA or MAPA in order to get an appropriate blend that has a high absorption rate. It can be observed that with slight increase in MAPA concentration from 1M to 2M with constant 5M DEEA a very high absorption flux is achieved.

4.5.2 Overall Mass Transfer Coefficient

The overall mass transfer coefficient for different concentration of blended system is plotted in fig 4.21.

From sketched area it is noticed that overall mass transfer coefficient increases with the increase in temperature. The same behavior is observed with concentration of the amine solution as well, that over all mass transfer coefficient increases with the concentration. Indicating more ease for the mass transfer at higher concentrations than at lower concentrations. Overall mass transfer coefficient has direct dependency on absorption flux of CO_2 With the increase in absorption flux of CO_2 the overall mass transfer coefficient increases accordingly.

At lower blended concentrations the difference in values of overall mass transfer coefficient is small as the concentration increases, rise in overall mass transfer coefficient is observed but this increase is not very much noticeable but as concentration of DEEA approaches to 5M with 2M MAPA a rapid increase in overall mass transfer coefficient can be seen.

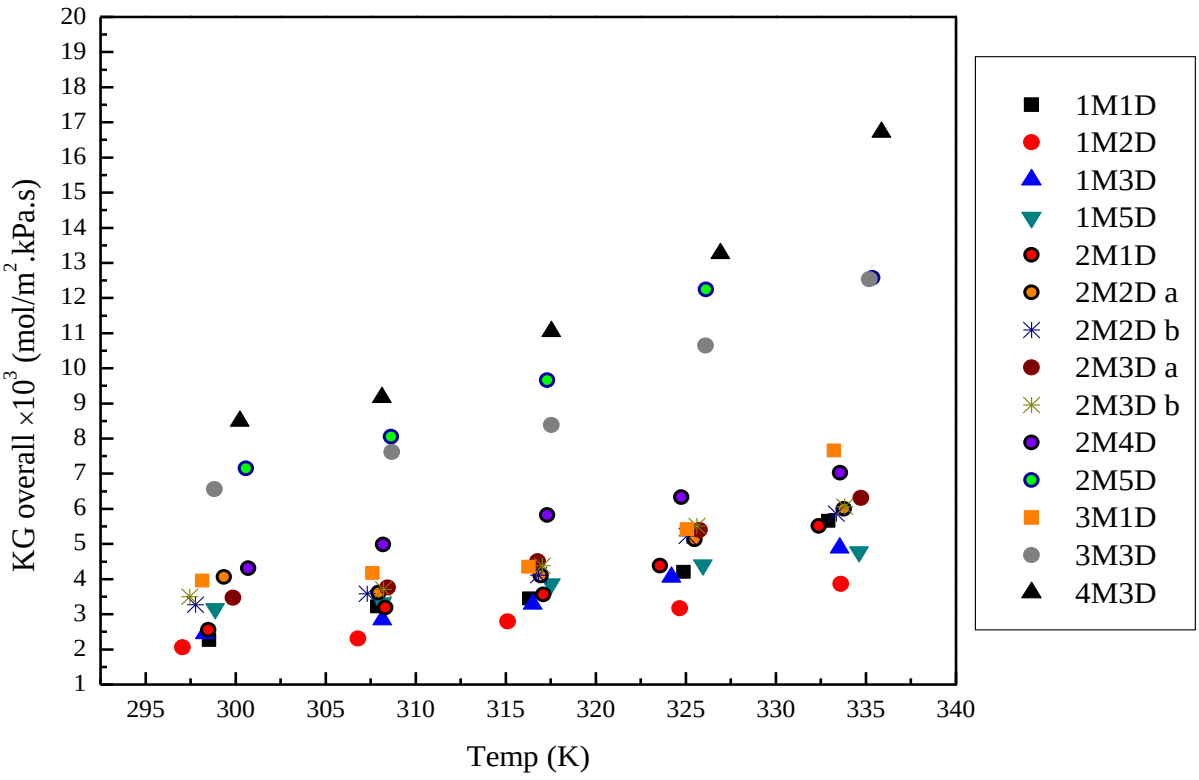

Fig 4.21: Overall mass transfer coefficient for Blended "MAPA+DEEA" system at different temperatures

Considering again two sets of blended systems, the mass transfer coefficient is higher in case of constant 2M MAPA with variant DEEA concentrations. While constant 1M MAPA system occupied the lower range. An attributed change in overall mass transfer coefficient values can be seen in case when 1M5D is compared with 2M5D.

Experimental data points for overall mass transfer coefficient of two blended systems i.e. 2M2D a, 2M2Db and 2M3Da, 2M3Db are in good agreement with each other certifying the reproducibility of data.

4.5.2.1 Overall Mass Transfer Coefficient Comparison (Current Work and Literature)

Literature was citied in order to estimate the behavior of current work and data already available. It is reported that no as such data of overall mass transfer coefficient for current blends or similar system is obtainable. Although kinetic evaluations are performed on blended systems like and MEA+TEA (Monoethanolamine + Triethanolamine) system by *"Shyh-Yun Horng et al., 2002* but overall mass transfer coefficient details are not presented in order to judge and estimate the trend and mass transfer efficiency of current work.

4.5.3 Observed Kinetic Rate Constant

Experimental values of observed kinetic rate constant are attached to appendix B1. While the graph for observed kinetic rate constant against temperature is plotted in fig 4.22.

Single step termolecular mechanism (Direct mechanism) is followed in order to interpret kinetics of blended system. The number of fitting parameters in this mechanism is less than that in the zwitterion mechanism. Termolecular mechanism can satisfactorily explain fractional and higher-order kinetic.

Graphical representation depicts that kinetics for CO_2 absorption is affected by temperature change. With the increase in temperature the kinetic rate constant increases accordingly. Similarly concentration of amine solution has influence on kinetic rate constant, by increasing the concentration the observed kinetic rate constant increases.

The observed kinetic rate constant has an inverse relation with the diffusivity of CO_2, if this diffusivity decreases than kinetic rate constant increases in the same trend. Similarly by varying the enhancement factor (Ea) the observed kinetic rate constant vary, as Ea has direct relation with it.

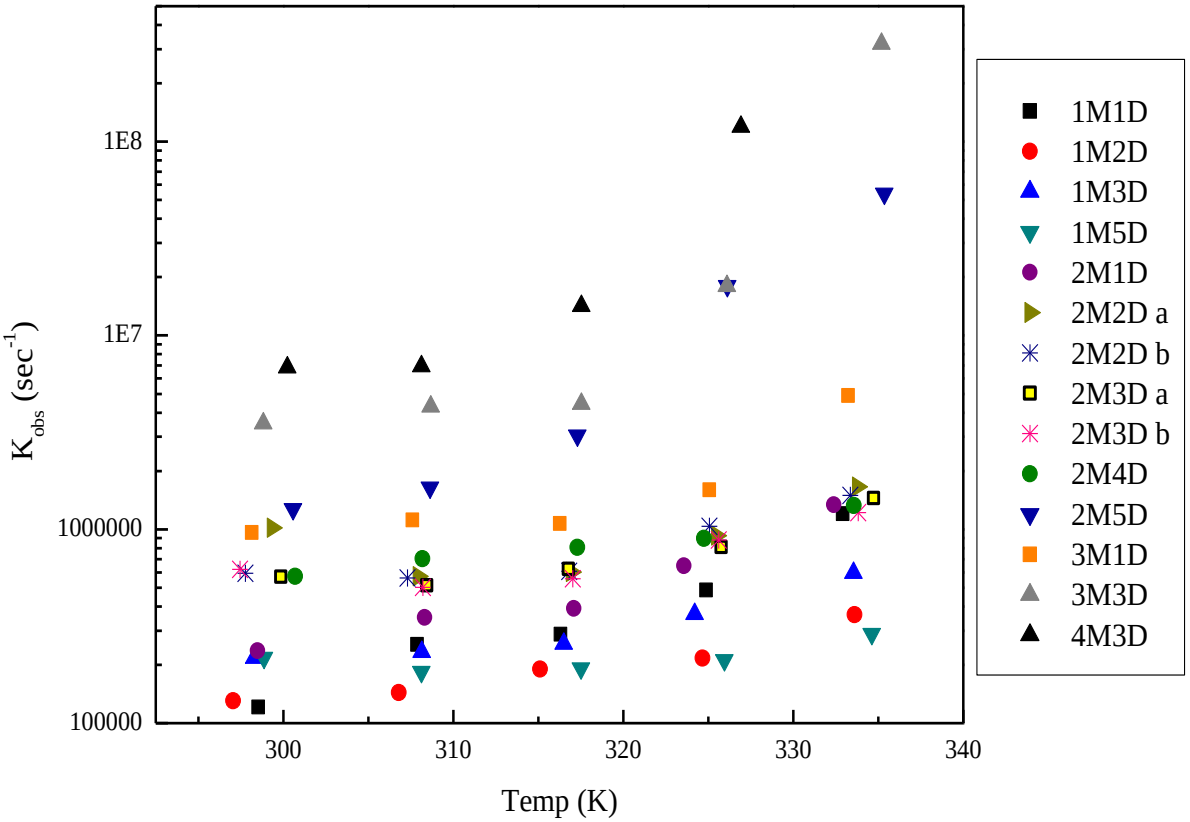

Fig 4.22: Observed kinetic rate constant for Blended "MAPA+DEEA" system at different temperatures

Kinetic rate constant in case of constant 1M MAPA and variable DEEA have low numerical values in contrast to 2M MAPA and variable DEEA. While if concentrations of DEEA are kept constant then a drastic rise in kinetic rate constant is observed in 1M5D and 2M5D.

Reproducibility of the experimental data points is also done by replicate runs at all temperature for 2M2D a, 2M2Db and 2M3Da, 2M3D b.

4.5.3.1 Comparison of Observed Kinetic Rate Constant (Current Work and Literature)

Literature was studied in order to analyze the behavior of current work. According to review no as such data on observed kinetic rate constant for blended systems is presented yet. Although kinetic evaluations are performed on blended systems like and MEA+TEA (Monoethanolamine + Triethanolamine) system by *"Shyh-Yun Horng et al., 2002* but the behavior and trend of observed kinetic rate constant is not explained in this published data.

On other hand side if two sets of blended systems of current work are compared with each other it is concluded that higher concentration of MAPA leads to high observed kinetic rate constant. Two blended systems attracts more attention 1M5D and 2M5D, the concentration of DEEA are same but slight increase in concentration of MAPA ends up with a very high observed kinetic rat constant.

4.5.4 Second Order Kinetic Rate Constant

Experimental kinetic rate constants for blended system are presented in fig 4.23.

Parity plot of kinetic rate constant has a direct dependency over temperature and concentration of amine solution. It is determined that with the increase in temperature the kinetic rate constant increases accordingly.

Considering again the two sets of blended systems, by increasing the concentration of MAPA from 1 to 2M there is a rise in rate constant and very high values (rate constant) are reported for 2M5D when it is compared to 1M5D.

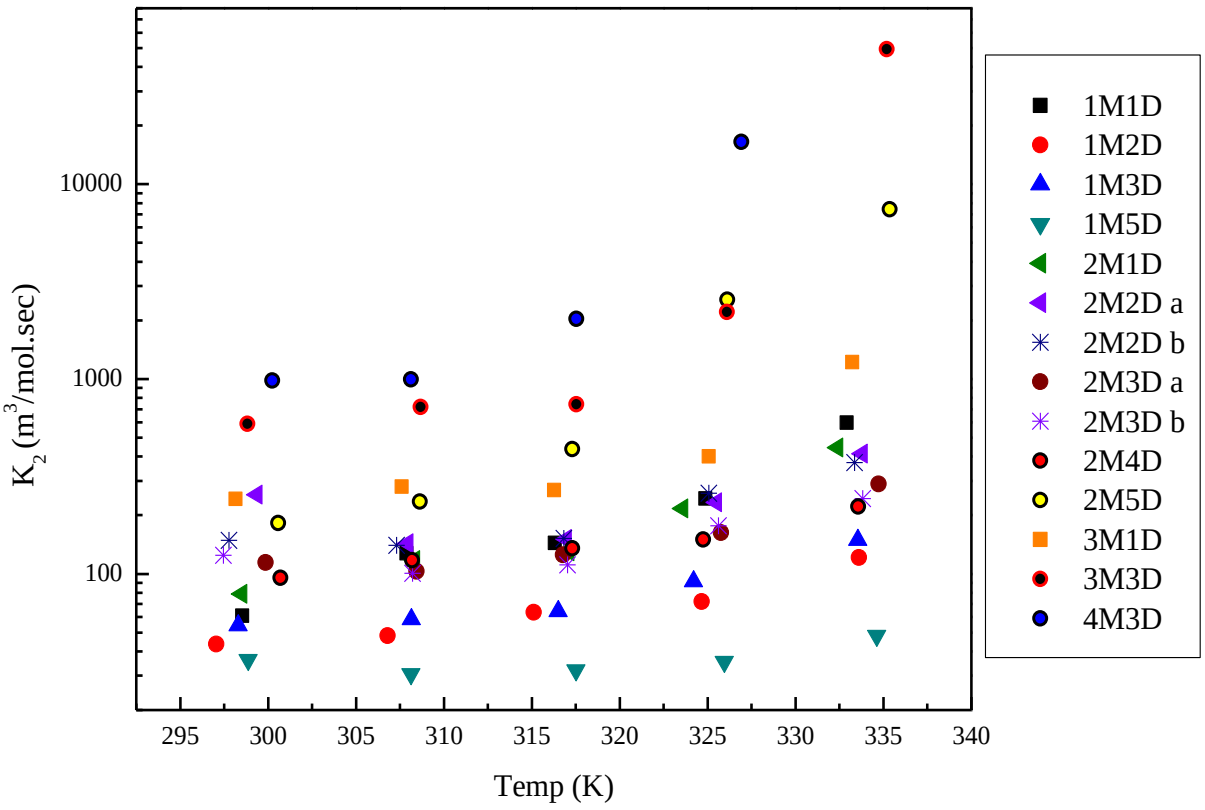

Fig 4.23: Second order kinetic rate constant for Blended "MAPA+DEEA" system at different temperatures

The difference in the values of rate constants at lower concentration and lower temperatures are small, it because of very close physiochemical properties at lower temperatures and lower concentrations which affects the K_2 values. The solubility data affects the K_2 values more than density and viscosity. A rough trend is observed in case of 1M5D that rate constant are lower than 1M1D/1M2D/1M3D/ it might be because of very low values of henry constant in case of 1M5D as compared to that of other blends. 4M3D has higher kinetic rate constant in blended systems at all temperature.

Reproducibility is also achieved by replicate runs of 2M2D a, 2M2D b and 2M3D a , 2M3D b, all the data points are fashioned in the same trend showing good agreement with each other.

4.5.4.1 Comparison of Second Order Kinetic Rate Constant (Current Work and Literature)

Literature review revealed no specific data on second order kinetic rate constant of blended systems. Although kinetic characterization are performed on blended systems like and MEA+TEA (Monoethanolamine + Triethanolamine) system by *"Shyh-Yun Horng et al., 2002"* but data on kinetic rate constant is not presented.

In addition to it, if two sets of blended systems of current work are compared with each other it is concluded that increase in concentration of MAPA leads to high kinetic rate constant. Two blended systems absorbs more consideration 1M5D and 2M5D, the concentration of DEEA are same but slight increase in concentration of MAPA ends up with a very high observed kinetic rat constant.

4.6 Comparison of Aqueous MAPA System & Aqueous Blended System (Current Work)

Two systems are studied in this whole work, the aqueous MAPA system and the blended (MAPA+DEEA) system. The intent of the current work is to judge the behavior of blended systems when the concentration of one amine solution is increases keeping the other constant. Two sets are discussed already in which 1M MAPA is kept constant and then 2M MAPA with variant DEEA.

It is convenient to analyze variations in data points of all the calculated parameters from physical properties till kinetics when one amine is blended with another in different concentrations, so MAPA system along with blends are compared together.

Experimentally determined densities of single (MAPA) system along with blended systems are presented in fig 4.24.

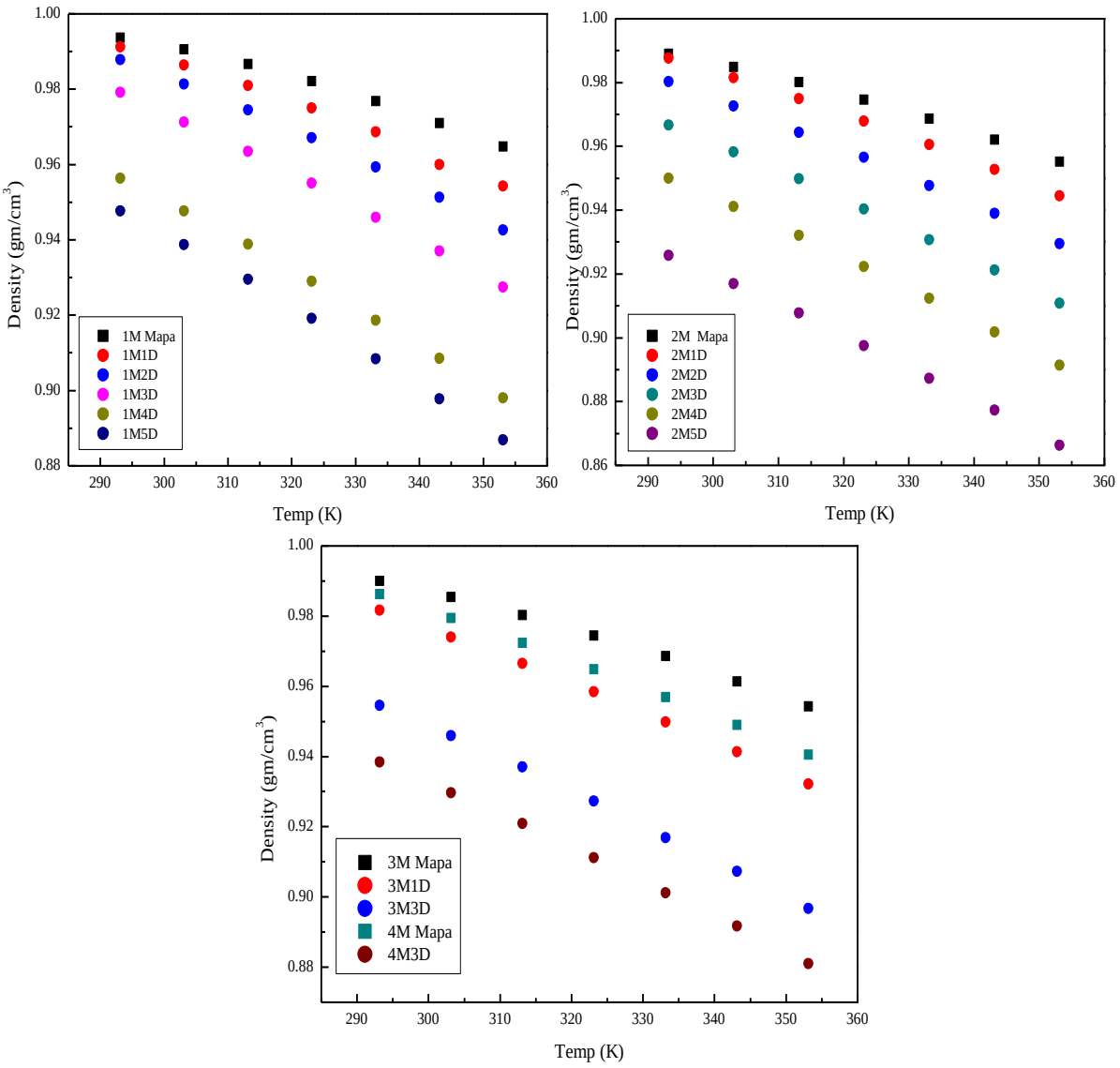

Fig 4.24: Experimental densities of "MAPA" system and Blended "MAPA+DEEA" system at different temperatures

The graphical explanation in each set represents that with the increase in DEEA concentration the density of blended solution decreases. In all cases aqueous MAPA system has higher numerical values, as DEEA is induced density decreases accordingly. 1M4D system was not performed experimentally but in this case in order to judge changes at each concentration, density is interpolated from 1M3D and 1M5D. So slightly change manner from its remaining blends can be seen in 1M4D.

In the same fashion experimental viscosities are also compared for both systems as expressed in fig 4.25.

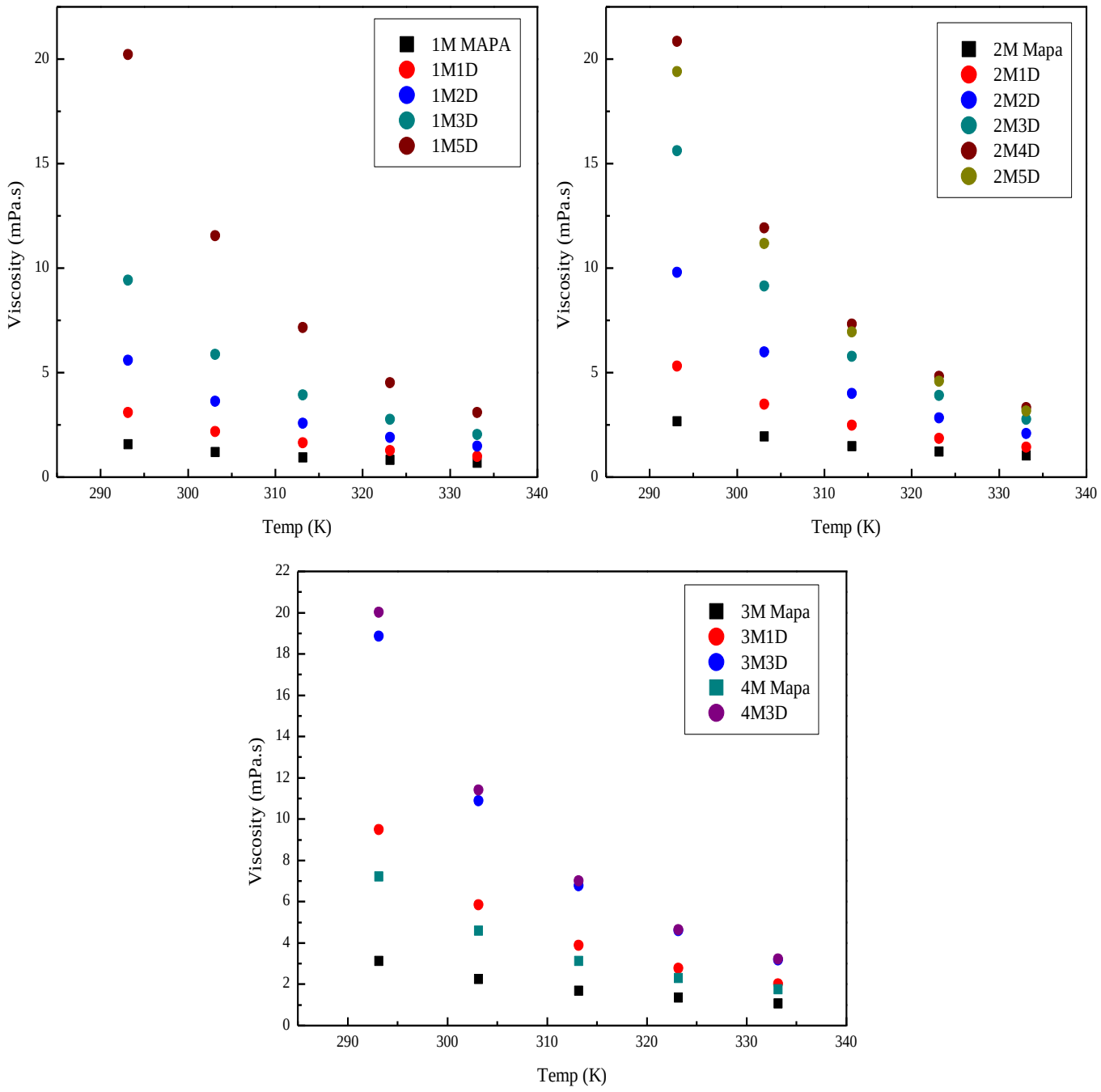

.

Fig 4.25: Experimental viscosities of "MAPA system and Blended "MAPA+DEEA" system

It is concluded that with the increase in DEEA concentration in all blended schemes the viscosity of system increases as single MAPA system has low numerical values in terms of viscosities.

Viscosities of the blended systems are close at lower concentration but a drastic rise can be seen as DEEA concentration approaches to 5M. In second sketch of fig 4.25 a rough trend is detected as 2M4D has higher viscosities as compared to that of 2M5D at higher temperature, it is believed as an experimental error as parallel measurements/runs of samples were not done. Furthermore in third graph of fig 4.25 the viscosities of 3M3D and 4M3D are following the same trend indicating no effect on viscosity change with increase in MAPA concentration.

Solubility measurements that were performed will also be a part of analysis as plotted in fig 4.26

From fig 4.26 it is recognized that with the increase in DEEA concentration henry's constant decreases in all cases. Henry constant is higher in case of single MAPA system. A slight deviation from trend is also observed in case of 3M1D as plotted in third graph of fig 4.26.

Similarly kinetic evaluations are also performed by comparing the MAPA system along with blends.

Observed kinetic rate constants of aqueous MAPA system and blended system are inspected consecutively as plotted in fig 4.27. That are resulted in, increase observed kinetic rate constant at higher concentrations of DEEA i.e. 5M in the light of second graph. While 1M5D is again showing rough behavior because of very low henry's constant values. As kinetic calculations are very much sensitive to henry's constant values. On other side at lower concentrations of DEEA in blended systems the trends are likely same as of aqueous MAPA system indicating very little effect of DEEA in blends at lower concentration.

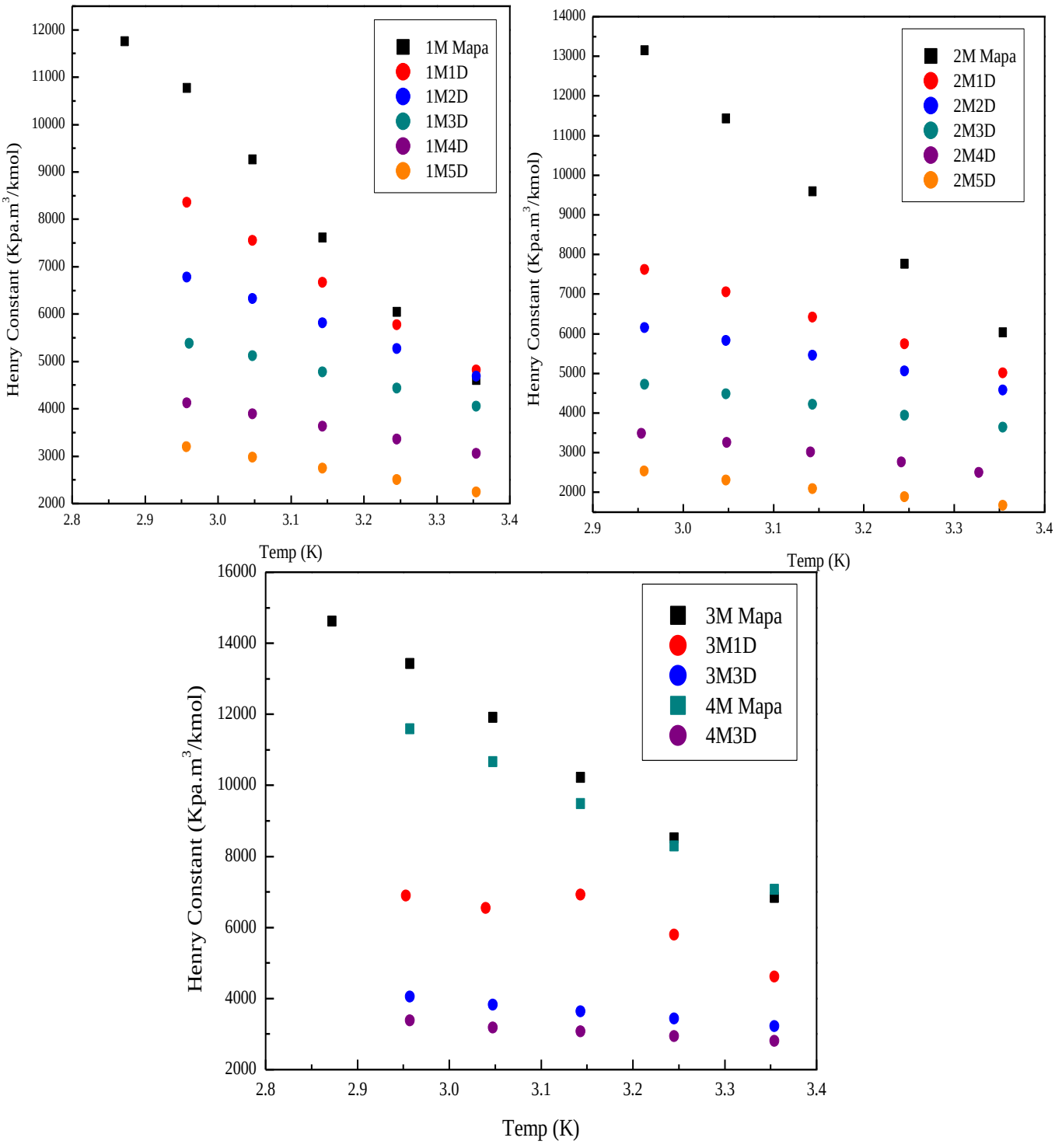

Fig 4.26: Experimentally determined henry's constant for "MAPA" system and Blended "MAPA+DEEA" system

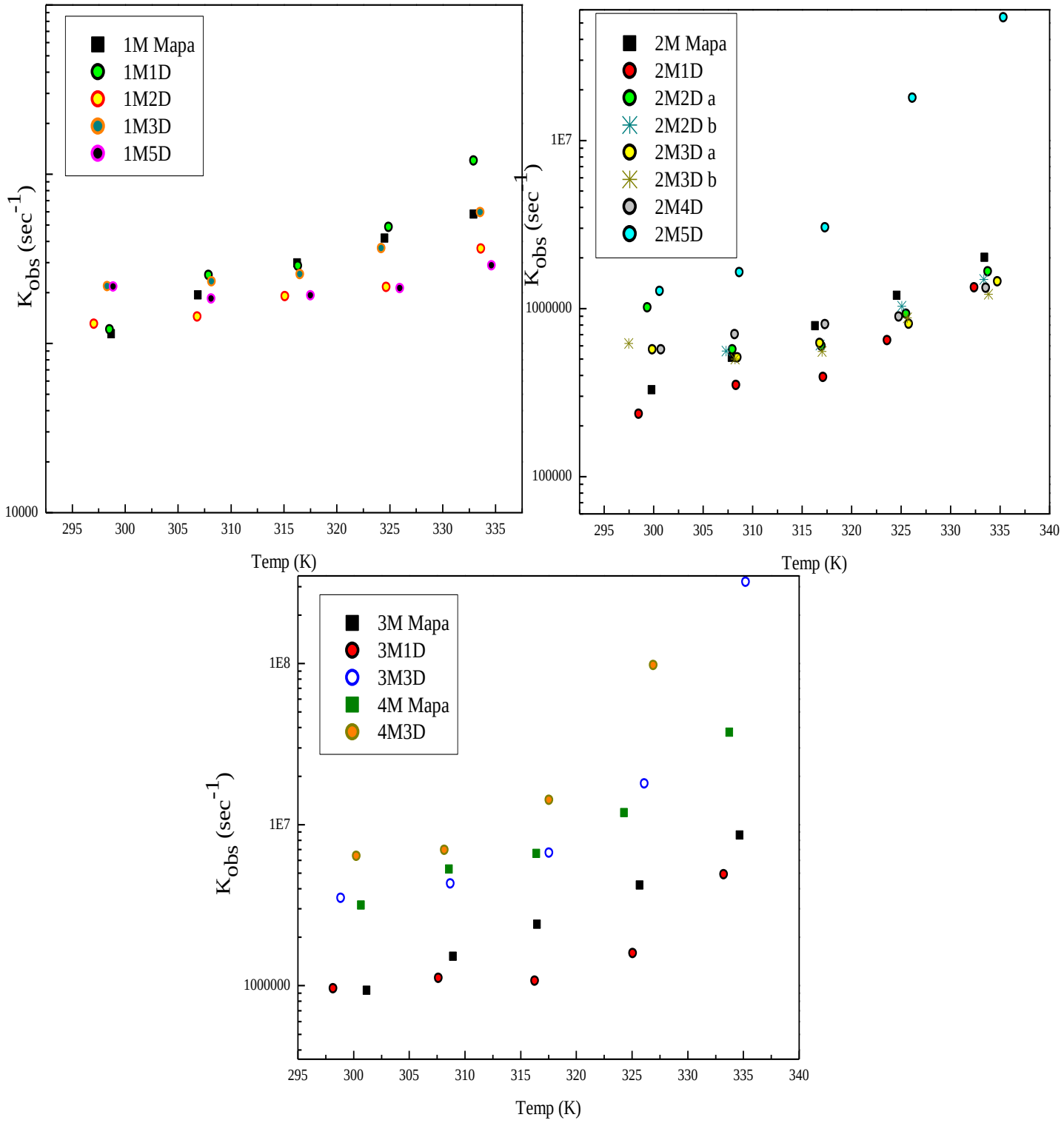

Fig 4.27: Observed kinetic rate constant of "MAPA" system and Blended "MAPA+DEEA" system

Conclusions and Proposed Future Work

The kinetic of CO_2 absorption in aqueous MAPA system and blends of MAPA+DEEA has been studied using the string of discs contactor by the single step-termolecular mechanism (Direct mechanism) approach, proposed by *"Crooks et al., 1989"*.

Kinetic evaluations were done at a temperature ranging from 298.15K-338.15K for both systems. The results indicate that this mechanism can be applied to determine the reaction mechanism of MAPA system and blended "MAPA+DEEA" system. Reproducibility is also analyzed by performing replicate runs of blended system (2M2D and 2M3D).

In addition, physical properties as density and viscosity have been examined to determine the physico-chemical parameters. The solubility of N_2O in both systems was also measured in order to estimate the solubility of CO_2. The solubility should be measured accurately as it affects the second order rate constant much of all. The results of 5M MAPA system and 1M5D system indicates the sensitivity of henry's constant in kinetic evaluation.

Literature was citied in order to analyze the trend of current work. The literature data available is in agreement with the current work.

In future work it is proposed to evaluate the henry's constant values of 5M MAPA system and 1M5D system in replicate runs to ensure its reproducibility. Henry's constant was measured for alternative amine systems, while the remaining was calculated by interpolation of data. It is proposed to examine the henry's constant for each amine system rather than interpolation.

In order to understand the effect of promoter in case of blended system it is preferred to study the kinetics of DEEA system alone as well. In string of discs contactor as amine solution is continuously dripping out in outlet flask so samples should be collected after each run of 5L of solution and analyze them to see the exact effect of the CO_2 absorption.

References

- Anton Paar MCR 100, Picture retrieved from "*Aerosol and Particle Technology Laboratory (APTL)*" http://apt.cperi.certh.gr/.

- Anton Paar DMA 4500M *"Density meter",* Picture retrieved from: info.us@anton-paar.com

- Aronu, E. Ugochukwu,Hartono, A., Hallvard F.Svendsen, *"Density, Viscosity and N_2O Solubility of aquoues amino acid salt and amine amino acid salt solution",* Journal of Chemical Thermodynamics,(**2011**).

- Arunkumar Samanta, S.S. Bandyopadhyay *"Absorption of carbon dioxide into piperazine activated aqueous N-methyldiethanolamine"* Chemical Engineering Journal 171 (**2011**) 734–741

- Astarita, G., Savage, D. W., Bisio, A., *"Gas Treating with Chemical Solvent",* John Wiley & Sons., New York, (**1983**).

- Ardi Hartono, Eirik F.daSilva, Hallvard F.Svendsen *"Kinetics of carbon dioxide absorption in aqueous solution of diethylenetriamine (DETA)",* Chemical Engineering Science 64 (**2009**) 3205 – 3213

- Basma Yaghi and Omar Houache *"Solubility of Nitrous Oxide in Amine Aqueous Solutions"* Journal of Engineering, computing and architecture. ISSN 1937-7197 Volume 2 issue 1 (**2008**).

- Bentiez-Garacia, J.,G. Ruiz-ibanex, H. A. Al-Ghawas and O.C. Sandall, (**1991**), Chem, eng. Sci. 46, 2927.

- Bird, R, B., Stewart, W.E., Lighfoot, E. N. *"Transport phenomena",* 2nd edition, John Wiley & Son, Inc., New York, (**2002**)

- Blauwhoff, P. M. M.; Versteeg, G. F.; van Swaaij, W. P. M. *"A Study on the Reaction between CO2 and Alkanolamines in Aqueous Solutions"*. Chem. Eng. Science. (**1983**)**,** 38, 1411–1429

- Blauwhoff, P. M. M.; Versteeg, G. F.; van Swaaij, W. P. M. *"A Study on the Reaction between CO2 and Alkanolamines in Aqueous Solutions"*. Chem. Eng. Science. (**1984**)**,** 39(2), 207–25

- Brian, P. L. T. *"Gas Absorption Accompanied by an Irreversible Reaction of General Order"*. AIChE J. (**1964**)**,** *10*, 5–10.

- BP, 2005, "*BP Statistical Review of World Energy"*, Retrieved from http://www.bp.com

- Caplow, M., *"Kinetics of Carbamate Formation and Breakdown",* J. Am. Chem Soc., 90, 6795-6803 (**1968**).

- Crooks, J. E:, and Donnellan, J. P.*, "Kinetics and Mechanism of the Reaction between Carbon Dioxide and Amine in Aqueous Solution",* J. Chem. Soc., Perkins Trans., II, 331-333, (**1989**)

- Clarke, J. K. A., *"Kinetics of Absorption of Carbon Dioxide in Monoethanolamine Solutions at Shorts Contact Time"*, Ind. Eng. Chem. Fundam., 3, 239-245, (**1964**)

- Carbon capture project, *CCP* (**2008**); Retrieved from http:// CO_2captureproject.org

- Daniel P. Hagewiesche, Sami S. Ashour, Hani A. Al-Ghawasorville & Orvillec. Sandall *"Absorption of carbon dioxide into aqueous blends of monoethanolamine and n methyldiethanolamine*" Chem. Eng. Science 0009-2509(**1994**) 00489-7.

- Danckwert, P.V., *"The Reaction of CO_2 with Ethanolamine"*, Chem. Eng. Science 34,443-446 (**1979**).

- Da Silva, E. F.; Svendsen, H. F. Ab *"Initio Study of the Reaction of Carbamate formation from CO_2 and Alkanolamines"*. Ind. Eng. Chem. Res. (**2004**)**,** *43,* 3413–3418.

- Donaldson, T. L.; Nguyen, Y. N. *"Carbon Dioxide Reaction Kinetics and Transport in Aqueous Amine Membranes"* Ind. Eng. Chem. Fundam. (**1980**)**,** *19,* 260–266.

- Dindore, V. Y. "*String of Disc Contactor: Process Details and Experimental Set Up";* SINTEF Report; Trondheim, (**2004**).

- DeCoursey, W. J. Absorption with Chemical Reaction: *"Development of a New Relation for the Danckwerts Model"*. Chem. Eng. Sci. (**1974**)**,** *29*, 1867–1872.

- DeCoursey, W. J. *"Enhancement Factor for Gas Absorption with Reversible Reaction"*. Chem. Eng. Sci. (**1982**)**,** *37*, 1483–1489.

- Danckwerts, P. V.; Kennedy, A. M. *"Kinetics of Liquid–Film Process in Gas Absorption. Part I: Models of the Absorption Process"*. Trans. Inst. Chem. Eng. (**1954**), *32*, S49–S52.

- Danckwerts, P. V., (**1970**), *"Gas-Liquid Reaction",* McGraw-Hill, New York.

- Donaldson, T.; Nguyen, Y. N. "*Carbon Dioxide Reaction Kinetics and Transport in Aqueous Amine Membranes*" Ind. Eng. Chem. Fundam. (**1980**), 19, 260-266.

- Edwards, T. J.; Newman, J.; Prausnitz, J. M., *"Thermodynamics of Aqueous Solutions Containing Volatile Weak Electrolyte Solutions",* AIChE J., 21, 248–259, (**1975**).

- Erwin D. Snijder, Marcel J. M. te Riele, Geert F. Versteeg; and W. P. M. van Swaaij *"Diffusion Coefficients of Several Aqueous Alkanolamine Solutions"* J. Chem. Eng. Data (**1993**),38,475-480.

- Froment, G. F.; Bischoff, K. B. "*Chemical Reactor Analysis and Design";* John Wiley & Sons: New York, (**1990**).

- Hartono, A., Juliussen, O., Svendsen, H. F.,*"Solubility of N_2O in Aqueous Solution of Diethylenetriamine (DETA)"*, J. Chem. Eng. Data., 53 (11), 2696–2700, (**2008**).

- Haruo Hikia, Satoru asai Yoshio katsu and Seiichi ikuno*, "Absorption of Carbon Dioxide into Aqueous Monoethanola mine Solutions"* AlChE Journal (Vol. 25, No. 5) Sep (**1979**).

- Hatta, S., Technological Reports of Tôhoku University, 10, 613-622.

- Higbie, R.,*"The Rate of Absorption of a Pure Gas into a Still Liquid during Short Periods Exposure",* Trans.Am.Inst.Chem.Eng.31, 365-389, (**1935**).

- IPCC, Intergovernmental Panel on Climate Change, (**2007**). Synthesis Report: *"Contribution of working groups 1,2,3 to fourth assessment report of the intergovernmental panel on climate change core writing*", Pachauri,R.K. and Reisinger, A. (Eds.). IPCC, Geneva, Switzerland.

- IPCC. (**2005**). "IPCC Special Report, *"Carbon Dioxide Capture and Storage",* Technical Summary Retrieved from: http://www.ipcc.ch/pdf/special reports/srccs/srccs_technicalsummary.pdf

- IEA GHG "*Putting carbon dioxide back in the ground'* IEA Greenhouse Gas R&D Programme, (**2002**), ISBN 1 898373 28 0.

- IEA, International Energy Agency, (**2010**) a. *"World energy outlook"* , Executive summary.

- IEA, International Energy Agency, (**2010**) b. *"Key world energy statistics".*

- Jose´ D. Figueroa , Timothy Fout , Sean Plasynski, Howard McIlvried, Rameshwar D. Srivastava Deshmukh, R. D.*; "Advances in CO_2 capture technology*"—The U.S. Department of Energy's Carbon Sequestration Program (**2008**).

- Jørgensen, E.; Faurholt, C. *"Reaction between Carbon Dioxide and Amino Alcohols II. Triethanolamine".* Acta Chem. Scand. (**1954**)**,** *8,* 1141–1144.

- Juelin Li, Amr Henni, and Paitoon Tontiwachwuthikul *"Reaction Kinetics of CO_2 in Aqueous Ethylenediamine, Ethyl Ethanolamine, and Diethyl Monoethanolamine Solutions in the Temperature Range of 298-313 K, Using the Stopped-Flow Technique"* Ind. Eng. Chem. Res. (**2007**), 46, 4426-4434.

- Koomey, J. G., Krause, F. (**2009**). "*Why two degrees really matters".* Retrieved from http://thinkprogress.org/climate/2009/12/06/205058/copenhagen-two-degrees-warmingtarget/?mobile=nc.

- Kohl, A.; Nielsen, R. "*Gas Purification";* Gulf Publishing Company: Houston, (**1997**).

- Littel, R.J., Versteeg, G. F., van Swaaij, P.M., *"Solubility and diffusivity for the absorption of COS, CO_2 and N_2O in amine solutions"*, J.Chem.Eng.Data, 37(1), 49-55, (**1992**).

- Li, M.-H.; Lai, M.-D. *"Solubility and Diffusivity of N_2O and CO_2 in (Monoethanolamine + N-Methyldiethanolamine + Water) and in (Monoethanolamine +2-Amino-2-methyl-1-propanol + Water)".* J. Chem. Eng. Data (**1995**), 40, 486−492.

- Liebenthal, U.; Pinto, D.D.D.; Monteiro, J. G. M.-S.; Svendsen, H. F.; Kather, A. "*Overall process analysis and optimization for CO2 capture from coal fired power plants based on phase change solvents forming two liquid phases".* 11th International Conference on Greenhouse Gas Control Technologies, 18 - 22 November (**2012**), Kyoto, Japan

- Mandal, B. P.; Kundu, M.; Padhiyar, N. U.; Bandyopadhyay, S. S. *"Physical Solubility and Diffusivity of N_2O and CO_2 into Aqueous Solutions of (2-Amino-2-methyl-1-propanol + Monoethanolamine) and (N-Methyldiethanolamine + Monoethanolamine)".* J. Chem. Eng. Data (**2005**), 50, 352−358.

- Mannford Doble, M. "*Ph.D. Thesis"*, Cambridge University, (**1996**)

- Mohammad R.M. Abu-Zahra, John P.M. Niederer, Paul H.M. Feron; Geert F. Versteeg, CO2 capture from power plants: Part II. "*A parametric study of the economical performance based on mono-ethanolamine"*. March (**2007**).

- Onda, K.; Sada, E.; Kobayashi, T.; Fujine, M. *"Gas Absorption Accompanied by Complex Chemical Reactions – I Reversible Chemical Reactions".* Chem. Eng. Sci. (**1970**), *25*, 753–760.

- Olander, D. R. *"Simultaneous Mass Transfer and Equilibrium Chemical Reaction".* AIChE J. (**1960**)**,** *6*, 233–239.

- Plaza, M.G., García, S., Rubiera, F., Pis, J.J. and Pevida, C. (**2010**). *"Post-Combustion CO_2 Capture with a Commercial Activated Carbon: Comparison of Different Regeneration Strategies".* Chem. Eng. J. 163: 41–4

- P.H.M. Feron and C.A. Hendriks *"CO_2 Capture Process Principles and Costs"* Oil & Gas Science and Technology – Rev. IFP, Vol. 60 (**2005**), No. 3, pp. 451-459.

- Peter Folger, "*Carbon Capture: A Technology Assessment, Specialist in Energy and Natural Resources Policy"* July 19, (**2010**).

- Peter W. Derks, Kees J. Hogendoorn, and Geert F. Versteeg *"Solubility of N_2O in and Density, Viscosity, and Surface Tension of Aqueous Piperazine Solutions"* J. Chem. Eng. Data (**2005**), *50,* 1947-1950.

- Perry, R. H.; Pigford, R. L. *"Kinetics of Gas–Liquid Reactions".* Ind. Eng. Chem. (**1953**)**,** *45*, 1247–1253.

- Porter, K. E. *"The Effect of Contact–Time Distribution on Gas Absorption with Chemical Reaction"*. Trans. Instn. Chem. Engrs. (**1966**)**,** *44*, T25–T36.

- Pinsent, B. R. W., Pearson, L., Roughton, F. W. J.*, "The Kinetics of Combination of Carbon Dioxide with Hydroxide Ions",* Trans. Faraday Soc., 52, 1512-1520, (**1956**).

- Prausnitz, J. M.; Lichtenthaler, R. N.; and de Azevedo, E. D., *"Molecular Thermodynamics of Fluid-phase Equilibira"*, (3rd ed.), Prentice Hall PTR; New Jersey (**1999**).

- Prachi Singh n, W.P.M.vanSwaaij, D.W.F.(Wim)Brilman *"Kinetics study of carbon dioxide absorption in aqueous solutions of 1,6hexamethyldiamine(HMDA) and 1,6-hexamethyldiamine, N,N0 di-methyl(HMDA,N,N0)"* Chemical Engineering Science 66 (**2011**) 4521–4532.

- P.W.J. Derks, T. Kleingeld, C. van Aken, J.A. Hogendoorn, G.F. Versteeg *"Kinetics of absorption of carbon dioxide in aqueous piperazine solutions"* Chemical Engineering Science 61 (**2006**) 6837 – 6854.

- Sholeh Ma'mun *"Selection and Characterization of New Absorbents for Carbon Dioxide Capture*" Doctoral thesis Faculty of Natural Science and Technology, Department of Chemical Engineering, NTNU Trondheim, Norway (**2005**).

- Shyh-Yun Horng and Meng-Hui Li *"Kinetics of Absorption of Carbon Dioxide into Aqueous Solutions of Monoethanolamine + Triethanolamine"* Ind. Eng. Chem. Res.(**2002),** *41,* 257-266

- Secor, R. M.; Beutler, J. A. *"Penetration Theory for Diffusion Accompanied by a Reversible Chemical Reaction with Generalized Kinetics".* AIChE J. **(1967),** *13*, 365–373.

- Stephens, E. J.; Morris, G. A. *"Determination of Liquid–Film Absorption Coefficient: A New Type of Column and Its Application to Problems of Absorption in Presence of Chemical Reaction".* Chem. Eng. Prog. (**1951**)**,** *47,* 232–242.

- Tiepel, E.W.; Gubbins, K. E.;Can. J., *"Theory of gas solubility in mixed solvent systems"*, Chem. Eng. (**1972**), 50, 361–365.

- Versteeg, G. F.; van Dijck, L. A. J.; van Swaaij, W. P. M. "*On the kinetics between CO2 and Alkanolamines both in Aqueous and Nonaqueous Solutions".* An Overview. Chem. Eng. Commun. (**1996**), 144, 113-158.

- Versteeg, G. F., van Swaiij, W. P. M., *"Solubility and Diffusivity of Acid Gases (CO_2, N_2O) in Aqueous Alkanolamines Solutions"*, J. Chem. Eng. Data., 33, 29-34, (**1988**).

- Versteeg, G. F.; van Swaiij; W. P. M.,*"Solubility and Diffusivity of Acid Gases (Carbon Dioxide and Nitrous Oxide) in Aqueous Alkanolamine Solutions",* J. Chem. Eng. Data, 33, 29-34, (**1988**).

- *Why CCS?* (2012). Retrieved from the Zero website: http://www.zero.no/ccs/introduction/whyccs.

Appendix A: Physiochemical Properties

Table A1: Experimental density data of aqueous MAPA system at temperatures 20-80 ^{0}C

Temp ^{0}C	Temp K	Concentration mol/l	Weight fraction	Density gm/cm^3		Difference gm/cm^3
80	353.15	**5M Mapa***	0.4407	0.92760	0.92760	0
70	343.15	5M Mapa	0.4407	0.93688	0.93687	0.001067
60	333.15	5M Mapa	0.4407	0.94555	0.94554	0.001058
50	323.15	5M Mapa	0.4407	0.9545	0.95448	0.002095
40	313.15	5M Mapa	0.4407	0.96281	0.96281	0
30	303.15	5M Mapa	0.4407	0.97124	0.97123	0.00103
20	293.15	5M Mapa	0.4407	0.97925	0.97926	-0.00102
80	353.15	**4M Mapa**	0.3651	0.94046	0.94045	0.001063
70	343.15	4M Mapa	0.3651	0.94894	0.94893	
60	333.15	4M Mapa	0.3651	0.95696	0.95695	0.001045
50	323.15	4M Mapa	0.3651	0.96488	0.96486	0.002073
40	313.15	4M Mapa	0.3651	0.97233	0.97233	0
30	303.15	4M Mapa	0.3651	0.97945	0.97944	0.001021
20	293.15	4M Mapa	0.3651	0.98626	0.98626	0
80	353.15	**3M Mapa**	0.2718	0.95419	0.95419	0
70	343.15	3M Mapa	0.2718	0.96134	0.96134	0
60	333.15	3M Mapa	0.2718	0.96864	0.96863	0.001032
50	323.15	3M Mapa	0.2718	0.97446	0.97445	0.001026
40	313.15	3M Mapa	0.2718	0.98023	0.98023	0
30	303.15	3M Mapa	0.2718	0.98546	0.98546	0
20	293.15	3M Mapa	0.2718	0.99003	0.99003	0
80	353.15	**2M Mapa**	0.1803	0.95515	0.95515	0
70	343.15	2M Mapa	0.1803	0.96213	0.96212	0.001039
60	333.15	2M Mapa	0.1803	0.96863	0.96862	0.001032
50	323.15	2M Mapa	0.1803	0.97464	0.97463	0.001026
40	313.15	2M Mapa	0.1803	0.98006	0.98007	-0.00102
30	303.15	2M Mapa	0.1803	0.9849	0.98491	-0.00102
20	293.15	2M Mapa	0.1803	0.98905	0.98905	
80	353.15	**1M Mapa**	0.0891	0.96472	0.96472	0
70	343.15	1M Mapa	0.0891	0.97102	0.97101	0.00103
60	333.15	1M Mapa	0.0891	0.97685	0.97684	0.001024
50	323.15	1M Mapa	0.0891	0.9821	0.98209	0.001018
40	313.15	1M Mapa	0.0891	0.98665	0.98665	0
30	303.15	1M Mapa	0.0891	0.99057	0.99057	0
20	293.15	1M Mapa	0.0891	0.99359	0.9936	-0.00101

* Bold text just represents starting of the sample

Table A2: Density Parameters (Eq4.1)

Solvent	Parameters				
MAPA	K1	K2	K3	K4	K5
	0.48691	71.3021	1.9389E4	411.5582	59046.5252

Table A3: Experimental density data of aqueous Blended system at temperatures 20-80 ^{0}C

Temp ^{0}C	Temp K	Concentration mol/l	Weight fraction	Density gm/cm^3		Difference
80	353.15	**2M1D***	0.1205	0.94453	0.94452	0.001059
70	343.15	2M1D	0.1205	0.95275	0.95274	0.00105
60	333.15	2M1D	0.1205	0.96046	0.96044	0.002082
50	323.15	2M1D	0.1205	0.9679	0.96788	0.002066
40	313.15	2M1D	0.1205	0.97484	0.97484	0
30	303.15	2M1D	0.1205	0.98141	0.98141	0
20	293.15	2M1D	0.1205	0.98764	0.98764	0
80	353.15	**2M2D**	0.2477	0.92947	0.92947	0
70	343.15	2M2D	0.2477	0.93892	0.93892	0
60	333.15	2M2D	0.2477	0.94766	0.94765	0.001055
50	323.15	2M2D	0.2477	0.95651	0.9565	0.001045
40	313.15	2M2D	0.2477	0.96429	0.96431	-0.00207
30	303.15	2M2D	0.2477	0.9726	0.9726	0
20	293.15	2M2D	0.2477	0.98025	0.98026	-0.00102
80	353.15	**2M3D**	0.3735	0.91075	0.91075	0
70	343.15	2M3D	0.3735	0.92127	0.92128	-0.00109
60	333.15	2M3D	0.3735	0.93068	0.93066	0.002149
50	323.15	2M3D	0.3735	0.94031	0.94029	0.002127
40	313.15	2M3D	0.3735	0.94978	0.94978	0
30	303.15	2M3D	0.3735	0.95827	0.95828	-0.00104
20	293.15	2M3D	0.3735	0.96662	0.96663	-0.00103
80	353.15	**2M4D**	0.4821	0.89138	0.89138	0
70	343.15	2M4D	0.4821	0.90180	0.90180	0
60	333.15	2M4D	0.4821	0.91227	0.91226	0.001096
50	323.15	2M4D	0.4821	0.92228	0.92227	0.001084
40	313.15	2M4D	0.4821	0.93207	0.93208	-0.00107

30	303.15	2M4D	0.4821	0.94115	0.94117	-0.00213
20	293.15	2M4D	0.4821	0.94996	0.94997	-0.00105
80	353.15	**2M5D**	0.6499	0.86631	0.86630	0.001154
70	343.15	2M5D	0.6499	0.87730	0.87729	0.00114
60	333.15	2M5D	0.6499	0.88728	0.88726	0.002254
50	323.15	2M5D	0.6499	0.89753	0.89751	0.002228
40	313.15	2M5D	0.6499	0.90771	0.90773	0.002228
30	303.15	2M5D	0.6499	0.91685	0.91689	-0.00436
20	293.15	2M5D	0.6499	0.92572	0.92572	0
80	353.15	**1M3D**	0.3649	0.92745	0.92745	0
70	343.15	1M3D	0.3649	0.93708	0.93707	0.001067
60	333.15	1M3D	0.3649	0.94596	0.94595	0.001057
50	323.15	1M3D	0.3649	0.95499	0.95497	0.002094
40	313.15	1M3D	0.3649	0.96351	0.96351	0
30	303.15	1M3D	0.3649	0.97125	0.97126	-0.00103
20	293.15	1M3D	0.3649	0.97915	0.97916	-0.00102
80	353.15	**1M5D**	0.6293	0.88690	0.88690	0
70	343.15	1M5D	0.6293	0.89775	0.89774	0.001114
60	333.15	1M5D	0.6293	0.90833	0.90832	0.001101
50	323.15	1M5D	0.6293	0.91919	0.91918	0.001088
40	313.15	1M5D	0.6293	0.9295	0.92952	-0.00215
30	303.15	1M5D	0.6293	0.93875	0.93882	-0.00746
20	293.15	1M5D	0.6293	0.94769	0.9477	-0.00106
80	353.15	**3M3D**	0.3716	0.89669	0.89668	0.001115
70	343.15	3M3D	0.3716	0.90722	0.90721	0.001102
60	333.15	3M3D	0.3716	0.91679	0.91678	0.001091
50	323.15	3M3D	0.3716	0.92735	0.92734	0.001078
40	313.15	3M3D	0.3716	0.93704	0.93706	-0.00213
30	303.15	3M3D	0.3716	0.94595	0.94598	-0.00317
20	293.15	3M3D	0.3716	0.95455	0.95455	0
80	353.15	**4M3D**	0.3789	0.88102	0.88101	0.001135
70	343.15	4M3D	0.3789	0.89166	0.89164	0.002243
60	333.15	4M3D	0.3789	0.90113	0.90112	0.00111
50	323.15	4M3D	0.3789	0.91116	0.91114	0.002195

40	313.15	4M3D	0.3789	0.92088	0.92089	-0.00109
30	303.15	4M3D	0.3789	0.9297	0.92975	-0.00538
20	293.15	4M3D	0.3789	0.93845	0.93846	-0.00107
80	353.15	**3M1D**	0.1215	0.93216	0.93215	0.001073
70	343.15	3M1D	0.1215	0.94130	0.94129	0.001062
60	333.15	3M1D	0.1215	0.94985	0.94983	0.002106
50	323.15	3M1D	0.1215	0.95842	0.95841	0.001043
40	313.15	3M1D	0.1215	0.96651	0.96651	0
30	303.15	3M1D	0.1215	0.97402	0.97405	-0.00308
20	293.15	3M1D	0.1215	0.98166	0.98166	0
80	353.15	**1M2D**	0.2385	0.94255	0.94255	0
70	343.15	1M2D	0.2385	0.95127	0.95126	0.001051
60	333.15	1M2D	0.2385	0.95926	0.95925	0.001042
50	323.15	1M2D	0.2385	0.96713	0.96711	0.002068
40	313.15	1M2D	0.2385	0.97441	0.97442	-0.00103
30	303.15	1M2D	0.2385	0.98134	0.98136	-0.00204
20	293.15	1M2D	0.2385	0.98783	0.98783	0
80	353.15	**1M1D**	0.1198	0.95426	0.95424	0.002096
70	343.15	1M1D	0.1198	0.96001	0.96001	0
60	333.15	1M1D	0.1198	0.96858	0.96859	-0.00103
50	323.15	1M1D	0.1198	0.97496	0.97495	0.001026
40	313.15	1M1D	0.1198	0.981	0.981	0
30	303.15	1M1D	0.1198	0.98638	0.98638	0
20	293.15	1M1D	0.1198	0.99117	0.99118	-0.00101

* Bold text just represents starting of the sample and denotations are made to simplify as M indicates MAPA concentration and D represents DEEA concentration.

Table A4: Experimental density data of Water at temperatures 20-80 ^{0}C

Temp ^{0}C	Temp K	Density gm/cm^3		Difference gm/cm^3
80	353.15	0.97190	0.97190	0
70	343.15	0.97785	0.97785	0
60	333.15	0.98329	0.98328	0.001017
50	323.15	0.98813	0.98812	0.001012
40	313.15	0.92220	0.92230	0.01084
30	303.15	0.99572	0.99572	0
20	293.15	0.99819	0.99819	0

Table A5: Experimental viscosity data of aqueous MAPA system at temperatures 20-60 ^{0}C

Temp ^{0}C	Temp K	Concentration mol/l	Weight fraction	viscosity mPa.s
20	293.15	**1M Mapa**	0.0891	1.5566
30	303.15	1M Mapa	0.0891	1.1907
40	313.15	1M Mapa	0.0891	0.94221
50	323.15	1M Mapa	0.0891	0.81542
60	333.15	1M Mapa	0.0891	0.67336
20	293.15	**2M Mapa**	0.1803	2.6734
30	303.15	2M Mapa	0.1803	1.937
40	313.15	2M Mapa	0.1803	1.467
50	323.15	2M Mapa	0.1803	1.2039
60	333.15	2M Mapa	0.1803	1.0331
20	293.15	**3M Mapa**	0.2718	3.1306
30	303.15	3M Mapa	0.2718	2.2364
40	313.15	3M Mapa	0.2718	1.6743
50	323.15	3M Mapa	0.2718	1.3518
60	333.15	3M Mapa	0.2718	1.0663
20	293.15	**4M Mapa**	0.3651	7.2112
30	303.15	4M Mapa	0.3651	4.5946
40	313.15	4M Mapa	0.3651	3.1331
50	323.15	4M Mapa	0.3651	2.2954
60	333.15	4M Mapa	0.3651	1.7526
20	293.15	**5M Mapa**	0.4407	12.386
30	303.15	5M Mapa	0.4407	7.3773
40	313.15	5M Mapa	0.4407	4.796
50	323.15	5M Mapa	0.4407	3.4407
60	333.15	5M Mapa	0.4407	2.3698

Table A6: Viscosity Parameters (Eq 4.2)

Solvent	Parameters				
MAPA	K1	K2	K3	K4	K5
	2.74E-3	10.1592	5.4578E5	1713.87	7.594E5

Table A7: Experimental viscosity data of aqueous Blended system at temperatures 20-60 ^{0}C

Temp ^{0}C	Temp K	Concentration mol/l	Weight fraction	viscosity mPa.s
20	293.15	**1M1D**	0.1198	3.0937
30	303.15	1M1D	0.1198	2.1819
40	313.15	1M1D	0.1198	1.6352
50	323.15	1M1D	0.1198	1.2693
60	333.15	1M1D	0.1198	0.98868
20	293.15	**1M5D**	0.6293	20.204
30	303.15	1M5D	0.6293	11.548
40	313.15	1M5D	0.6293	7.1605
50	323.15	1M5D	0.6293	4.5125
60	333.15	1M5D	0.6293	3.0891
20	293.15	**2M1D**	0.1205	5.3125
30	303.15	2M1D	0.1205	3.4849
40	313.15	2M1D	0.1205	2.4714
50	323.15	2M1D	0.1205	1.8387
60	333.15	2M1D	0.1205	1.4196
20	293.15	**2M5D**	0.6499	19.399
30	303.15	2M5D	0.6499	11.162
40	313.15	2M5D	0.6499	6.9377
50	323.15	2M5D	0.6499	4.5792
60	333.15	2M5D	0.6499	3.1508
20	293.15	**1M3D**	0.3649	9.4204
30	303.15	1M3D	0.3649	5.8713
40	313.15	1M3D	0.3649	3.9228
50	323.15	1M3D	0.3649	2.7554
60	333.15	1M3D	0.3649	2.0258
20	293.15	**2M3D**	0.3735	15.604
30	303.15	2M3D	0.3735	9.1397
40	313.15	2M3D	0.3735	5.7826
50	323.15	2M3D	0.3735	3.9006
60	333.15	2M3D	0.3735	2.7671

20	293.15	**2M2D**	0.2477	9.7858
30	303.15	2M2D	0.2477	5.9787
40	313.15	2M2D	0.2477	3.9981
50	323.15	2M2D	0.2477	2.8172
60	333.15	2M2D	0.2477	2.0735
20	293.15	**2M4D**	0.4821	20.85
30	303.15	2M4D	0.4821	11.912
40	313.15	2M4D	0.4821	7.3068
50	323.15	2M4D	0.4821	4.824
60	333.15	2M4D	0.4821	3.3207
20	293.15	**1M2D**	0.2385	5.5779
30	303.15	1M2D	0.2385	3.6268
40	313.15	1M2D	0.2385	2.5792
50	323.15	1M2D	0.2385	1.9029
60	333.15	1M2D	0.2385	1.4656
20	293.15	**3M1D**	0.1215	9.4809
30	303.15	3M1D	0.1215	5.8409
40	313.15	3M1D	0.1215	3.8862
50	323.15	3M1D	0.1215	2.7677
60	333.15	3M1D	0.1215	2.0081
20	293.15	**4M3D**	0.3789	20.009
30	303.15	4M3D	0.3789	11.393
40	313.15	4M3D	0.3789	7.0032
50	323.15	4M3D	0.3789	4.6393
60	333.15	4M3D	0.3789	3.2137
20	293.15	**3M3D**	0.3716	18.842
30	303.15	3M3D	0.3716	10.883
40	313.15	3M3D	0.3716	6.7687
50	323.15	3M3D	0.3716	4.5851
60	333.15	3M3D	0.3716	3.1592

Table A8: Experimental Henry constant for aqueous MAPA system at temperatures 25-65, 75 ^{0}C

Temp ^{0}C	Temp K	Concentration mol/l	Weight fraction	Henry constant Kpa.m^3/kmol
75.01	348.16	**1M Mapa**	0.0882	11752.06
65.00	338.15	1M Mapa	0.0882	10768.72
55.01	328.16	1M Mapa	0.0882	9258.76
45.00	318.15	1M Mapa	0.0882	7607.85
35.00	308.14	1M Mapa	0.0882	6038.92
25.00	298.15	1M Mapa	0.0882	4604.09
65.00	338.15	**2M Mapa**	0.1769	13144.02
55.00	328.15	2M Mapa	0.1769	11433.84
45.00	318.15	2M Mapa	0.1769	9592.199
35.00	308.15	2M Mapa	0.1769	7765.935
25.00	298.15	2M Mapa	0.1769	6027.405
75.00	348.15	**3M Mapa**	0.265	14620.42
65.01	338.16	3M Mapa	0.265	13430.22
55.00	328.15	3M Mapa	0.265	11909.76
45.00	318.15	3M Mapa	0.265	10223.16
35.00	308.15	3M Mapa	0.265	8514.56
25.00	298.15	3M Mapa	0.265	6846.90
65.00	338.15	**4M Mapa**	0.355	11589.29
55.00	328.15	4M Mapa	0.355	10662.55
45.00	318.15	4M Mapa	0.355	9488.659
35.00	308.15	4M Mapa	0.355	8284.601
25.00	298.15	4M Mapa	0.355	7072.297
65.00	338.15	**5M Mapa**	0.4396	8279.26
55.00	328.15	5M Mapa	0.4396	7893.02
45.00	318.15	5M Mapa	0.4396	7527.60
35.00	308.15	5M Mapa	0.4396	7151.62
25.01	298.16	5M Mapa	0.4396	6720.89

Table A9: Henry constant Parameters (Eq 4.3)

Solvent	Parameters				
MAPA	K1	K2	K3	K4	K5
	3487.92	8.4368E6	6.364E8	2005.66	868706

Table A10: Experimental Henry constant for aqueous Blended system at temperatures 25-65^{0}C

Temp ^{0}C	Temp K	Concentration mol/l	Weight fraction	Henry constant Kpa.m^3/kmol
65.00	338.15	**1M1D**	0.2056	8354.82
55.00	328.15	1M1D	0.2056	7551.85
45.00	318.15	1M1D	0.2056	6666.86
35.00	308.15	1M1D	0.2056	5768.55
25.00	298.15	1M1D	0.2056	4816.92
65.00	338.15	**1M2D**	0.3250	6776.15
55.00	328.15	1M2D	0.3250	6321.83
45.00	318.15	1M2D	0.3250	5806.96
35.00	308.15	1M2D	0.3250	5264.40
25.00	298.15	1M2D	0.3250	4684.46
64.64	337.79	**1M3D**	0.4410	5380.96
55.02	328.17	1M3D	0.4410	5113.44
45.00	318.15	1M3D	0.4410	4778.75
35.00	308.15	1M3D	0.4410	4429.17
25.00	298.15	1M3D	0.4410	4047.83
65.02	338.17	**1M5D**	0.6740	3199.37
55.00	328.15	1M5D	0.6740	2975.15
45.00	318.15	1M5D	0.6740	2746.53
35.00	308.15	1M5D	0.6740	2504.59
25.00	298.15	1M5D	0.6740	2244.65
65.00	338.15	**2M1D**	0.2940	7619.42
55.00	328.15	2M1D	0.2940	7049.54
45.00	318.15	2M1D	0.2940	6414.20
35.01	308.16	2M1D	0.2940	5743.75
25.00	298.15	2M1D	0.2940	5014.80
65.00	338.15	**2M2D**	0.4165	6155.31
55.00	328.15	2M2D	0.4165	5824.96
45.01	318.16	2M2D	0.4165	5453.70
35.00	308.15	2M2D	0.4165	5055.61
25.00	298.15	2M2D	0.4165	4574.75
65.00	338.15	**2M3D**	0.5280	4718.02
55.00	328.15	2M3D	0.5280	4475.10
45.00	318.15	2M3D	0.5280	4213.48
35.00	308.15	2M3D	0.5280	3935.56
25.00	298.15	2M3D	0.5280	3635.78
65.37	338.52	**2M4D**	0.6451	3488.38
54.88	328.03	2M4D	0.6451	3255.41
45.20	318.35	2M4D	0.6451	3012.26
35.35	308.50	2M4D	0.6451	2763.69

27.39	300.54	2M4D	0.6451	2496.76
65.03	338.18	**2M5D**	0.7623	2532.93
55.00	328.15	2M5D	0.7623	2305.57
45.00	318.15	2M5D	0.7623	2091.84
35.00	308.15	2M5D	0.7623	1881.89
25.00	298.15	2M5D	0.7623	1666.59
25.00	298.15	**4M3D**	0.7042	2801.41
35.00	308.15	4M3D	0.7042	2936.051
45.00	318.15	4M3D	0.7042	3068.896
55.00	328.15	4M3D	0.7042	3182.564
65.00	338.15	4M3D	0.7042	3375.625
25.00	298.15	**3M1D**	0.3816	4620.699
35.00	308.15	3M1D	0.3816	5793.154
45.00	318.15	3M1D	0.3816	6917.365
55.00	328.15	3M1D	0.3816	6551.545
65.00	338.15	3M1D	0.3816	6890.137
25.00	298.15	**3M3D**	0.6160	3219.001
35.00	308.15	3M3D	0.6160	3436.301
45.00	318.15	3M3D	0.6160	3641.763
55.00	328.15	3M3D	0.6160	3829.485
65.00	338.15	3M3D	0.6160	4047.48

Appendix B: Kinetics

Appendix B1: Kinetics data of aqueous MAPA System

1M MAPA

T	LMa	10^5. kl	10^2. kg	10^2. kg	10^{-3}. H_{CO_2}	LMP CO_2	LMP *CO_2	10^3. N_{CO_2}	10^3. kg	10^3. KG	KG/kg	E	k_2	kobs (1/s)	$10^3.N_{CO_2}$ (mod)
(^{0}C)	(mol CO^2/ mol Amine)	(m/s)	(m/s)	(mol/m^2 kpa s)	(kpa m^3/mol)	(kpa)	(kpa)	(mol/ m^2 s)	(mol/m^2 kpa s)	(mol/m^2 kpa s)	(%)				(mol/ m^2 s)
25.53	0.00	5.59	3.84	1.53	3.35	0.26	0.000	0.80	3.75	3.01	19.67	225.1	114.28	1.1368E+5	0.92
33.73	0.00	6.85	3.90	1.52	4.26	0.25	0.000	0.85	4.27	3.33	21.91	265.9	195.01	1.9334E+5	0.90
43.11	0.00	8.27	3.95	1.50	5.21	0.25	0.000	0.92	4.89	3.68	24.63	307.9	302.47	2.9847E+5	0.94
51.37	0.00	9.84	3.96	1.46	5.95	0.25	0.000	0.98	5.54	4.02	27.55	335.3	425.35	4.1786E+5	0.99
59.76	0.01	11.09	3.58	1.29	6.65	0.24	0.000	1.03	6.26	4.21	32.71	375.6	592.35	5.7912E+5	1.01

2M MAPA

T	LMa	10^5. kl	10^2. kg	10^2. kg	10^{-3}. H_{CO_2}	LMP CO_2	LMP* CO_2	10^3. N_{CO_2}	10^3. kg	10^3. KG	KG/kg	E	k_2	kobs (1/s)	$10^3.N_{CO_2}$ (mod)
(^{0}C)	(mol CO^2/ mol Amine)	(m/s)	(m/s)	(mol/m^2 kpa s)	(kpa m^3/mol)	(kpa)	(kpa)	(mol/ m^2 s)	(mol/m^2 kpa s)	(mol/m^2 kpa s)	(%)				(mol/ m^2 s)
26.64	0.00	3.65	3.86	1.54	4.61	0.26	0.000	0.79	3.84	3.07	19.90	484.2	163.38	3.2813E+5	0.99
34.74	0.00	4.73	3.98	1.55	5.56	0.24	0.000	0.85	4.49	3.48	22.43	527.1	255.16	5.1044E+5	1.01
43.15	0.00	6.02	4.01	1.52	6.50	0.24	0.000	0.96	5.39	3.98	26.15	582.5	397.33	7.9103E+5	1.08
51.42	0.00	7.18	4.07	1.50	7.38	0.24	0.000	1.06	6.45	4.51	30.04	662.6	604.13	1.1966E+6	1.14
60.26	0.00	7.68	3.68	1.32	8.31	0.24	0.000	1.17	7.91	4.95	37.43	855.7	1022.80	2.0135E+6	1.16

3M MAPA

T	LMa	10^5. kl	10^2. kg	10^2. kg	10^{-3}. H_{CO_2}	LMP CO_2	LMP $*CO_2$	10^3. N_{CO_2}	10^3. kg	10^3. KG	KG/kg	E	k_2	kobs (1/s)	$10^3.N_{CO_2}$ (mod)
(^{0}C)	(mol CO^2/ mol Amine)	(m/s)	(m/s)	(mol/m^2 kpa s)	(kpa m^3/mol)	(kpa)	(kpa)	(mol/ m^2 s)	(mol/m^2 kpa s)	(mol/m^2 kpa s)	(%)				(mol/ m^2 s)
28.04	0.00	3.50	3.96	1.58	5.35	0.25	0.000	1.01	5.36	4.00	25.33	819.6	308.86	9.3585E+5	1.14
35.77	0.00	4.24	3.90	1.52	6.24	0.23	0.000	1.07	6.61	4.61	30.34	973.4	503.91	1.5203E+6	1.14
43.31	0.00	5.21	3.99	1.51	7.02	0.22	0.000	1.16	8.29	5.36	35.38	1117.3	798.32	2.3978E+6	1.16
52.53	0.00	6.79	4.04	1.49	7.86	0.20	0.000	1.25	11.09	6.35	42.75	1285.5	1412.27	4.2177E+6	1.17
61.51	0.00	7.76	3.89	1.39	8.62	0.22	0.000	1.59	15.61	7.36	52.86	1736.2	2904.41	8.6145E+6	1.34

4M MAPA

T	LMa	10^5. kl	10^2. kg	10^2. kg	10^{-3}. H_{CO_2}	LMP CO_2	LMP $*CO_2$	10^3. N_{CO_2}	10^3. kg	10^3. KG	KG/kg	E	k_2	kobs (1/s)	$10^3.N_{CO_2}$ (mod)
(^{0}C)	(mol CO^2/ mol Amine)	(m/s)	(m/s)	(mol/m^2 kpa s)	(kpa m^3/mol)	(kpa)	(kpa)	(mol/ m^2 s)	(mol/m^2 kpa s)	(mol/m^2 kpa s)	(%)				(mol/ m^2 s)
27.52	0.00	1.67	3.96	1.58	5.39	0.21	0.000	1.05	7.16	4.93	31.15	2313.4	783.07	3.1721E+6	0.93
35.42	0.00	2.49	4.03	1.57	5.99	0.21	0.000	1.25	9.75	6.02	38.27	2350.2	1311.75	5.2822E+6	1.05
43.26	0.00	3.52	4.11	1.56	6.52	0.22	0.000	1.46	11.77	6.70	43.09	2181.7	1655.20	6.6238E+6	1.26
51.13	0.00	4.69	4.14	1.53	6.99	0.20	0.000	1.61	16.83	8.01	52.43	2511.2	2978.96	1.1845E+7	1.31
60.57	0.00	4.79	3.88	1.40	7.53	0.21	0.000	2.02	30.08	9.53	68.32	4736.7	9501.06	3.7440E+7	1.45

5M MAPA

T	LMa	10^5. kl	10^2. kg	10^2. kg	10^{-3}. H_{CO_2}	LMP CO_2	LMP $*CO_2$	10^3. N_{CO_2}	10^3. kg	10^3. KG	KG/kg	E	k_2	kobs (1/s)	$10^3.N_{CO_2}$ (mod)
(^{0}C)	(mol CO_2/ mol Amine)	(m/s)	(m/s)	(mol/m^2 kpa s)	(kpa m^3/mol)	(kpa)	(kpa)	(mol/ m^2 s)	(mol/m^2 kpa s)	(mol/m^2 kpa s)	(%)				(mol/ m^2 s)
27.68	0.00	1.15	4.08	1.64	5.00	0.27	0.000	1.75	11.06	6.60	40.35	4808.0	2002.13	9.7025E+06	1.21
35.25	0.00	1.58	4.00	1.56	5.11	0.25	0.000	1.85	14.23	7.43	47.76	4603.7	2477.46	1.1926E+07	1.37
43.59	0.00	2.21	4.00	1.51	5.23	0.22	0.000	1.98	21.33	8.85	58.51	5050.7	3981.92	1.9020E+07	1.48
52.51	0.00	3.13	4.02	1.48	5.35	0.27	0.000	2.88	39.83	10.77	72.95	6830.5	10367.64	4.9046E+07	2.05
60.92	0.00	3.48	3.84	1.38	5.46	0.29	0.000	3.45	80.85	11.76	85.45	12727.6	40111.62	1.8812E+08	2.35

Appendix B2: Kinetics data of aqueous Blended "MAPA+DEEA" System

1M1D

T	LMa	10^5. kl	10^2. kg	10^2. kg	10^{-3}. H_{CO_2}	LMP CO_2	LMP $*CO_2$	10^3. N_{CO_2}	10^3. kg	10^3. KG	KG/kg	E	k_2	kobs (1/s)
(^{0}C)	(mol CO^2/ mol Amine)	(m/s)	(m/s)	(mol/m^2 kpa s)	(kpa m^3/mol)	(kpa)	(kpa)	(mol/ m^2 s)	(mol/m^2 kpa s)	(mol/m^2 kpa s)	(%)			
25.38	0.00	3.11	3.89	1.56	2.69	0.31	0.00	0.71	2.65	2.27	14.53	321.19	60.88	1.213E+05
34.72	0.00	4.21	3.92	1.53	4.11	0.22	0.00	0.71	4.07	3.22	21.05	398.39	127.59	2.541E+05
43.17	0.00	5.49	3.95	1.49	4.56	0.23	0.00	0.78	4.47	3.44	23.05	372.02	143.95	2.866E+05
51.73	0.00	6.98	3.76	1.38	4.98	0.20	0.00	0.85	6.03	4.20	30.36	429.79	243.59	4.8488E+05
59.76	0.00	8.10	3.83	1.38	5.35	0.18	0.00	0.99	9.52	5.63	40.85	630.25	596.40	1.1864E+05

1M2D

T	LMa	10^5. kl	10^2. kg	10^2. kg	10^{-3}. H_{CO_2}	LMP CO_2	LMP $*CO_2$	10^3. N_{CO_2}	10^3. kg	10^3. KG	KG/kg	E	k_2	kobs (1/s)
(^{0}C)	(mol CO^2/ mol Amine)	(m/s)	(m/s)	(mol/m^2 kpa s)	(kpa m^3/mol)	(kpa)	(kpa)	(mol/ m^2 s)	(mol/m^2 kpa s)	(mol/m^2 kpa s)	(%)			
23.91	0.00	1.81	3.70	1.49	3.39	0.38	0.00	0.79	2.38	2.06	13.80	446.82	43.65	1.305E+05
33.65	0.00	2.71	3.80	1.48	3.71	0.34	0.00	0.79	2.74	2.31	15.63	375.09	48.06	1.437E+05
41.96	0.00	3.72	3.83	1.45	3.96	0.28	0.00	0.79	3.46	2.80	19.27	369.25	63.59	1.902E+05
51.52	0.00	4.99	3.88	1.42	4.21	0.28	0.00	0.88	4.07	3.17	22.23	343.44	72.16	2.157E+05
60.47	0.00	5.73	3.71	1.33	4.42	0.25	0.00	0.95	5.43	3.85	29.01	419.21	121.03	3.618E+05

1M3D

T	LMa	10^5. kl	10^2. kg	10^2. kg	10^{-3}. H_{CO_2}	LMP CO_2	LMP $*CO_2$	10^3. N_{CO_2}	10^3. kg	10^3. KG	KG/kg	E	k_2	kobs (1/s)
(^{0}C)	(mol CO^2/ mol Amine)	(m/s)	(m/s)	(mol/m^2 kpa s)	(kpa m^3/mol)	(kpa)	(kpa)	(mol/ m^2 s)	(mol/m^2 kpa s)	(mol/m^2 kpa s)	(%)			
25.14	0.00	1.21	3.80	1.53	2.98	0.32	0.00	0.78	2.93	2.46	16.05	722.81	54.45	2.173E+05
34.99	0.00	1.96	3.92	1.52	3.17	0.27	0.00	0.78	3.50	2.84	18.66	564.84	58.39	2.330E+05
43.35	0.00	2.77	4.00	1.51	3.31	0.26	0.00	0.86	4.21	3.29	21.77	503.31	64.25	2.563E+05
51.05	0.00	3.77	3.93	1.45	3.42	0.23	0.00	0.93	5.64	4.06	28.02	511.82	91.45	3.648E+05
60.39	0.00	4.29	3.83	1.38	3.54	0.22	0.00	1.07	7.58	4.89	35.53	627.41	148.97	5.940E+05

1M5D

T	LMa	10^5. kl	10^2. kg	10^2. kg	10^{-3}. H_{CO_2}	LMP CO_2	LMP $*CO_2$	10^3. N_{CO_2}	10^3. kg	10^3. KG	KG/kg	E	k_2	kobs (1/s)
(^{0}C)	(mol CO^2/ mol Amine)	(m/s)	(m/s)	(mol/m^2 kpa s)	(kpa m^3/mol)	(kpa)	(kpa)	(mol/ m^2 s)	(mol/m^2 kpa s)	(mol/m^2 kpa s)	(%)			
25.72	0.00	0.63	3.87	1.56	1.66	0.30	0.00	0.94	3.96	3.16	20.28	1050.51	36.25	2.170E+05
34.97	0.00	1.07	4.00	1.56	1.79	0.31	0.00	1.03	4.23	3.33	21.34	706.78	30.65	1.835E+05
44.37	0.00	1.70	3.95	1.49	1.91	0.28	0.00	1.09	5.22	3.86	25.90	586.44	32.05	1.918E+05
52.80	0.00	2.44	3.96	1.46	2.01	0.27	0.00	1.17	6.31	4.40	30.24	518.55	35.31	2.113E+05
61.46	0.00	2.61	3.77	1.35	2.10	0.27	0.00	1.27	7.38	4.77	35.37	593.70	48.21	2.884E+05

2M1D

T	LMa	10^5. kl	10^2. kg	10^2. kg	10^{-3}. H_{CO_2}	LMP CO_2	LMP $*CO_2$	10^3. N_{CO_2}	10^3. kg	10^3. KG	KG/kg	E	k_2	kobs (1/s)
(^{0}C)	(mol CO^2/ mol Amine)	(m/s)	(m/s)	(mol/m^2 kpa s)	(kpa m^3/mol)	(kpa)	(kpa)	(mol/ m^2 s)	(mol/m^2 kpa s)	(mol/m^2 kpa s)	(%)			
25.34	0.00	2.03	3.81	1.53	3.70	0.31	0.00	0.80	3.07	2.56	16.72	560.22	79.00	2.362E+05
35.16	0.00	2.98	3.91	1.53	4.12	0.28	0.00	0.89	4.03	3.19	20.89	557.39	117.34	3.508E+05
43.94	0.00	4.25	4.03	1.52	4.44	0.29	0.00	1.02	4.66	3.56	23.44	487.21	130.58	3.903E+05
50.43	0.00	5.29	3.82	1.41	4.65	0.26	0.00	1.13	6.36	4.38	31.11	558.71	216.02	6.454E+05
59.24	0.00	6.22	3.68	1.32	4.92	0.23	0.00	1.29	9.42	5.50	41.56	746.79	444.84	1.329E+06

2M2D a

T	LMa	10^5. kl	10^2. kg	10^2. kg	10^{-3}. H_{CO_2}	LMP CO_2	LMP $*CO_2$	10^3. N_{CO_2}	10^3. kg	10^3. KG	KG/kg	E	k_2	kobs (1/s)
(^{0}C)	(mol CO^2/ mol Amine)	(m/s)	(m/s)	(mol/m^2 kpa s)	(kpa m^3/mol)	(kpa)	(kpa)	(mol/ m^2 s)	(mol/m^2 kpa s)	(mol/m^2 kpa s)	(%)			
26.20	0.00	1.21	3.70	1.48	3.39	0.24	0.00	0.99	5.60	4.06	27.42	1568.31	255.14	1.017E+06
34.79	0.00	1.74	3.89	1.51	3.60	0.31	0.00	1.12	4.75	3.61	23.87	981.17	143.15	5.706E+05
43.79	0.00	2.62	3.93	1.48	3.78	0.29	0.00	1.19	5.66	4.10	27.58	817.42	150.60	6.002E+05
52.34	0.00	3.65	3.94	1.45	3.92	0.25	0.00	1.30	7.94	5.12	35.42	853.40	232.63	9.270E+05
60.62	0.00	4.02	3.69	1.33	4.05	0.24	0.00	1.45	10.90	5.99	45.07	1099.78	413.74	1.648E+06

2M2D b

T	LMa	10^5. kl	10^2. kg	10^2. kg	10^{-3}. H_{CO_2}	LMP CO_2	LMP $*CO_2$	10^3. N_{CO_2}	10^3. kg	10^3. KG	KG/kg	E	k_2	kobs (1/s)
(^{0}C)	(mol CO^2/ mol Amine)	(m/s)	(m/s)	(mol/m^2 kpa s)	(kpa m^3/mol)	(kpa)	(kpa)	(mol/ m^2 s)	(mol/m^2 kpa s)	(mol/m^2 kpa s)	(%)			
24.62	0.00	1.13	3.94	1.59	3.42	0.28	0.00	0.92	4.12	3.27	20.61	1247.08	148.75	5.932E+05
34.16	0.00	1.51	3.99	1.56	3.58	0.26	0.00	0.92	4.66	3.59	23.02	1109.94	140.33	5.597E+05
43.67	0.00	2.67	3.93	1.48	3.78	0.25	0.00	1.02	5.68	4.11	27.67	803.97	151.87	6.056E+05
51.92	0.00	3.61	3.82	1.40	3.92	0.22	0.00	1.17	8.34	5.23	37.27	905.09	259.14	1.033E+06
60.20	0.00	3.98	3.74	1.35	4.05	0.25	0.00	1.46	10.36	5.85	43.51	1054.96	373.06	1.486E+06

2M3D a

T	LMa	10^5. kl	10^2. kg	10^2. kg	10^{-3}. H_{CO_2}	LMP CO_2	LMP $*CO_2$	10^3. N_{CO_2}	10^3. kg	10^3. KG	KG/kg	E	k_2	kobs (1/s)
(^{0}C)	(mol CO^2/ mol Amine)	(m/s)	(m/s)	(mol/m^2 kpa s)	(kpa m^3/mol)	(kpa)	(kpa)	(mol/ m^2 s)	(mol/m^2 kpa s)	(mol/m^2 kpa s)	(%)			
26.70	0.00	0.83	3.88	1.55	2.70	0.27	0.00	0.92	4.46	3.47	22.31	1444.84	114.31	5.702E+05
35.29	0.00	1.42	4.00	1.56	2.82	0.28	0.00	1.05	4.95	3.76	24.14	984.32	102.84	5.129E+05
43.63	0.00	1.95	3.90	1.48	2.93	0.27	0.00	1.20	6.48	4.50	30.47	973.66	125.16	6.239E+05
52.62	0.00	2.85	3.93	1.45	3.03	0.26	0.00	1.40	8.59	5.40	37.19	913.75	162.51	8.098E+05
61.58	0.00	2.96	3.83	1.37	3.12	0.25	0.00	1.55	11.65	6.30	45.91	1231.14	289.30	1.441E+06

2M3D b

T	LMa	10^5. kl	10^2. kg	10^2. kg	10^{-3}. H_{CO_2}	LMP CO_2	LMP $*CO_2$	10^3. N_{CO_2}	10^3. kg	10^3. KG	KG/kg	E	k_2	kobs (1/s)
(^{0}C)	(mol CO^2/ mol Amine)	(m/s)	(m/s)	(mol/m^2 kpa s)	(kpa m^3/mol)	(kpa)	(kpa)	(mol/ m^2 s)	(mol/m^2 kpa s)	(mol/m^2 kpa s)	(%)			
24.32	0.00	0.74	3.93	1.59	2.66	0.28	0.00	0.99	4.49	3.50	22.05	1613.68	124.56	6.212E+05
35.07	0.00	1.24	3.98	1.55	2.82	0.29	0.00	1.09	4.88	3.71	23.94	1104.53	100.57	5.014E+05
43.87	0.00	1.98	4.02	1.52	2.92	0.26	0.00	1.15	6.15	4.38	28.83	911.32	111.33	5.550E+05
52.47	0.00	2.84	3.90	1.43	3.02	0.26	0.00	1.41	8.97	5.51	38.54	956.32	176.70	8.805E+05
60.68	0.00	2.99	3.85	1.39	3.11	0.27	0.00	1.65	10.76	6.06	43.69	1121.16	243.43	1.212E+06

2M4D

T	LMa	10^5. kl	10^2. kg	10^2. kg	10^{-3}. H_{CO_2}	LMP CO_2	LMP $*CO_2$	10^3. N_{CO_2}	10^3. kg	10^3. KG	KG/kg	E	k_2	kobs (1/s)
(^{0}C)	(mol CO^2/ mol Amine)	(m/s)	(m/s)	(mol/m^2 kpa s)	(kpa m^3/mol)	(kpa)	(kpa)	(mol/ m^2 s)	(mol/m^2 kpa s)	(mol/m^2 kpa s)	(%)			
27.56	0.00	0.67	3.80	1.52	1.83	0.31	0.00	1.34	6.01	4.31	28.38	1649.31	95.49	5.713E+05
35.03	0.00	1.05	3.83	1.49	1.96	0.29	0.00	1.47	7.50	4.99	33.50	1395.31	117.50	7.030E+05
44.15	0.00	1.67	3.94	1.49	2.09	0.27	0.00	1.56	9.57	5.82	39.15	1197.87	134.87	8.067E+05
51.60	0.00	2.25	3.84	1.42	2.18	0.29	0.00	1.82	11.44	6.33	44.65	1110.09	149.78	8.955E+05
60.42	0.00	2.57	3.87	1.39	2.28	0.28	0.00	1.95	14.17	7.02	50.48	1256.21	221.27	1.323E+06

2M5D

T	LMa	10^5. kl	10^2. kg	10^2. kg	10^{-3}. H_{CO_2}	LMP CO_2	LMP $*CO_2$	10^3. N_{CO_2}	10^3. kg	10^3. KG	KG/kg	E	k_2	kobs (1/s)
(^{0}C)	(mol CO^2/ mol Amine)	(m/s)	(m/s)	(mol/m^2 kpa s)	(kpa m^3/mol)	(kpa)	(kpa)	(mol/ m^2 s)	(mol/m^2 kpa s)	(mol/m^2 kpa s)	(%)			
27.43	0.00	0.69	3.83	1.54	1.26	0.23	0.00	1.63	13.36	7.15	46.50	2438.57	182.39	1.273E+06
35.49	0.00	1.06	3.89	1.51	1.35	0.24	0.00	1.96	17.19	8.05	53.18	2189.79	235.11	1.640E+06
44.16	0.00	1.67	3.95	1.50	1.45	0.21	0.00	2.04	27.28	9.66	64.59	2379.53	435.65	3.039E+06
52.98	0.00	2.45	3.98	1.46	1.55	0.19	0.00	2.27	74.54	12.23	83.59	4741.77	2555.82	1.782E+07
62.20	0.00	2.50	3.89	1.40	1.66	0.24	0.00	2.96	122.64	12.55	89.77	8193.63	7411.70	5.164E+07

3M1D

T	LMa	10^5. kl	10^2. kg	10^2. kg	10^{-3}. H_{CO_2}	LMP CO_2	LMP $*CO_2$	10^3. N_{CO_2}	10^3. kg	10^3. KG	KG/kg	E	k_2	kobs (1/s)
(^{0}C)	(mol CO^2/ mol Amine)	(m/s)	(m/s)	(mol/m^2 kpa s)	(kpa m^3/mol)	(kpa)	(kpa)	(mol/ m^2 s)	(mol/m^2 kpa s)	(mol/m^2 kpa s)	(%)			
25.00	0.00	1.17	3.78	1.52	3.42	0.30	0.00	1.17	5.35	3.96	25.98	1558.49	241.85	9.640E+05
34.45	0.00	1.97	3.85	1.50	4.14	0.30	0.00	1.24	5.79	4.17	27.84	1215.65	280.23	1.117E+06
43.12	0.00	2.74	3.76	1.42	4.54	0.31	0.00	1.35	6.26	4.35	30.59	1038.31	269.05	1.072E+06
51.91	0.00	3.57	3.90	1.43	4.70	0.27	0.00	1.47	8.71	5.42	37.80	1146.91	399.65	1.592E+06
60.09	0.00	4.26	3.95	1.42	4.65	0.21	0.00	1.61	16.51	7.64	53.73	1802.05	1218.09	4.851E+06

3M3D

T	LMa	10^5. kl	10^2. kg	10^2. kg	10^{-3}. H_{CO_2}	LMP CO_2	LMP $*CO_2$	10^3. N_{CO_2}	10^3. kg	10^3. KG	KG/kg	E	k_2	kobs (1/s)
(^{0}C)	(mol CO^2/ mol Amine)	(m/s)	(m/s)	(mol/m^2 kpa s)	(kpa m^3/mol)	(kpa)	(kpa)	(mol/ m^2 s)	(mol/m^2 kpa s)	(mol/m^2 kpa s)	(%)			
25.68	0.00	0.66	3.83	1.54	2.38	0.22	0.00	1.42	11.44	6.56	42.62	4131.47	587.53	3.515E+06
35.53	0.00	1.12	3.87	1.50	2.46	0.20	0.00	1.54	15.43	7.62	50.65	3391.39	718.75	4.299E+06
44.39	0.00	1.74	3.96	1.49	2.53	0.23	0.00	1.94	19.09	8.38	56.09	2785.23	740.64	4.427E+06
52.95	0.00	2.49	4.01	1.47	2.60	0.20	0.00	2.16	38.36	10.63	72.27	4018.49	2207.91	1.319E+07
62.05	0.00	2.57	3.75	1.34	2.67	0.20	0.00	2.55	181.23	12.50	93.11	19033.87	49375.66	2.949E+08

4M3D

T	LMa	10^5. kl	10^2. kg	10^2. kg	10^{-3}. H_{CO_2}	LMP CO_2	LMP $*CO_2$	10^3. N_{CO_2}	10^3. kg	10^3. KG	KG/kg	E	k_2	kobs (1/s)
(^{0}C)	(mol CO^2/ mol Amine)	(m/s)	(m/s)	(mol/m^2 kpa s)	(kpa m^3/mol)	(kpa)	(kpa)	(mol/ m^2 s)	(mol/m^2 kpa s)	(mol/ m^2 kpa s)	(%)			
27.10	0.00	0.66	3.92	1.57	2.07	0.25	0.00	2.13	18.47	8.49	54.03	5784.91	980.65	6.839E+06
34.99	0.00	1.01	3.99	1.56	2.10	0.27	0.00	2.44	22.35	9.17	58.96	4648.75	995.62	6.941E+06
44.39	0.00	1.75	4.03	1.52	2.13	0.27	0.00	3.00	40.24	11.04	72.57	4917.13	2032.89	1.416E+07
53.77	0.00	2.45	4.00	1.47	2.18	0.29	0.00	3.84	135.82	13.25	90.25	12150.05	16496.85	1.148E+08
62.72	0.00	2.42	3.92	1.40	2.23	0.29	0.00	4.79	-86.78	16.64	119.1	7967.04	6827.11	4.746E+07

Appendix C: Graphical Representation

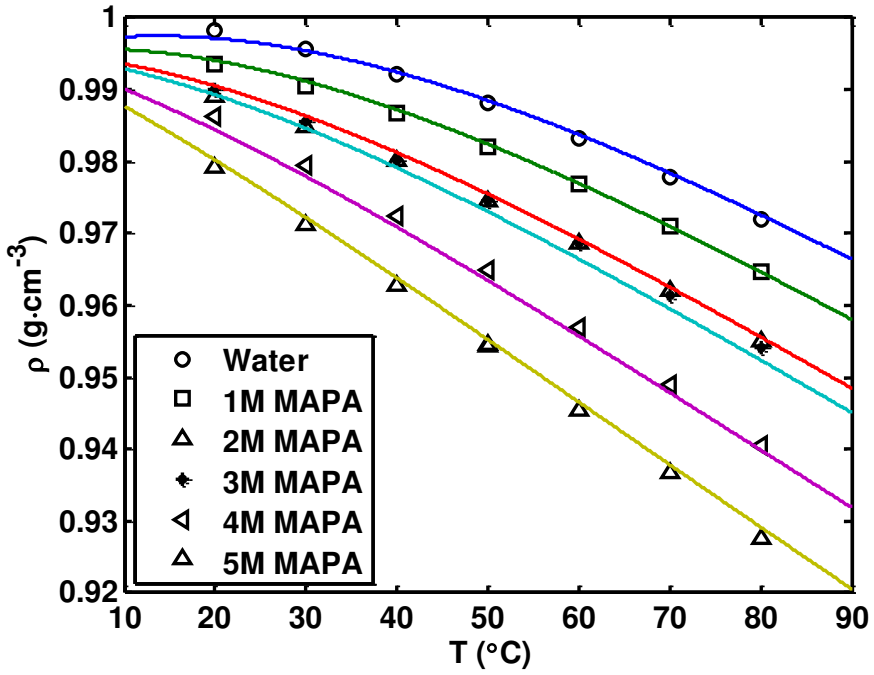

Graph C1: Density vs temperature curves MAPA system based on modeling

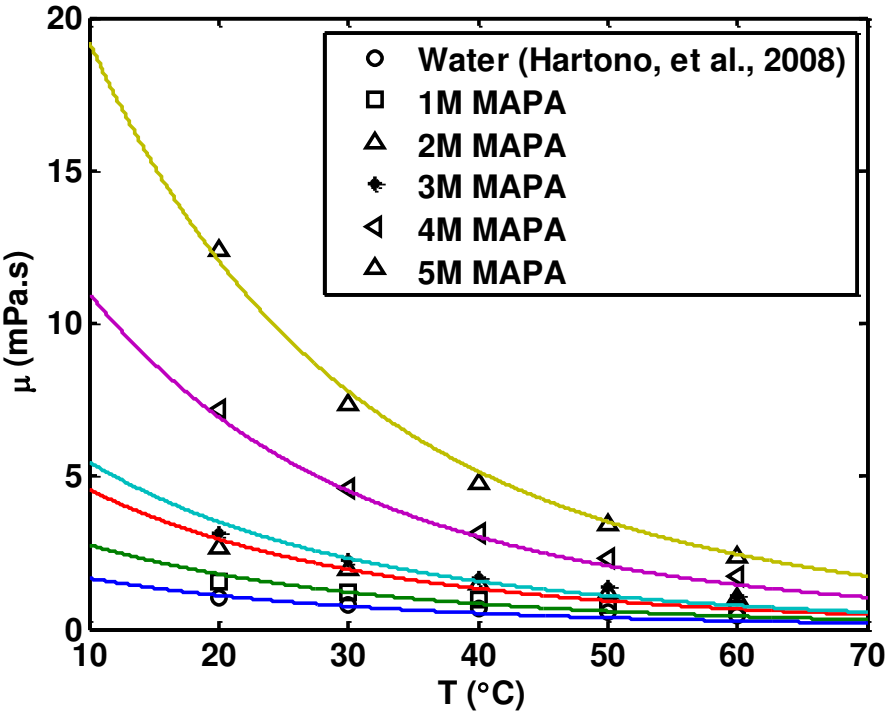

Graph C2: Viscosity vs temperature curves for MAPA system based on modeling

Appendix D: Risk Assessment Form of In Used Equipment

NTNU	Hazardous activity identification process	Risikovurdering	Nummer	Dato
		HMS-avd.	HMSRV2601	2/6/2013
		Godkjent av	Side	Erstatter
HMS				

Unit: *Kjemisk prosessteknologi* **Date:** 2/6/2013

Line manager: *Hallvard F. svendesen (CO2 capture group)*

Participants in the identification process (including their function): Hammad Majeed (Operator), Juliana manterio(Co supervisor)

Short description of the main activity/main process: Kinetics and modelling in CO2-amine systems

ID no.	Activity/process	Responsible person	Laws, regulations etc.	Existing documentation	Existing safety measures	Comment
1	Cleaning of equipment	Operator			Wearing Proper PPE	Exhaust Valve is very important for volatile chemicals
2	Preparation of sample	Operator			Wearing Proper PPE	To be prepared in specified chamber where air flow is availible
3	Sample loading in equipment	Operator			Wearing Proper PPE	
4	Sample taking from equipment	Operator			Wearing Proper PPE	
5	Draining of chemical from equipment	Operator			Wearing Proper PPE	waste container to be disposed properly or recycled
6	Cleaning of equipment after experiment	Operator			Wearing Proper PPE	Vent valve should be open during cleaning and drying period
7	Gas bottles(N2, CO2)	Operator				

NTNU	Risk assessment	Utarbeidet av	Nummer	Dato
		HMS-avd.	HMSRV2603	2/6/2013
		Godkjent av	Side	Erstatter
HMS /KS				

Unit: *Kjemisk prosessteknologi* **Date:** 2/6/2013

Line manager: *Hallvard F. svendesen (CO2 capture group)*

Participants in the identification process (including their function): *Hammad Majeed (Operator), Juliana manterio (Co Supervisor)*

Signatures: Hammad Majeed

ID no.	Activity from the identification process form	Potential undesirable incident/strain	Likelihood:	Consequence:				Risk value	Comments/status Suggested measures
			Likelihood (1-5)	Human (A-E)	Environment (A-E)	Economy/ material (A-E)	Reputation (A-E)	Human	
1	Cleaning of equipment	breakage of glass ware, Chemcial fumes	3	A	A	A	A	A3	
2	Preparation of sample	spillage of amines, Alcohol	4	B	B	B	A	B4	Use of fume cupboard
3	Sample loading in equipment	spillage of chemical	4	B	A	B	A	B4	Fume mask is mandatory
4	Sample taking from equipment	spillage of chemical	4	B	A	A	A	B4	
5	Draining of chemical from equipment	spillage of chemical	4	B	A	A	A	B4	
6	Cleaning of equipment after experiment	breakage of glass ware	3	A	B	A	A	A3	Exhaust value should be open
7	Preparation of disc in SDC onc in 5 years		1	D	A	A	A	1D	